# NEW NEUTRON DETECTOR USING MAGNETICALLY FOCUSED ELECTRONS FOR FAST REACTOR NEUTRON FLUX MEASUREMENTS

A THESIS

Presented to

The Faculty of the Division of Graduate Studies

by

Samir Abdul-Majid Alzaidi

In Partial Fulfillment

of the Requirements for the Degree

Doctor of Philosophy

in the School of Nuclear Engineering

Georgia Institute of Technology

October, 1976

NEW NEUTRON DETECTOR USING MAGNETICALLY FOCUSED ELECTRONS

FOR FAST REACTOR NEUTRON FLUX MEASUREMENTS

Approved:

G. G. Eichholz, Chairman

M. V. Davis

R. W. Fink

D. S. Harmer

E. T. Patronis

Date approved by Chairman: 10-4-76

# ACKNOWLEDGMENTS

Many individuals have contributed to the work presented here. Without their efforts, its successful completion would not be possible. To each of them I would like to express my sincere appreciation.

I am deeply grateful to my adviser, Dr. G. G. Eichholz, for his guidance, encouragement, patience, useful suggestions, the long hours he spent with me discussing several problems related to this work, and for his valuable review of the manuscript.

I express my deep appreciation to Dr. M. V. Davis, Dr. R. W. Fink, Dr. D. S. Harmer, Dr. E. T. Patronis, and Dr. C. J. Roberts, my reading committee members, for all kinds of help and encouragement which they gave to me during the course of this work, and to Dr. L. E. Weaver, Director of the School of Nuclear Engineering, for his support, cooperation, and assistance. My deep appreciation goes also to Dr. E. W. Thomas (School of Physics), Dr. B. R. Livesay (Engineering Experiment Station), Dr. R. K. Feeney (School of Electrical Engineering), and Dr. S. Spooner (School of Chemical Engineering) for much valuable advice and for generously lending equipment needed for this work.

I would like to express my sincere appreciation to Mr. B. D. Statham (School of Nuclear Engineering) who was most helpful in providing different kinds of assistance and useful information during all stages of this work; to Mr. W. B. Jeter (School of Engineering) for his fine work in machining several parts used in this research and for useful advice

and assistance in light pipe and scintillator polishing.

I am deeply grateful to the staff of the Georgia Tech Research Reactor; Mr. R. S. Kirkland was cooperative and helpful. Members of the Reactor Operation Group, Messrs. S. H. Kirbo, L. D. McDowell, D. L. Cox, D. K. Hill, Michael Skinner, and A. Cox, were very helpful, patient, and friendly, and I feel deeply indebted to them. The Health Physics Group including Messrs. R. M. Boyd, J. E. Taylor, and S. N. Millspaugh were patient and cooperative and to them I would like to express my appreciation. And many thanks go to Mr. P. D. Field, Mr. R. C. McFarland, and Mr. J. M. Burke for all kinds of friendly assistance which they provided during the experimental phases of this research.

I express many thanks to the Iraqi Government for all kinds of help, interest, and encouragement given to me during the course of this research.

Thanks go to all of my friends and colleagues in the school for making the work more enjoyable and to Mrs. Lydia S. Geeslin for her professional work in typing and preparing the manuscript.

My family, especially my mother, are offered many thanks for their love and confidence; and special thanks go to my wife, Kawther, for being very patient, understanding, and helpful and for her continuous encouragement and inspiration.

TABLE OF CONTENTS


| | | Page |
|---|---|---|
| ACKNOWLEDGMENTS | | ii |
| LIST OF TABLES | | vi |
| LIST OF ILLUSTRATIONS | | vii |
| SUMMARY | | ix |
| Chapter | | |
| I. | INTRODUCTION | 1 |
| II. | REVIEW OF PRESENT NEUTRON FLUX DETECTORS IN REACTOR APPLICATIONS | 13 |
| | The Fission Chamber | 14 |
| | Boron Detectors | 20 |
| | Self-Powered Detectors | 22 |
| | Neutron Thermopile Detectors | 27 |
| | Neutron Detection by Induced Radioactivity | 33 |
| | SiC Semiconductor Detectors | 38 |
| | Cerenkov Detectors | 42 |
| | Microwave Detectors | 45 |
| | Spark Counters | 48 |
| | Detectors Employing Radiation Elements and Secondary Electrons | 49 |
| | Gas Scintillation Detectors | 51 |
| | Summary | 51 |
| III. | A NEW NEUTRON DETECTOR USING MAGNETICALLY FOCUSED ELECTRONS | 53 |
| | Introduction | 53 |
| | Description of the Detector | 54 |
| | The Magnetic Field | 56 |
| | The Electron Trajectory | 58 |
| | Neutron Converter | 62 |
| | Electron Detector | 64 |
| | Possible Gamma-ray Interference | 67 |
| | Other Properties of the Detector | 71 |

TABLE OF CONTENTS (Continued)


| Chapter | | Page |
|---|---|---|
| IV. | EXPERIMENTAL DETAILS AND PROCEDURE | 74 |
| | General | 74 |
| | Magnetic Field Measuring Device | 77 |
| | The Counting System | 80 |
| | Preliminary Test Arrangements | 82 |
| | The Vacuum System | 84 |
| | The Georgia Tech Research Reactor (GTRR) | 85 |
| V. | RESULTS | 90 |
| | Hot Filament Electron Focusing | 90 |
| | Focusing $^{35}S$ Beta Particles | 93 |
| | Detector Response Using Gadolinium, Cadmium, Silver, and Indium Converters in the Biomedical Facility | 96 |
| | Effect of Solenoid Curvature | 98 |
| | Effect of Pressure on the Count Rate | 105 |
| | Use of the H-8 Horizontal Beam Facility | 105 |
| | Detector Time Response | 110 |
| | Detector Sensitivity to Gamma-ray Interference | 110 |
| VI. | DISCUSSION OF RESULTS | 114 |
| | Detector Performance | 114 |
| | Design Features | 121 |
| | Possible Sources of Error in the Experiment | 124 |
| | Stability | 126 |
| VII. | CONCLUSIONS | 127 |
| BIBLIOGRAPHY | | 129 |
| VITA | | 142 |

# LIST OF TABLES


| Table | | Page |
|---|---|---|
| 1. | Potential Converter Materials . . . . . | 65 |
| 2. | Gamma-ray Background Fields: Beamport H-8 with Graphite Rod Inserted. . . . . | 107 |
| 3. | Detector Count Rate at Different Power Levels with and without Magnetic Field. . . . . | 108 |

# LIST OF ILLUSTRATIONS


| Figure | | Page |
|---|---|---|
| 1. | Magnitude of Radiation Induced Current vs Peak Reactor Power | 5 |
| 2. | Magnitude of Radiation Induced Current vs Peak Reactor Power | 5 |
| 3. | Resistivity of Some Insulators as a Function of Temperature | 8 |
| 4. | Conductivity vs $(T)^{-1}$ for Alpha Alumina (Lucalox) | 9 |
| 5. | Schematic Diagram of the Neutron Detector Using Magnetically Focused Electrons. | 55 |
| 6. | Solenoid Position with Respect to the x,y,z Coordinates | 69 |
| 7. | Projection of Electron Path in x-y Plane (continuous lines) of Two Electrons Having the Same Velocity $v_{xy}$ a) $v_{xy}$ is small b) $v_{xy}$ is large. | 70 |
| 8. | Cross Section of the Solenoid $O_1$ and the Circle of Electron Trajectory $O_2$ | 72 |
| 9. | Schematic Diagram of the Neutron Detector Assembly and Electron Counting System | 75 |
| 10. | Magnetic Field vs Induced Voltage in the Hall Probe | 79 |
| 11. | Schematic Diagram of Electron Focusing System from Hot Filament | 83 |
| 12. | Mid-plane Section of the Georgia Tech Research Reactor | 86 |
| 13. | Schematic of Detector Position Inside H-8 Beam Hole. | 88 |
| 14. | Photograph Showing the Detector Outside the Beam Hole with the Paraffin Catcher Removed. | 89 |

LIST OF ILLUSTRATIONS (Continued)


| Figure | | Page |
|---|---|---|
| 15. | Simplified Circuit of Electron Focusing from Hot Filament. . . . . | 91 |
| 16. | Anode Current vs Anode Voltage at Focusing Voltage $V_1$ = 0 and Three Different Values of Magnetic Field. . . . . | 92 |
| 17. | Anode Current vs Anode Voltage at Focusing Voltage $V_1$ = -2000 Volts (electron energy = 2000 eV) and Two Values of Magnetic Field . . . . . | 94 |
| 18. | Anode Current vs Electron Energy at Three Values of Magnetic Field and Anode Voltage V = 67 Volts. . . . . | 95 |
| 19. | Count Rate vs Magnetic Field of Sulfur-35 Beta Source. . . . . | 97 |
| 20. | Count Rate vs Reactor Power and Neutron Flux of Gadolinium Converter and Gamma-ray in the Biomedical Facility . . . . . | 99 |
| 21. | Count Rate vs Reactor Power and Neutron Flux of Cadmium Converter in the Biomedical Facility . . . . . | 100 |
| 22. | Count Rate vs Reactor Power and Neutron Flux of Silver Converter in the Biomedical Facility. . . . . | 101 |
| 23. | Count Rate vs Reactor Power and Neutron Flux of Indium Converter in the Biomedical Facility at Two Values of Magnetic Field . . . . . | 102 |
| 24. | Position of Converter in the Curved Section of the Solenoid . . . . . | 104 |
| 25. | Count Rate vs Pressure of Gadolinium Converter in H-3 Beam Hole at 1000 kW . . . . . | 106 |
| 26. | Count Rate vs Reactor Power and Neutron Flux of Gadolinium Converter in H-8 Beam Hole. . . . . | 109 |
| 27. | Count Rate vs Time During Reactor Start Up Using Gadolinium Converter. . . . . | 111 |
| 28. | Schematic of Detector Solenoid Position for Intense Gamma Irradiation from H-8 Beam Hole. . . . . | 112 |

## SUMMARY

A neutron detector utilizing conversion electrons or beta particles has been investigated. The detector utilizes a long evacuated pipe along which the electrons are focused onto a distant electron detector, which is located in the low neutron flux region. This arrangement avoids the need for conducting electrical signals directly from high flux regions, which arises in other detectors, and thus circumvents problems due to radiation damage and breakdown noise in the cables.

The detector consists of a thin long evacuated tube on which a solenoid coil is wound. One end of the system is curved to an angle of about $60^{o}$ to reduce neutron and gamma-ray streaming. The in-core end of the detector contains a neutron converter. At the other end of the pipe there is an electron detector, consisting of a thin plastic scintillator, a long Plexiglas pipe, and a photomultiplier. The signal from the photomultiplier is counted in the conventional counting fashion.

When the neutron converter is exposed to a neutron flux, electrons emitted are constrained in a spiral path by the applied magnetic field. They will follow the pipe and the curved portion must be larger in diameter to accommodate the perpendicular component of motion. Secondary electrons and electrons due to gamma-ray interaction with the tube wall will not be propagated along the tube. They make tight spiral paths and return to the wall.

Experiments have been performed, using thin films of gadolinium

deposited on stainless steel as the converter material, in the Georgia Tech Research Reactor, with a magnetic field of 740 gauss. A sensitivity of $2.6 \times 10^{-2}$ counts per second per unit flux was obtained. With an indium foil, 0.076 cm thick, a sensitivity of $2.6 \times 10^{-3}$ counts per second per unit flux was obtained in a magnetic field of 800 gauss, whereas a 0.038 cm thick silver foil resulted in a value of $1.8 \times 10^{-3}$ counts per unit flux and 0.0025 cm thick cadmium resulted in a value of $1.3 \times 10^{-3}$ counts per second per unit flux.

To test the sensitivity of the system to gamma-ray interference the straight portion of the detector was exposed to a gamma-ray field of 2000 R/hr with no detectable increase in background counts. While the experiment so far has been confined to thermal neutrons only, it is anticipated that a detector of the type described could function equally well in a fast neutron field with an appropriate converter material.

# CHAPTER I

## INTRODUCTION

During the operation of a nuclear reactor, adequate instrumentation is needed to ensure the correct and safe operation of the reactor by providing information on system performance. Such measurements should demonstrate that the reactor performance is as predicted by the designer and that any unexpected departure from a design condition can be indicated rapidly and be corrected. The measurements may also give information on whether this correction is practical during operation or if the reactor must be shut down immediately before any damage can take place.

Several types of measurements are usually made in nuclear reactors; these include measurement of neutron flux, temperature, coolant flow, liquid level, strain in reactor vessel, pressure, and measurements of the quantity of any radioactive material in the coolant. Other instrumentation may be in use with particular reactor designs.

Neutron flux measurement is important because it gives an indication of the reactor power and core conditions in the reactor. For power level determination measurement of the neutron flux level is used widely and preferred over other methods because it is more sensitive, fairly accurate and thus gives more information regarding the power distribution in the reactor than other methods. An uneven power distribution results in inefficient utilization of the fuel. The operator may be able to correct this situation once it is known by him.

For a given setting of control rods, it is generally assumed that the neutron flux is proportional to the power generated. Although the relation is more complex, generally a simple assumption of direct proportionality is adequate. A change of control rod position alters the neutron flux which is calibrated for the power using the neutron level indication.

A neutron flux detector is an important instrument in reactor safety too. The ideal requirement is to minimize plant shut down and to ensure that the reactor scrams only when absolutely necessary. False scrams should be avoided to prevent possible fuel material fatigue due to thermal stresses and to prevent losing operation time. Reliable instrumentation is a necessity. The design criterion is that the fuel pin clad temperature must be kept below the maximum hot-spot temperature which is chosen to give an insignificant probability of cladding failure. Installing a thermocouple to the fuel cladding to measure the temperature is very difficult because of the very high power density in that region and because the presence of the thermocouple itself may significantly change the heat flux distribution. The operating conditions have to be deduced from the power input to the local region of the core. A small size in-core, prompt detector can give information on any local high flux condition which might cause fuel cladding failure. Hence an indirect purpose of detecting local flux levels would be to prevent reactor scrams and to increase power generation.

Temperature measurement in the coolant may be used together with or as an alternative to the neutron level measurement as an indication of reactor power level. In this method only the average reactor power can

be obtained and no indication of the local power distribution is obtained. Because of the high thermal capacity of the reactor core this method may have a relatively slow time response following a change in power level.

A measurement of gamma ray fluxes may also be used as an indicator of power level. Two types of gamma photons contribute to the gamma ray intensity inside the nuclear reactor. The first are those associated with the fission process. They are prompt, their intensity is proportional to the reactor power, and they tend to have a higher energy spectrum. The second are those associated with the decay of the fission products. They have a slow time response associated with their gradual decay, they tend to have lower energies, and their intensity is not necessarily proportional to the momentary reactor power. Gamma-ray detectors cannot distinguish easily between the two groups, except by selecting specific energy windows and, therefore, their reading in general will not be proportional to the actual reactor power. Another detector has been described recently which depends on the Cherenkov threshold and can distinguish between the two types of gamma photons. Its properties and limitations are discussed in the next chapter. The only advantage of such a gamma-ray detector over a neutron detector is that it does not have a burnup problem though it may suffer radiation damage and a gradual increase in background counts.

The first requirement of any detector for in-core reactor applications is that it should withstand the reactor environment. The high gamma-ray intensity produces large interference in most existing neutron detectors. In fast reactors the degradation problem is even more severe than in thermal reactors. For instance, in a Liquid Metal Fast Breeder Reactor

the in-core gamma intensity is about $10^9$ R/hr (1). In detectors operating in a pulse mode the gamma-ray build up can produce pulses which may exceed the discriminator level. If the detector is operating in the current mode, the gamma photons produce an interfering current by ionization as in the case of gas-filled ionization chambers and self-powered detectors. The cable of the detector can be a large source of noise due to gamma-ray effects on the insulator. The noise may exceed the signal of the detector in a fast reactor environment. The gamma-ray photoelectric and Compton effects on the sheath, the insulator, and the central conductor can produce a negative current. This is because the surface area and the number of atoms per unit length of the sheath and the insulator are larger than that of the central conductor and more electrons are ejected from the sheath and the insulator and reach the central conductor; moreover, some of the electrons ejected from the conductor are reflected by the insulator. The net effect is that the sheath would be positively charged with respect to the central conductor, which causes the negative signal. Coaxial and multiconductor wire cable have been irradiated in-core in a reactor with a peak flux of $0.95 \times 10^{16}$ nv to find the gamma-ray transient effects (29). Fourteen inches of the cable were exposed to the radiation. The induced current in the central conductor of the coaxial cable with no applied voltage is shown in Figures 1 and 2 (29) together with the type of the cables. Another test showed that the current produced in the individual conductors of the multiconductor cable was approximately equal but that current produced in the shield of the coaxial cable was much larger than that produced in the central conductor. The gamma-ray-induced change in conductivity under steady state radiation

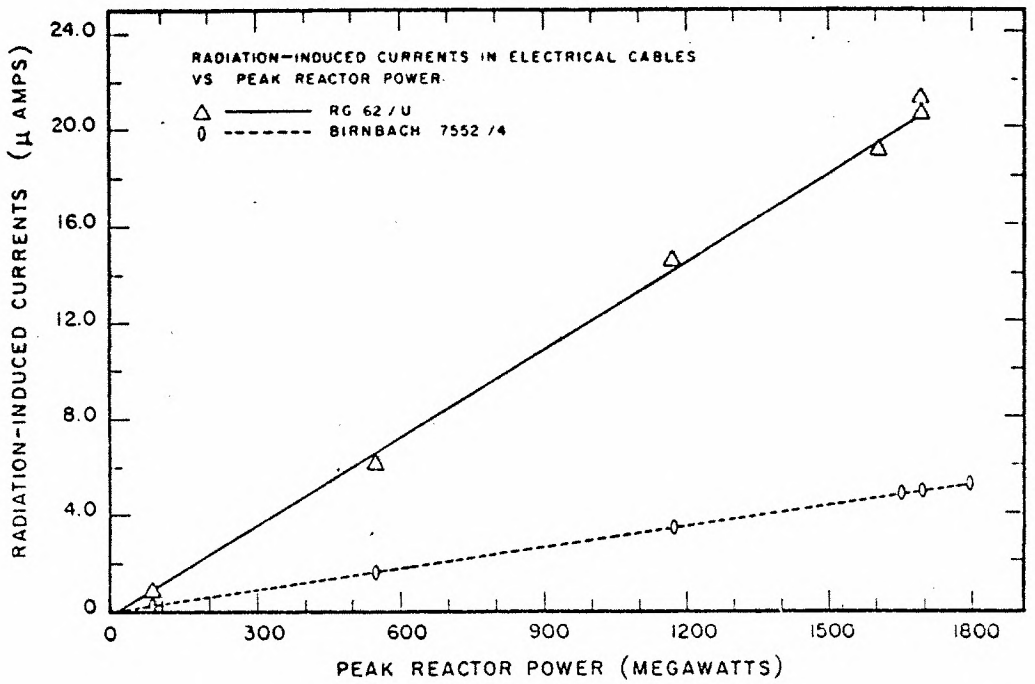


Figure 1. Magnitude of Radiation Induced Current vs Peak Reactor Power (29)

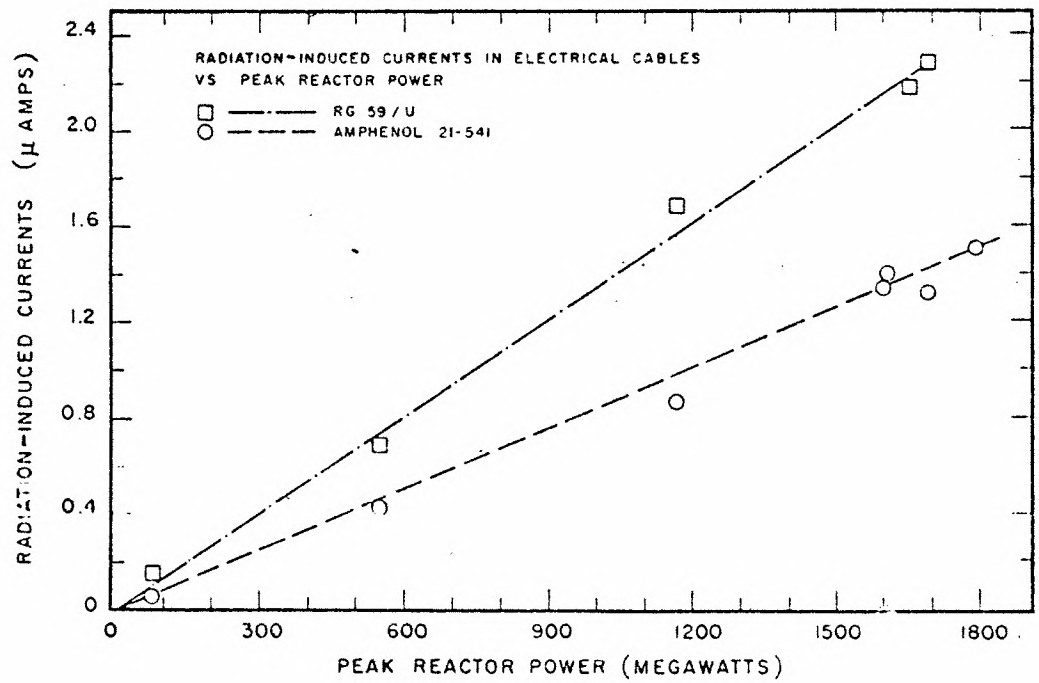


Figure 2. Magnitude of Radiation Induced Current vs Peak Reactor Power (29)

conditions follows the empirical equation (30)

$$\sigma - \sigma_0 = K \dot{r}^{\Delta}$$

where $\sigma$ and $\sigma_0$ are the conductivity of the insulator with and without gamma-ray field, respectively; K, $\Delta$ are empirical constants; $\dot{r}$ is the gamma-ray dose rate. A theoretical treatment of the transient gamma radiation effects on cables is given in references 27 and 31. A knowledge of the gamma-ray spectrum is required to calculate the induced current in the models presented by the two references.

Permanent damage on the detector and its cable will also result from long-term irradiation by fast and thermal neutrons and by energetic charged particles. Insulators are more susceptible to radiation than conductors. Fast neutrons and charged particles produce damage by atomic displacements while thermal neutrons do so by producing impurities by the process of transmutation. The resistivity of $Al_2O_3$ decreased by a factor of 100 in an integrated fast flux of $2 \times 10^{18}$ n/cm$^2$ at 250°C. Magnesium oxide also showed a large decrease in resistivity (36,37). The conductivity of the metals is affected by irradiation but the high temperature of the core tends to anneal out most of the damage. More details about irradiation effects on the electrical properties of various insulating materials are found in references 36 and 37.

The high temperature in the reactor core or close to the core is another important factor causing the ultimate failure of most common neutron detectors. In the Liquid Metal Fast Breeder Reactor the detector must survive a temperature of 300 - 1400°F (1). An increase in

temperature causes an increase in leakage current in many detectors by reducing the electric resistivity of the insulators. A breakdown will result if the applied voltage across the insulator is high. Due to the difference in the linear thermal expansion, electric bonding between two materials may break down at an elevated temperature such as the break of the contact between the solid-state detector and its connectors or the break of the contact between the uranium dioxide coating and the thermocouple lead in the neutron thermometer detector.

The increased temperature on the cable, in many cases, causes a cable noise much larger than the detector noise especially with a high applied voltage. For this reason detector designers are trying to substitute something else for the cable, such as a light pipe or wave guide. Usually a ceramic type of insulator is used in reactor cables since such insulators have good heat transmission properties and have a longer lifetime under irradiation than conventional insulators. When the temperature of a five-meter long rod of MgO is increased from 350°C to 650°C in vacuum, the resistance changes from $10^{13}$ to $10^{8}$ ohm at an applied voltage of 100 V (11). In Figure 3 (14) the resistivity of some common insulators as a function of temperature is shown. Other data are given in references 26 and 28. The effect of combined gamma radiation and an increase in temperature will decrease the resistance further than either of these two effects alone, as shown in Figure 4 (26). Other properties of the cable will also change at an elevated temperature. The apparent open-circuit capacitance and the apparent short circuit inductance for mineral-insulated cable were studied over a frequency range of 10 kHz to 100 MHz at different temperatures up to 400°C (32). The study showed

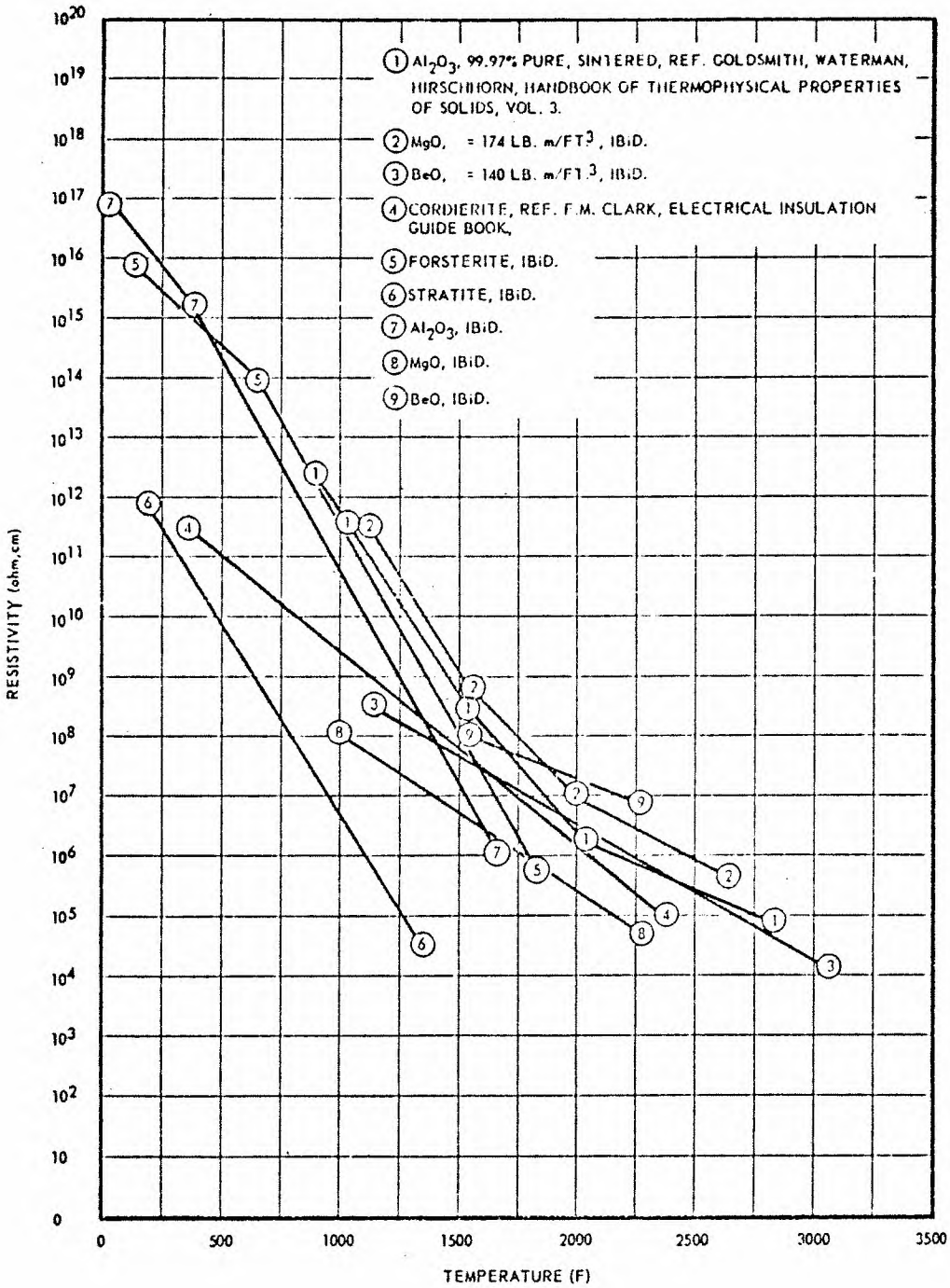


Figure 3. Resistivity of Some Insulators as a Function of Temperature (14)

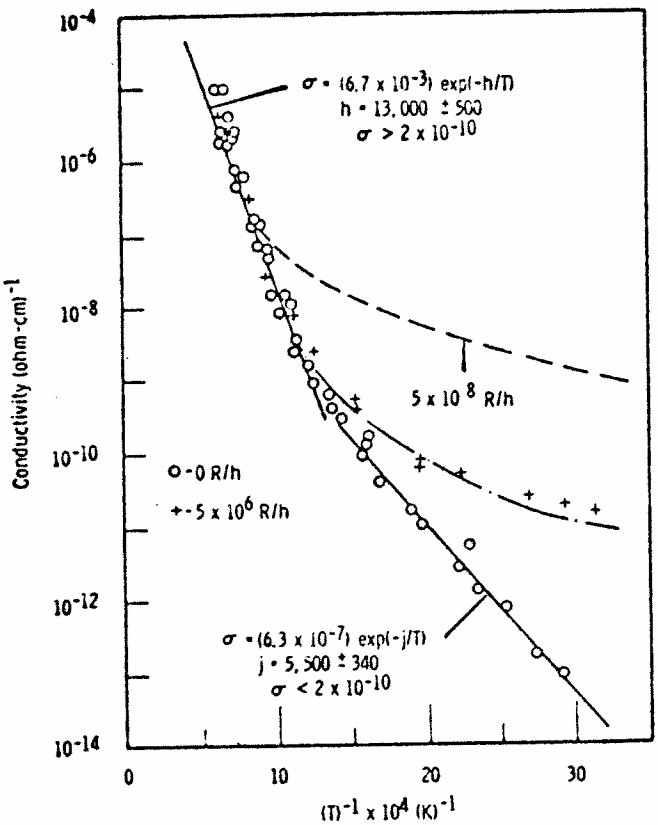


Figure 4. Conductivity vs $(T)^{-1}$ for Alpha Alumina (Lucalox) (26)

that limit the lifetime of the chamber. The upper temperature that some chambers can withstand is 500-600°C (16). The sealant of the chamber cannot withstand higher temperatures as a rule. Any thermal shock will also affect drastically the integrity of the sealant. Metal-glass (alumina-metal) joints are used in this temperature range. The combined radiation and temperature effects increase the long-range damage by one order of magnitude.

Hoitink et al. (20,21,22) have made an extensive study of some commercially available fission neutron counters in $10^6$ R/hr gamma-ray fields and at elevated temperatures. The detectors operated satisfactorily at 300°F (150°C) but the gamma field reduced the sensitivity due to pulse pile up. At 900°F (482°C) the detectors could not operate due to the large noise generated as a consequence of the temperature stress on the detector insulators. In long operation at relatively high temperatures (~ 300°F, 150°C), three of six counters failed. The failure in one of the counters was caused by a deposition of some impurities (carbon, chlorine, and sodium) on the insulators of the detector. The two other detectors failed because of a change in the characteristics of the gas either from the entry of the air or from the evolution of contained contamination into the gas where detector characteristics are highly dependent on the gas composition. They also studied the effect of induced noise pulses in the cable of fission counters for fast reactors using a cable made of quartz fiber insulator, stainless steel and copper for central wires, and a stainless steel sheath. They concluded that above 400°F (205°C) the interfering pulses became serious but the chamber can operate at or below 300°F (149°C). They also

strong dependence of these parameters on both the frequency and the temperature. The change in resistance and capacitance produced an error by shunting the signal which will attenuate a dc signal and distort an ac signal. In addition the increase in temperature causes a thermocouple effect which makes the output a function of the temperature rather than of the original signal. Chemical compatibility with the surrounding materials and mechanical strength might also change under elevated temperatures or large temperature changes and affect the electric properties of the cable.

Besides being able to survive in high radiation levels and at high temperatures the detector should cover a wide range of neutron fluxes. The flux should be covered adequately from the start-up range to the full power condition. This may include about nine decades in most reactors and no single detector can be expected to cover the whole range. In the start-up range very sensitive detectors are required. If this lower end of the range is not covered adequately, then the operator must withdraw the control rods carefully until the flux reaches the lower detector threshold. This is known as a blind start up and can possibly lead to a dangerous situation and should be avoided (4). Among the detectors used in this low range in thermal reactors are boron chambers since they have a high efficiency of about five counts per unit flux and since interfering gamma-ray intensity is low during start up. Less sensitive detectors are used in the intermediate and power ranges such as the fission counter which has an efficiency of one count per unit flux or the self powered detector of efficiency around $10^{-23}$ - $10^{-21}$ amperes per unit flux, depending on the type of emitter. In fast reactors, where other detectors may

deteriorate, activation methods are usually used but are much less convenient.

Detectors that are associated with reactor control should have very rapid time response. The operator must know without any delay any change in the flux due to changing or unexpected conditions. If an undesirable situation exists which may require reactor shutdown, then the shutdown should occur as rapidly as possible since any delay may cause damage.

It is always desirable to have a detector of small size, especially for in-core measurements. A large size in-core detector would interfere with the reactor design and could produce a flux depression near the detector position. If the reactor core must be closely packed for high power density or if the core design prevents in-core installation, then the detector can be put outside the core with a corresponding loss in sensitivity. In any case the detector should be positioned such that there is no gamma-ray or neutron streaming to any accessible area along the instrument channel.

Because of the difficulties associated with the insertion and removal of any reactor in-core instruments, such a detector should have reasonable service life. This is determined by the burn-up characteristics of the detector and its susceptibility to radiation damage in the reactor environment.

Other factors to consider in designing a neutron detector are the chemical compatibility of the detector material to avoid a situation where the effect of high radiation field and high temperature may encourage undesirable chemical interactions between the detector material

and its surroundings and also within the detector itself. The device cost, the consequence and probability of failure, any corrections required to compensate for burnup, and the requirement for initial and periodic calibration must be considered as well (53).

At the present time, available in-core and out-of-core detectors in most thermal reactors work satisfactorily. In fast reactors many of these detectors would be expected to fail because of the more severe reactor environment. Existing detectors may also be insufficient to provide enough information needed for the safe operation of the fast reactor with the higher safety margin required. For this reason new or improved detectors will be needed.

Since many of the anticipated problems seem to be associated with the deterioration of the detector cable, a detector which does not use any cable in the core or close to the core and which is insensitive to intense gamma-ray fields and high temperatures may solve the problem. This is the target that we tried to achieve in this work through the design of a new detector which depends on transferring electrons in vacuum by magnetic focusing out of the core region into a remote region where they can be detected with less interference or without radiation-induced degradation.

# CHAPTER II

## REVIEW OF PRESENT NEUTRON FLUX DETECTORS IN REACTOR APPLICATIONS

The purpose of this chapter is to review critically the characteristics of previously available neutron flux detectors that have been proposed for nuclear reactor applications, their useful range of applications, and their limitations. The detectors reviewed include the fission chamber, boron chamber, self-powered detectors, neutron thermometers, activation foils, SiC semiconductor detector, Cerenkov detectors, microwave detectors, spark counters, secondary electrons detector, and gas scintillation detectors. The fission chamber is widely used now in thermal reactors and it is available commercially. It operates in the pulsed mode or integrated mode in the intermediate or full power range. The boron chamber has high sensitivity when operated in the individual pulse mode and usually is used during start-up. At high neutron flux it saturates very fast and usually is withdrawn from the reactor at a high power level. The self-powered detector is also widely used in the full power range of a thermal reactor though it is insensitive at low flux levels. Its slow response time makes it undesirable as a detector for reactor control. Neutron thermometers (neutron thermopiles) have been used in some places in the past and are still used in many reactors today during intermediate and full power ranges. Activation methods of detection have many useful applications in thermal reactors and in fast reactors at different power levels. The SiC semiconductor detector is still in the developmental

stage; in its present condition it fails at about $10^{16}$ nvt. The Cerenkov detectors are also in the developmental stage and the gas type detector seems to be promising. Microwave detectors also seem promising. These and other detectors will be reviewed critically in this chapter to indicate under what conditions a new detector may be needed to supplement existing technology.

## The Fission Chamber

### Basic Characteristics

The fission chamber (2,3,5-17) is a gas-filled chamber consisting of two electrodes between which high voltage is applied. The neutron-converters are fissionable materials deposited on one electrode. The charged fission fragments emitted when the detector is exposed to a neutron flux produce ionization in the gas. The positive ions and the electrons produced are collected by the two electrodes. Either individual pulses or integrated current are measured. The large amount of energy released per fission makes the detector very attractive in heavy gamma fields because the fission signals are easily detected. The most probable energy for the heavy fission fragment is 60.2 MeV, for the light fragments, 94.5 MeV. The cross sections in the thermal region for some fissionable materials are relatively high but drop drastically at higher energies. The fission fragments emerge at about $180^{o}$ with each other; therefore, usually only one fragment is responsible for the pulse in the pulse counter since only one fragment will dissipate its energy in the gas. The range of the fission fragments in $UO_2$ is about 10 $mg/cm^2$; therefore, the $UO_2$ thickness must be less than about 1-2 $mg/cm^2$. Since

the fission fragments carry a large charge, the ionization density is higher in the initial part of their path and decreases with distance traversed. As the energy of the fragment drops below the ionization potential of the gas, the fragment will lose the rest of its energy by elastic collisions.

All of the fissionable materials used (U, NP, Pu) are alpha emitters but this does not constitute an interfering problem since their half lives are very large and discrimination against alpha-induced pulses can be made. The alpha particle produces intense ionization close to the end of its path. The dimension and pressure of the chamber can be adjusted such that only a small portion of alpha particle ionization would contribute to the observed pulse.

The pulse height due to a single fission event is not constant due to a) the thickness of the fission material coating, b) the distribution in energy and the angle of ejection of the fragment, c) any nonuniformity of the foil thickness, d) possible cracks in the fissile material coating through which the fission fragment can pass more easily (which results in a high-energy pulse), and e) differences in the incident neutron energy in fast neutron reactions. Collimation of the fission fragment can be obtained by putting a perforated plate over the $UO_2$ coating; the overall efficiency will be reduced in this case, however.

To extend the lifetime of the fission detector a combination of fertile and fissile materials, e.g., $^{235}U$ and $^{238}U$ can be used (3,11). The right combination of these depends on the neutron flux and spectrum.

Use of the Fission Chamber for Reactor Neutron Flux Measurements

For thermal reactor flux measurements, fission chambers of different designs have been built by different designers. In most cases the chamber met the requirement of small size down to 1/4 inch in diameter (5-8). The filling pressure in the chamber is several atmospheres to reduce the volume. The reported sensitivity is usually around one count per second per unit flux for fission counters. The applied voltage should be such that the charges are collected rapidly but not so high as to increase the leakage current. Usually a few hundred volts are applied. The insulator in the chamber and the cable are typically $Al_2O_3$, MgO, fused quartz, $SiO_2$, or others. Xenon, argon, or other noble gases with a small percentage of polyatomic gas such as methane are used as the filling gases. Stainless steel (free of manganese) or titanium alloy make a good material for the electrodes.

The build up of fission product gases especially the xenon causes a decrease in the sensitivity with time (14).

Since the cables used between an in-core chamber and an external indicator are long, the capacitance associated with them is not negligible (30 ft of coaxial cable has a capacitance of more than 1000 pF). This tends to reduce the pulse height, decreasing the signal to noise ratio at the read out in the pulse chamber. A step-down pulse transformer (17) can be used at certain stages to improve pulse transfer; a transistor preamplifier (FET) of the type used in other detectors would be unsuitable in a reactor environment.

Other sources of interference in the chamber are due to:

1. the prompt gamma-rays in the reactor

2. induced gamma and beta activities in the chamber materials
3. fission product activity in the fission material coating
4. the fission product activity in the reactor core.

It would be expected that the response to the interfering activities is much less in helium-filled detectors. The reason is that the stopping power for the electrons varies with atomic number (A) and for fission fragments as $A^{1/3}$; therefore, the ionization from the interfering activities is reduced in helium compared with heavier gases (5). When the detector operates as an integrated-mode compensation chamber (6), all the interfering activities are eliminated except the activity of the fission fragment in the coating.

Other problems such as radiation effects on the polyatomic gases, residual surface impurities of the device, the welding of small size parts that might introduce impurities could also affect the properties of the chamber.

If the individual pulse rate is measured, then the interfering pulses from the gamma-ray background can be much reduced using the Campbelling technique of discrimination provided the gamma pulse rate is small compared to that of the neutrons. The Campbell theory states that the variance of the current from a source of random current pulse ($|\overline{I^2}| - |\overline{I}|^2$) is proportional to the average pulse rate and the square of the pulse height. Measuring the variance instead of the pulse rate will give good discrimination against gamma-rays. Details about the Campbelling technique are given in references 38-42.

For in-core or in-vessel use, especially in fast reactors, the higher temperature and greater radiation effects are two of the largest factors

reported that the noise pulses produced in the cable due to the gamma-ray field at high temperatures (> 400°F, 205°C) were similar to those due to neutrons, and hence discrimination against gamma-rays becomes very difficult. Roux et al. (23,24) have described a fission counter which operates at 750°F (450°C), and has a sensitivity of one count per second per unit flux at a gamma-ray intensity of $3 \times 10^6$ R/hr. The gas filling was 90% Ar + 10% $N_2$. The detector was operated at 400 V and gamma-shielded with tungsten and molybdenum; lead was rejected because it has a low melting point. Gooding (16) has described a chamber which operates at ~ 500°C inside a gas-cooled reactor and has a sensitivity of $5 \times 10^{-14}$ amp per unit flux. Hara (25) has reported that a fission counter for fast reactors with a short pulse-resolution time has been built. The detector could cover a wide monitoring range.

In conclusion, one can say that fission chambers and fission counters are used widely for continuous in-core flux measurement of thermal reactors. If operated as pulse chambers such detectors have the advantage of prompt response, good sensitivity, and fairly good discrimination against gamma-ray interference but may overload. In fast reactors the detectors fail to operate because of the following reasons:

1. In high temperature and high radiation fields the insulator and sealant deteriorate resulting in high leakage current especially with a high applied voltage.

2. When working as a pulse counter the gamma build-up pulses interfere with the neutron pulse.

3. Diffusion of impurities from the walls produces negative ions that tend to eliminate the pulse or reduce the pulse rate.

4. Deterioration of the uranium thin film coating.

Other problems that are shared with detectors for thermal reactors are:

5. The build-up of fission gases (especially xenon) produces a change in sensitivity with time.

6. Interfering signals from the decay of the fission products in the fission material coating.

7. The dissociation of polyatomic gases in high gamma-ray fields.

## Boron Detectors

### Basic Characteristics

Boron detectors ($BF_3$ gas filled or boron-lined) are gas-filled detectors which can be designed as ionization chambers of proportional counters. The reactions used are

$$\text{a)} \quad {}^{10}B + n \rightarrow {}^{7}Li + \alpha + 2.792 \text{ MeV}$$

or

$$\text{b)} \quad {}^{10}B + n \rightarrow {}^{7}Li^{*} + \alpha + 2.31 \text{ MeV}$$

and

$${}^{7}Li^{*} \rightarrow {}^{7}Li + 480 \text{ keV}$$

In 92% of the capture events of the thermal neutrons the 480 keV gammas are liberated, but for high-energy neutrons this percentage changes (e.g., at 2 MeV neutrons only 1/3 of the reactions go by process (b). The lifetime of ${}^{7}Li^{*}$ is $7.7 \times 10^{-14}$ sec. The cross section of the reaction for 2200 m/sec neutrons is 4010 barns and follows a 1/v law up to 30 keV. A large portion of the available energy is taken by alpha particles (~ 1.47 MeV) since they have a smaller mass. The boron is usually

enriched up to 96% of $^{10}B$ when used in such detectors. For neutrons above 5 MeV, other particles such as p, d, and t are emitted; however, the cross section for these reactions is comparatively small. Since the range of the 1.47 MeV alpha in boron is 0.78 mg/cm$^2$, the thickness of the boron therefore should be less than 0.7 mg/cm$^2$ in a boron lined detector.

Use of Boron Chamber for Reactor Neutron Flux Measurements

The effect of increasing the temperature on the $BF_3$ gas-filled detector has been studied by Lockwood et al. (44). A considerable shift in the pulse height distribution was found. The pulse height and the count rate dropped very fast. The effect was thought to be due to release of the electronegative impurities from the detector wall.

The effect of high counting rates in $BF_3$ counters was studied by Soberman and Korff (45). At ~ $10^6$ counts/min their detector deteriorated and did not recover for a long time even after increasing the voltage. This effect was thought to be due to the formation of negative fluoride ions produced by the dissociation of $BF_3$ gas under high flux conditions. Fluorine gas, which is highly electronegative, was found on analyzing the gas content after the neutron irradiation.

Milojevic, Kurepa, and Ribnikar (46) studied the effect of contamination materials such as $SiF_4$, HF, and NO on $BF_3$ counters. The results showed that even small traces of impurities could change the plateau characteristic.

When used as a pulse counter, the $BF_3$ chamber does not survive the high gamma intensity of the core where the buildup of gamma pulses causes large interference because the Q-value of the $^{10}B(n,\alpha)^7Li$ is not high. Abson et al. (47) have reported that the $BF_3$ counter can be operated in

a gamma field only up to 100-200 R/hr. For this reason and because of the temperature and large burn-up limitation, the $BF_3$ counter cannot be used for continuous in-core measurements. It tends to be used only during start up or shut down (48) where the detector is more sensitive than the fission counter, and it must be withdrawn at other times. The reported sensitivity (48) was five counts per second per unit flux for a six inch long, one inch diameter detector, filled at about 70 torr pressure.

When used as a pulse counter, the boron-lined counter shares the same problems of temperature and gamma-ray interference with the $BF_3$ counter. When used as an integrating chamber, compensation for gamma-rays can be made with an accuracy of about 1-2%. When put in the shield surrounding a thermal reactor it can be used for power monitoring and can be designed to cover about seven decades if a relatively large size chamber (8 inches long, 3 1/2 inches in diameter) is used (48). The large volume serves to increase the sensitivity. Roux (49) has increased the sensitivity by using a parallel-plate, multisection chamber with 0.1 cm separation between the parallel plates. In fast reactors the boron detectors cannot survive in the core or even close to the core because of rapid burnup.

## Self-Powered Detectors

### Basic Characteristics

The self-powered detector (50-68) was first described by Hilborn (50) based on an idea presented by Mikelman, Erofeev, and Rozenblyum (51) in 1961. The detector has received much attention and has found wide application, especially for in-core instrumentation. Good reviews on the

subject have been presented by Hilborn (30), Loosemore and Knill (52), Boland (53), Stevens (54), Worsham and Ball (55), and Hawkings (66).

The neutron-sensitive self-powered detector consists of a metallic central emitter, an insulator, and a coaxial collector. The central emitter emits an electron after absorbing a neutron. The electron penetrates the insulator and will leave the emitter positively charged; accordingly, there will be a potential difference between the collector and the emitter, and when an ammeter is connected between the two, a small current will flow.

It is not necessary that all the electrons are terminated in the collector (which is usually grounded). It is only important that the electrons leave the emitter. The purpose of the collector is to protect the insulator and the emitter from environmental electrical and other interference and to provide a return current path.

Three types of emitter-collector combinations have been used:

a. Emitters which have a large cross section for the reaction $(n,\gamma)$ followed by beta decay with a collector that has a small cross section for the same reaction. The activated emitter should decay by beta emission with a very short half life. The response of this kind of detector is not prompt because of the decay half life. Emitter material such as $^{103}Rh$, $^{51}V$, $^{107,109}Ag$, $^{55}Mn$, $^{235}U$, and $^{238}U$ can be used.

b. Emitters which undergo electron conversion after neutron absorption with a collector that has a small cross section for this reaction. Emitter materials such as $^{113}Cd$, $^{149}Sm$, $^{155,157}Gd$, $^{164}Dy$, and $^{199}Hg$ are of this type.

c. Emitters which undergo pure (n,γ) reactions. The emitted gamma photon ionizes target atoms by the photoelectric and Compton effects. An emitter of high-Z material and a collector of low-Z material should be used where the difference in gamma ionization causes a current to flow. Emitter materials such as cobalt and Zircaloy can be used in this case.

The insulator between the emitter and the collector should withstand high temperatures, high radiation intensities, and have a small neutron absorption cross section. Three types of insulators are usually considered. These are $Al_2O_3$, MgO, and BeO. Both Al and Mg emit betas after activation by neutrons, but the cross sections are very small; and they are preferred over BeO which is both toxic and relatively costly. Other possible insulators are thoria, zirconia, or quartz.

The collector should also have a low beta activation cross section. It should be compatible with the surrounding materials, be stable in the reactor core, and provide good electric shielding. Usually Inconel sheath is used. Stainless steel type 304 could be used, but it contains some manganese which undergoes an (n,γ) reaction. Nichrome has also been used in some earlier detectors.

Use of Self-Powered Detectors for Reactor Neutron Flux Measurements

When used for in-core measurements one of the problems of the beta-emitter self-powered detector is its time response which depends on the half life of the emitter. In experiments performed by Loosemore and Knill (52) a rhodium detector reached 90% of its final value in a constant flux in 2.5 minutes and 99% in 11 minutes. A vanadium detector should reach 90% of its steady value in 12.5 minutes.

Another problem is the relatively small sensitivity. The sensitiv-

ity depends on several factors such as the cross section, the half life of the emitter, and the size and geometry of the detector. Cylindrical geometry is usually used with an outside diameter of about 1-2 mm. The sensitivity of commercially available Rh detectors is about $0.23 \times 10^{-21}$ amp/nv·cm and that for V detectors is about $7.7 \times 10^{-23}$ amp/nv·cm (53). Since the emitter materials are sensitive to thermal, epithermal, and fast neutrons the detector will give different readings if the neutron spectrum changes; therefore, each detector has to be calibrated in the particular reactor spectrum.

Other materials close to the detector location can affect the reading of the detector. Baldwin and Rogers (59) measured the effect of shielding materials on the detector background. The detector gave different signals in different types of shielding.

The difficulties in producing a detector of uniform sensitivity per unit length were demonstrated in an experiment by Strindehag and Söderlund (60). They measured the sensitivity of two Rh self-powered detectors, each 3.3 meters long. Ten cm of the detector only was exposed to the neutron flux at a time and the rest of the detector was covered by boron plastic. A maximum variation of 4% from the average value was observed.

The largest problem of the self-powered detector is its sensitivity to gamma-ray fluxes. Electrons from the insulator and the collector reach the emitter and produce a negative current. Since a long cable is usually associated with this detector the gamma-ray effect in producing a negative charge in the central conductor can overcome or cancel the signal

current. This is the main reason for the failure of the detector in fast reactors (62). Most applications of the self-powered detectors are for in-core thermal reactors (52,55,59,63) in fields up to $10^{15}$ $n/cm^2$-sec(62). A good improvement for fast neutron measurements has been made by Mochizuki et al. (65) who compensated for the gamma signal by using two emitters of close (Z) material: one sensitive to neutrons and the other not. Combinations such as Rh-Pd, Rh-Mo, or V-Ni can be used. Besides this transient gamma effect the beta activation of the sheath and the insulator may also create negative signals due either to any impurity in the material or due to the activation in the material itself.

The effect of an increase in temperature and radiation damage is less important. Although they cause a change in the resistivity of the insulator the voltage across it is so small that only negligible leakage current will occur.

Price and Karvinen (61) reported that the resistance of MgO and $Al_2O_3$ showed a decrease during start up and recovered after some time under continuous irradiation. The background signal in the cable is also affected by the material (such as fissionable materials) adjacent to the cable.

Compensation for cable noise can be obtained by running a cable of the same length without the emitter in a balanced array. Another way of compensation is to use two internal lead wires with only one of them connected to the emitter. The latter kind of compensation has been found to be inaccurate, as different compensation currents were found when the cable was rotated around its axis. This is probably due to a change of the adjacent materials close to each internal wire. When the inner

conductors were spiraled around each other with a pitch of 2 cm, a better compensation was obtained.

The advantages of the self-powered detectors are their ruggedness, small size, moderately low cost, and relative low burn-up rate. In fast reactors the detector failed to operate satisfactorily because of:

1. Large noise to signal ratio due to gamma-ray and other sources of interference such as activation in the insulator, the sheath of the detector, and the cable.

2. Insensitivity to small flux changes especially for fast neutrons where the detector cross section is small.

3. The slow time response due to the particular half life of the excited emitter.

## Neutron Thermopile Detectors

### Basic Characteristics

This detector measures the temperature rise in a neutron-converter material when exposed to the neutron flux. The temperature rise is calibrated for neutron flux. It consists of several thermocouple junctions where alternative junctions are surrounded by a neutron converter. Neutron interactions such as (n,$\alpha$), (n,p), or (n,fission) increase the temperature in the neutron sensitive junction when the secondary particle is stopped in the material and, therefore, will develop an emf between the hot and the cold junctions. The emf can be calibrated for the neutron flux. A detailed theoretical treatment is given in references 69 and 70.

In this detector at lower temperatures the loss of heat due to thermal radiation is very small compared to the heat loss by conduction

and the effect of the ambient temperature is negligible if the thermal conductivities and the heat transfer coefficients of the detector materials remain constant, which may not be the case in reactor measurements. The thermal conductivities of most materials vary with temperature and with time due to the radiation damage. The heat transfer coefficient depends on factors such as the mass velocity of the fluid flowing by the detector, the hydraulic diameter through which the fluid is flowing, the heat capacity of the fluid, the viscosity of the fluid, and the thermal conductivity of the fluid. Therefore, it might change with time and position. At high temperatures the heat transfer by radiation becomes more effective. The response of the detector depends on the thermal conductivity k, the density $\rho$, the specific heat $C_p$, the radius of the detector, and on the difference between the initial temperature $T_i$ and the ambient temperature $T_A$. A graph of $(T_A-T)/(T_A-T_I)$ on a log scale against $(kt)/(\rho C_p r^2)$ on ordinary scale will be a straight line with negative slope where T is the temperature at any time t following an abrupt power decrease.

The Detector Application for Reactor Neutron Flux Measurements

The early designers of the thermopile used boron as the neutron-converter (71-77) and chromel-alumel, chromel-copper, and platinum-molybdenum thermocouples. Lapsley (72) used a 10-unit thermopile and reported a sensitivity of 1 mV at $10^{11}$ n/cm$^2$-sec thermal. Labro et al. (74) used 36 units with 1 mm diameter boron at alternate junctions 20 mm apart. The detector response was linear up to ~ $10^{12}$ n/cm$^2$-sec and saturated at higher fluxes. The saturation is due to the heat loss by thermal radiation. The response time of the detector was 10 seconds. A

boron-10 detector which operated at 510°F (265°C) at a neutron fluence up to $10^{19}$ nvt, for a neutron flux of $5 \times 10^{12}$ - $2 \times 10^{14}$ without failure has been reported (77). The response time of the detector was 70 msec.

When fission materials are used for the neutron-converter the detector has a higher sensitivity, especially at low fluxes, less burn-up due to the smaller absorption cross section than boron, however $^{239}Pu$ will be produced. Such a detector also had faster response time. Herold (78) has described a fission detector (fission couple) which was linear up to a flux of $5 \times 10^{11}$ $n/cm^2$-sec and has a response time of a few seconds. Lapsley (79) reported a transient time of the order of 0.5 minute and expected the gamma heating to be approximately 1% and the beta heating 3% of the fission heating. Guskov and Zvonarev (80) used $U_3O_8$, 75% $^{235}U$ enriched, uranium powder at one junction and $Pb_3O_8$ powder of the same amount (50 mg) on the other to compensate for the gamma heating since the two materials have very close atomic numbers Z. A uranium-tungsten pair was used by Morrison (81) for compensation. For complete compensation the two materials used should have the same specific heat, thermal conductivity, and heat transfer coefficients.

At high temperature (> 200°C) a chemical effect becomes significant and the oxidation of the thermocouple may change its properties. Surrounding the detector by inert gas will prevent this effect. Helium gas has been used (82) and enables the detector to operate at very high temperature. DuBridge (83) used argon gas and reported that the detector can operate at 1800°F (982°C). Kinzer (84) welded a cap over the detector and filled the space with argon gas to impede the heat transfer as well.

Extensive study on the fission couple for burst reactors was made by Morrison (85,86,87) for mapping purposes. The detector developed has chromel-constantan or chromel-alumel thermocouples; tungsten was used for compensation. The fissile and compensation materials had a spherical bead shape. The minimum dimension of the bead is limited by the fission fragment range in the material while the maximum dimension is limited by the self shielding of the material, especially in a thermal flux where the outer surface will have a higher temperature. The effect of thermocouple wire radius was also studied. The measured difference in temperature for 1 mil and 1/2 mil is the same, but is less the larger diameter thermocouples. Therefore, a four-lead thermocouple consisting of two one-half mil constantan, and two one-half mil chromel wires was suggested to give better support. Typical sensitivity of the detector was about $10^9$ $n/cm^2$-$^oC$. The time response reported was of the order of 15 microseconds (87). The length of the assembly varied from 4 to 18 inches (10-45 cm) and it was concluded that chromel-constantan are the most compatible materials for a fission couple.

An improved thermocouple detector which depends on the heat flow in a heat conductor proved to have better properties (94-97). The detector consisted of neutron sensitive materials, a thermal path for the heat to flow through, and a heat sink. The two junctions of the same thermocouple are put at two different points of the thermal conducting materials where a temperature difference is expected, or instead, two thermocouples are used. Mins (94) suggested that the coolant be used as the heat sink of the detector and that copper makes a good heat conducting material. Gee (96) built a detector of sensing-element dimensions

1/8" x 1/2" x 1" which has a 25-msec response time. The detector has a linear response with power but the output tended to decrease with time at constant power level and even gave a negative signal during the last stage of the shutdown. It was suspected that the silver bond between the thermocouple and the thermal conducting material was responsible for that behavior and that a gas enters the bonding and acts as a large heat resistance. Because of the complicated construction method, each detector must be calibrated separately. Azari et al. (97) gave a detailed theoretical treatment of this detector using an electrical analog. Two detectors (neutron and gamma) were built to measure the flux in a nuclear propulsion reactor. The response time was 80 seconds for the gamma detector and 95 seconds for the neutron detector.

Both $^{10}B$ and the fission couple have the severe limitation of burn-up as well as having different sensitivities at different neutron energies. Eichholz (98) used the reaction $^{14}N(n,p)^{14}C$. The reaction cross section at thermal neutron is 1.81 b and varies slowly with the neutron energy. This property eliminates the burn-up problem and the problem of change of sensitivity with neutron energy. Most ceramic nitrogen compounds have high melting points and are compatible with reactor materials and stable under radiation damage (such as SiN, AlN, TiN). The materials have a small Z which makes the gamma heating negligible.

Other detectors which depend on the heat properties can be included in this section. These consist of two resistances which are sensitive to a substantial change in temperature. One of them is either surrounded by or contains neutron-converter such that its temperature will increase when

exposed to the neutron flux and hence changes the resistance value with respect to the other resistance which does not contain a neutron converter. Bloom (99) has suggested the use of intrinsic or doped boron resistances, one enriched by $^{10}B$ and the other not. The intrinsic resistivity changes from $10^{-3}$ to $10^{6}$ ohm-cm when the temperature changes from room temperature to 2000°C. However, the resistance-temperature curve might change under high radiation effects or with time.

The thermopile detector has several advantages such as small size, ruggedness, ease of construction, relatively good sensitivity, reasonable linearity with thermal flux (up to ~ $10^{14}$ $n/cm^2$-sec), and reasonable lifetime. In fast reactors the possible reasons of detector failure are:

1. The high temperature may promote the oxidation of the detector material which would change its properties, the welding of the different parts may break down due to the different thermal linear expansion, and the detector signal will not be linear due to the heat losses by thermal radiation.

2. Large interfering signal from the gamma radiation effect on the cable similar to that encountered for the self-powered detector.

3. The thermal conductivities of the detector materials will change with time due to radiation damage and elevated temperature and hence differences in signal and time responses will result.

Besides the above reasons the detector may give rise to an interfering signal from the fission products if a fissionable neutron-sensitive material is used.

## Neutron Detection by Induced Radioactivity

### Basic Characteristics (100,111,147-149)

If an activable material is exposed to a neutron flux, secondary radiative decay may result. If R is the reaction rate, then

$$R = \int_V \int_E N(x,y,z)\ \sigma_a(E)\ \Phi(x,y,z)dE\ dxdydz$$

where

$N(x,y,z)$ is the particle concentration of the target at point $(x,y,z)$

$\Phi(x,y,z,E)$ is the differential neutron flux

$\sigma_a(E)$ is the activation cross section at neutron energy E. If $\Phi(x,y,z,E)$ is uniform across the detector, then at a given location

$$R = N_T \int_E \sigma(E)\ \Phi(E)dE$$

where $N_T$ is the total number of target atoms in the detector. The rate of change of the radioactive atoms N' is given by

$$\frac{dN'}{dt} = R - N'\lambda$$

where $\lambda$ is the disintegration constant of the product nuclide.

If R is constant (this means the neutron flux is constant) and $N_T$ is constant (low burnup), then the activity A is given by

$$A = \lambda N' = R(1-e^{\lambda t_0}) = A_s(1-e^{-\lambda t_0})$$

where

$t_0$ is the time of irradiation

$A_s$ is the saturation activity

To find the percentage of the counts that are due to fast neutron the detector is covered by cadmium, to absorb the thermal neutrons, and the activity of the foil is measured again. The fact that Cd is not totally transparent to epithermal neutrons makes it necessary to correct the measured value of the activity by multiplying by the correction factor, $F_{Cd}$, defined as

$$F_{Cd} = \frac{A_s \text{ (epithermal)}}{A_s \text{ (Cd covered)}}$$

Such corrections were studied experimentally in references 102 and 117-119. A good estimate of $F_{Cd}$ is found in reference 119.

Corrections must be made also for the perturbation caused by the foil in diffusing medium if the cross section of the foil material is high. The perturbation is due to (a) flux depression due to the absorption of the neutrons by the foil or (b) self shielding of the interior layers of the foil. Such corrections have been studied experimentally and have been discussed in references 103-108 and theoretically in references 109-111.

A standard method as well as good review of foil detection in thermal neutron fluxes is given in ASTM E263-70 (120).

In measuring the activity of the foils a beta self-absorption correction also has to be made. This correction is discussed in references 112-116.

Resonance detectors are used in the intermediate energy range. For a Cd covered detector the saturation activity is

$$A_s(Cd) = N_T \int_{E_c}^{\infty} \sigma_{1/v}(E)\ \Phi(E)dE + N_T \int_{E_c}^{\infty} \sigma_{res}(E)\ \Phi(E)dE$$

where $\sigma_a = \sigma_{1/v} + \sigma_{res}$ and $E_c$ = Cd cut-off energy.

Corrections for self shielding, for Doppler broadening of the resonance, and for flux depression must be included for thick detectors.

Threshold detectors are widely used in measuring fast neutrons. In these detectors the activation cross section is assumed to have a step function at an energy $E_s$. The saturation activity will be

$$A_s = N_T \sigma_a(E_s) \int_{E_s}^{\infty} \Phi(E)dE$$

The cross section $\sigma_a(E_s)$ is assumed to be zero below $E_s$ and constant at and above $E_s$. $E_s$ is defined such that

$$\int_0^{\infty} \sigma_a(E)\ \Phi(E)dE = \sigma(E_s) \int_{E_s}^{\infty} \Phi(E)dE$$

Accurate knowledge of the neutron spectrum is very important as the value $\sigma_a(E_s)$ depends strongly on the spectrum which in many cases is complicated.

A standard method for measuring fast neutrons is given in references 121-126.

Use of Foil Detectors for Reactor Neutron Flux Measurement

When foils are used for measurements in-core, special equipment is needed for inserting the foil in and out of the core. For wire activations, one end of the wire is connected to a drive cable. The wire and the cable slide inside a conduit. The conduit should be designed such that minimum friction occurs between the foil and cable and the conduit to avoid stretching or kinking the wire. In some cases special Teflon lining is provided to reduce the friction. Wiesemann and Ehrenpreis (127) have suggested the use of balls or pellets of any suitable shape that are transported through the conduit by gravity or by means of fluid such as air. Hatcher (128) has described a method for measuring each probe separately using a control unit. Spaa et al. (129) have suggested the use of a gas that passes through a chamber made of Al that is put in or very close to the core. When the gas leaves through a duct, its activity is measured by a counter. Knapp (130) measured the flux in an EBWR reactor with pellet activation and gave descriptions of the shape of the conduit used. Inconel was used for the material of the duct and the foil was made of a ceramic or alloy.

Sardina et al. (132) have described a method for measuring thermal neutrons which is insensitive to epithermal neutrons. In this method two isotopes are produced by successive neutron capture:

$$A + n \rightarrow B^{*}$$

$$B^{*} + n \rightarrow C^{*}$$

The activity of C depends on $\Phi^2$ while the activity of B depends on $\Phi$. The same method was treated in detail by M. R. Melendez (133) and experimental measurements of the activities of the induced isotopes ($^{165}$Dy - $^{166}$Dy) were made. Combinations of thermal foils and fast foils for measuring thermal and fast neutrons have been used. Detailed descriptions and formulations of the two detector method have been given by Papastergiou and Swanks (134). Fritzen and Jester (135) used 0.15% copper for thermal neutrons and high purity Al for fast neutrons. Page et al. (136) measured the fission distribution using $^{238}$U and $^{235}$U fission foils in EFBR. Köhler (137) measured the fast flux using $^{237}$Np and $^{232}$Th fission; the activity of $^{140}$Ba was utilized. McCune (138) used $^{232}$Th utilizing the activity of $^{137}$Cs after long-time irradiation. Withop et al. (139) measured the flux in EBR-II using $^{58}$Ni and $^{54}$Fe. They reported a difference of 60% from the flux measured in the same channels by ANL staff. The difference was interpreted as inaccurate measurements of the fast neutron spectrum by ANL staff. Page and Horne (140) measured the fast capture rate in $^{238}$U by utilizing the 100 keV gamma of $^{239}$Np.

The foil detector should withstand the core environment such as the high temperature and radiation effect and should have good corrosion resistance and compatibility with adjacent materials. Since many foils are usually required, the method of fabrication should be economic and they should be prepared in high purity. Hins (141) described a foil method for high temperature use by inserting the metal between two metal oxides. Ulseth, Jackson, and Combs (142) also described preparation of the foil and encapsulation material in the right chemical compounds.

The activity in the coolant in water cooled reactors can also be used as an indication of the reactor power (143). The activity of $^{16}N$ from the reaction $^{16}O(n,p)^{16}N$ can be used for this purpose. The reaction has a 9 MeV threshold and emits a 7.1 second gamma photon. The activity can be suitably measured by a scintillation detector (144) or by a silicon detector (145). Scott and Notea (146) have measured the delayed neutron from $^{17}N$ in the coolant using a $BF_3$ counter.

The foil detector has the advantage of being insensitive to gamma fields, it has a small size, and a choice of different detectors can be made for different energy ranges. The detector is unsuitable for fast reactors for the following reasons:

1. There is a delay in response time associated with the result evaluation and with the half life of the detector.

2. The detector is basically an integrating device and insensitive to minor flux variations during irradiation.

3. Special attention must be paid to the neutron spectrum which may be very difficult to measure.

## SiC Semiconductor Detectors (155-166)

The small size of this semiconductor makes it attractive for in-core measurement where many detectors could be used and the average power as well as the localized flux could be measured if a suitable material can be found.

It is well known that semiconductors are particularly susceptible to radiation damage and semiconductor devices in general are unsuitable for service in a high-level radiation environment. However, some studies

have been done on the possible use of some wide-gap semiconductors to serve as radiation-indicating diodes. One such material is silicon carbide. It has many desirable properties for in-core or close-to-the-core measurements. The band gap is about 2.9 eV (compared with 1.12 in Si and 0.72 in Ge) and its high melting point makes it stable in high temperature environments. A high concentration of carriers makes it more stable under radiation damage than pure Si, since radiation removes carriers by introducing traps in the forbidden band. The life time in SiC is 100 times larger than that in Si under the same irradiation conditions. Detectors have been developed to meet conditions of the core environment (155-159). The detector junction is made by diffusion using aluminum as the dopant (acceptor) diffused at temperatures above 1600°C into SiC which had previously been made n-type by introducing nitrogen impurities. The junction is made thin to permit the electrons and holes produced to be collected. In thick layers the recombination probability will increase and, therefore, the minority carrier lifetime decreases. The thickness of the depletion layer has to be sufficient to stop the fission fragments and alpha particles. A thin layer of $^{235}U$ is deposited on the surface to act as a converter. Such a detector has 100% efficiency for alpha particles and fission fragments and can operate very well at temperatures up to 800°C. No bias voltage is required (155). The observed resolution was poor compared with Si detectors when both detectors operate at low temperature. This poor resolution is due to the nonuniformity of the dead layer, a nonuniform depletion region, the relatively high energy required for electron-hole production (~ 10 eV), the low charge collection effi-

ciency, and the high noise level. The problem of making electrical contact was of major concern since the contact must be sufficiently small so it will not interfere with the counting process but still remain ohmic. The contact should be stable under the differential thermal expansion of the different parts of the system.

The detector was not expected to be stable under high integrated flux conditions and annealing of the detector (at ~ 1300°C) was suggested. All detector components such as the electrical contact must be stable at this temperature. Further study and development are needed to improve the junction, improve the surface stability at high temperature, develop a technique for uranium converter deposition, improve device encapsulation, and for development of the associated system such as the cables, the holders, etc. Babcock (162) has summarized the radiation effects on SiC and on SiC junction detectors. Under fast neutron irradiation ($E_n > 1$ keV) the estimated carrier removal is 2 carriers/cm$^3$ comparable to that of Si. The ability of SiC rectifiers to tolerate high initial carrier concentrations is the cause of their superiority. When irradiated by 2 MeV electrons at 25°C and 36 volt bias the charge collection efficiency dropped to half its original value after exposure to $1.2 \times 10^{16}$ electrons/cm$^2$. When irradiated by 2 MeV protons the collection efficiency decreased several times when exposed to less than $10^4$ protons/cm$^2$. Under fast neutron irradiation the detector is expected to function reasonably up to ~ $5 \times 10^{16}$ nvt. The main reason for the detector failure is the rapid deterioration of the coating under irradiation from fission fragments and fast neutrons. The irradiation effect is very complicated (161,162) but in general atomic displacement by elastic collisions will

produce vacancies and interstitials which will generate traps and recombination centers in the forbidden gap. The relative damage depends on the positions of these levels in the gap. Another effect of neutron irradiation is the capture of a neutron followed by beta decay. This will produce a donor atom. This damage is quite small compared to the first effect. In p-n junction detectors irradiation will reduce the pulse height, increase the pulse rise time, and increase the noise level.

Epstein and Ferber (163,164) have used a $^{238}U$ coating to make the detector sensitive to fast neutrons. The detector showed good fission resolution without using a bias voltage and the pulse height of the fission fragments was not reduced more than a few percent by a gamma field of $2 \times 10^5$ R/hr. The charge collection efficiency was fairly insensitive to the temperature.

From the above study we can conclude that the SiC detector has a limited life for in-core measurement of fast and thermal neutrons. The detector can operate reasonably at high temperatures (~ 700-800°C) but the radiation damage due to the fission fragments and the fast neutron is the reason for limiting the detector life. At ~ $10^{16}$ nvt annealing is necessary at ~ 1300°C, but this creates the problem of damaging the detector components such as the electrical contact. For this reason such detectors may be considered insufficiently advanced at this time to provide a practical alternative in-core flux detector.

## Cerenkov Detectors

### Basic Characteristics

When a charge particle passes through a medium it will polarize the nearby molecules which will behave as excited dipoles. If the particle is moving relatively slowly, the dipoles will be symmetric around the path and the resultant electric field will be zero at a large distance but when the particle moves very fast at speeds comparable to the speed of light, the dipoles will not be symmetric around the path and the resultant electric field is not zero at a great distance. Each dipole will emit electromagnetic pulses when it returns to its normal state. The radiation from the different elements will interfere destructively unless the particle has a velocity in the medium greater than the velocity of the light in that medium. In this case a constructive interference will result at a certain angle $\theta$ where

$$\cos\theta = \frac{1}{n\beta}$$

where n is the refractive index of the medium and $\beta$ is the ratio of the particle velocity to the velocity of light in vacuum.

From the above equation it follows that

1. The threshold velocity below which no radiation is observed occurs when $\beta = 1/n$.

2. The maximum angle of light emission for ultra-relativistic particles ($\beta=1$) is $\theta_{max} = \cos^{-1}(1/n)$.

3. The emitted light is in the visible or near visible region where $n > 1$. X-ray emission is impossible since $n < 1$.

Two conditions have to be fulfilled to get Cerenkov radiation:

1. The path length of the particle must be large compared to the wavelength of the light $\lambda$, otherwise diffraction becomes dominant.

2. The velocity of the particle must be almost constant during a track length of several $\lambda$.

A good review on this subject has been given by Moyer (169).

Use of Cerenkov Detectors for Reaction Neutron Flux Measurements

The threshold energy for an electron to produce Cerenkov radiation in water is 0.260 MeV. Therefore, the electrons in the water resulting either from gamma interaction or from the decay of the fission products will produce Cerenkov light. This phenomenon has been used to measure the power in a reactor (170-173). Some beta emitter fission products whose beta energy lies above the threshold can also be detected in the water coolant in this way (174-180).

The advantages of the use of the Cerenkov effect in water are the disappearance of the burn-up problems associated with most other neutron detectors, and the avoidance of cable and detector radiation damage. Such a detector does not disturb the neutron flux and has very good sensitivity. The main disadvantage of the Cerenkov water detector which limits its application for continuous power measurement is the inability to differentiate between the prompt fission gammas and the activities from the decay of the fission products and the practical difficulties in bringing out the light signal to a field-free region. Other disadvantages are

the change of the detector response with temperature changes due to the change in the density of the water, the large associated electronic equipment, and the possible error from gamma radiation that may enter the photomultiplier directly, causing ionization, or from stray light reaching the photocathode from sources other than the Cerenkov light. A solid medium instead of water, such as quartz, has been suggested but radiation damage and the high temperature will highly affect the transparency.

To solve the problem of the inability of the detector to distinguish between fission and decay gamma-rays, a Cerenkov detector that consists of a gas instead of water as the radiator has been suggested (181,182). Since Cerenkov threshold properties depend on the refractive index of the medium which in turn depends on the density of the medium, the pressure of the gas can be adjusted to emit Cerenkov light due to electrons resulting from fission gammas and not produce light due to the less energetic electrons from gamma decay. The gas must be chosen such that it will not emit scintillation light and has a clear threshold. Ethane and methane were found to have good threshold properties while in other gases such as noble gases and nitrogen the scintillation light emission is so intense that the threshold is not clearly defined at all.

The advantages of the gas-radiator Cerenkov detector are the same as those with the water radiator. In addition, it has some capability to distinguish between the fission gamma rays and the decay gamma rays. The detector is expected to have some disadvantages when put into operation. It is obvious that the detector has a large background of scintillation light due to different interacting betas or photons (including the

decay gamma). It is also sensitive to any β-particle which has an energy above the threshold energy. It is unable to detect a high localized neutron flux which is the main reason for in-core measurements. The radiation effects are expected to change the properties of the light pipe that has to be located in or close to the core. For these reasons Cerenkov detectors are not considered viable as in-core radiation detectors at this time.

## Microwave Detectors

Two kinds of neutron detectors utilize microwave phenomena. In the first detector (183) a microwave frequency-modulated signal generated by a klystron is allowed to pass through a waveguide to a gas chamber situated in the reactor core and separated from the waveguide by a window which allows the microwave to pass through but prevents the gas from leaking into the waveguide. The neutrons interact with the gas molecules giving an ionized product which has strong resonance absorption on the microwave spectrum and therefore will attenuate the microwave frequency over a portion of the bandwidth. The attenuation is proportional to the number of transmutation products. Reactions such as $^{14}N(n,p)^{14}C$ will form $CO_2$ in the presence of oxygen which has a spectrum line approximately 25 MHz in width at a frequency of approximately 23,250 MHZ.

In this detector the gas is continuously circulated in and out of the chamber in order to avoid the accumulation of the transmutation products.

Such a detector is expected to be completely insensitive to the gamma radiation; on the other hand, it has several disadvantages. The

gas has to be kept at constant pressure which is not easy to maintain due to variation of the temperature in the reactor. A constant supply of the gas has to be maintained as well. The activated outlet gas has to be controlled and should not be allowed to escape to the atmosphere. Constant proportions of two or more gases and a constant rate of flow have to be maintained all the time.

Another type of microwave detector has been described by Brown et al. (184-188). In this detector a microwave cavity is filled with helium-3 gas. Microwaves from a signal generator are allowed to pass through an evacuated waveguide to the cavity. Another waveguide is attached to the cavity connected to a microwave detector. When the cavity is exposed to the neutron flux the (n,p) reaction will produce a plasma in the gas. Free electrons are produced by the primary and secondary ionization processes and will change the effective permittivity of the gas and therefore the resonance frequency of the cavity. The observed change in the frequency is a good indication of the neutron flux.

The resonance frequency ($f_s$) dependence on the dielectric constant $\epsilon$ is governed by the relation

$$f_s^2 = k/\epsilon$$

where k is determined by the dimensions and the geometry of the cavity.

The change in the angular frequency $\omega$ can be expressed by the relation

$$\frac{2\Delta\omega}{\omega} = \frac{\omega_p^2/\omega^2}{1 + \frac{\nu^2}{\omega^2}}$$

where

$$\omega_p = \frac{n'e^2}{m\varepsilon_0}$$

$n'$ = free electron density

$e$ = electronic charge

$m$ = electron mass

$\varepsilon_0$ = dielectric constant before the plasma is set up

$\nu$ = collision frequency for momentum transfer

Therefore, $\omega$ changes with $n'$ which in turn changes with the neutron flux. Also, $n'$ is affected by factors such as the attachment and the recombination of ions.

A change in the temperature $\Delta T$ will change the dimensions of the cavity and therefore its resonance frequency. The new frequency f is

$$f_{(T)} = \frac{f_0}{1 + k\Delta T}$$

where $f_0$ is the frequency before the temperature changes.

Since the thermal cross section for $^3He\ (n,p)\ ^3H$ is very large (5900 b), the effect of gamma rays is quite small.

To test the usefulness of a microwave detector as a flux monitor, a cavity of 0.7 cm radius and 0.895 cm long, filled by $^3He$ gas at 0.7

atm (530 torr) was used (184). The cavity and the waveguides were contained in an aluminum tube, sealed to keep the reactor coolant from entering. The waveguides were kept in vacuum to avoid any attenuation of the waves. Alumina metalized ceramic can be used as a thin window to the cavity which will allow the wave to enter the cavity and prevent the release of the gas.

This detector is reasonably insensitive to the gamma-ray field and has a very good time response (a few milliseconds). On the other hand, the problem of burn-up is severe. The signal is nonlinear with the flux and has a humped, unexplained behavior. It is also sensitive to temperature variations and to gas contamination. Radiation damage will also change the properties of the cavity seal with time.

## Spark Counters

Corrugated-plate spark counters for neutron detection have been described by Eichholz (167,168). The principle of the detector depends on the localized spark discharge created between two wires or just a wire or a conducting wedge parallel to a flat plate kept at high potential difference when a charged particle passes through. Slotted boron nitride was placed between the ridges as the neutron converter, where the alpha particles created by neutron irradiation initiates the discharge. The magnitude of the spark depends on the electrode gap spacing, the applied voltage, the type and pressure of the gas, and the circuit time constant. The sensitivity depends on the converter-gap geometry and on the number of the spark gaps.

A detector a few centimeters long, made of compact stainless steel

filled with pure argon gas was used. The detector operated linearly up to $10^8$ n/cm$^2$-sec when put in the beam hole at the face of the Georgia Tech Research Reactor. The sensitivity observed was $6.7 \times 10^{-8}$ counts per incident neutron. The detector was not able to operate normally above $10^{10}$ n/cm$^2$-sec when put inside the reactor due to the high gamma field which generates a steady current due to the ionization. The effect of increased temperature does not change the sensitivity appreciably, but the required voltage decreases. It was concluded that the detector can operate up to ~ 500°C and provide good discrimination against gamma rays and background in neutron flux up to ~ $10^{10}$ n/cm$^2$-sec and in gamma fields up to 500 R/hr.

The detector has good sensitivity and could be used during start-up or shut down of the reactor. Its sensitivity to high gamma flux and the high applied voltage which increases the leakage current prevent its use for continuous monitoring inside fast and thermal reactors.

## Detectors Employing Radiation Elements and Secondary Electrons (189-194)

The radiation element consists of two electrodes that are electrically insulated. One of them is coated by a neutron converter and the other is not, and the space between them is evacuated.

After neutron irradiation, positive charged particles created, such as the alpha particle in a (n,$\alpha$) reaction or the fission fragment in a (n,fission) reaction, and will be emitted from the neutron converter ejecting additional secondary electrons. When both the positive charged particles and the secondary electrons reach the second electrode they

make it negatively charged. If an ammeter is connected between the two electrodes, a current will flow in the circuit. The detector works with or without an applied voltage, though an external voltage is preferable to prevent space charge formation. Compensation for gamma signals and other interfering reactions can be made by making an identical chamber without the neutron-sensitive material so that the difference in the current between the two chambers will be due to the neutron flux alone. The sensitivity reported by a General Electric group is $1.3 \times 10^{-20}$ A/nv-cm$^2$ for boron and fission detectors, respectively, in a thermal flux (190). Fujii and Suita (191) filled the chamber with low-pressure gases such as argon or carbon dioxide at approximately 200 torr. The polarity showed strong dependence on the pressure and the gas used. Wilson (195) described a device which had $^{235}U$ emitter material. The current in the external circuit was due to the beta activity from the fission product rather than from secondary ionization. Ohmart (196) used two electrochemically dissimilar metals separated by an ionizable gas. The electrons produced in the gas by irradiation flow to the electrode which is more active chemically without an external applied voltage. The two electrodes could be aluminum and Teflon. The system was not very efficient. Linden (197) built a detector where the neutron-sensitive material was covered by a material such as MgO or $SiO_2$. The secondary electrons produced in this thin layer are attracted through an evacuated space to the collecting electrode by an applied field. Another type of detector was described that applied the same geometry but the electrons were ejected by the self-heating of the emitter rather than by ionization (198); this

is called a "thermionic detector." Secondary electron detectors have been used for dosimetry purposes too

Such a detector is not expected to survive in a fast reactor because of the cable problem. The gamma-ray interference is also severe. Another problem such as the build up of impurity gases such as helium from the $(n,\alpha)$ reaction or xenon will change its properties with time.

## Gas Scintillation Detectors

Gas scintillation detectors for in-core measurement were developed by Handschuh et al. (200). The detector consists of $^{235}U$ coated electrodes connected to a sinusoidal electric voltage supply in a chamber filled with a noble gas (e.g., argon) at a pressure between 200-300 torr. The light is transmitted through a tube which is polished inside and then detected outside the reactor. Such a detector is unable to detect a high-level localized neutron flux. It is sensitive to gamma-rays and radiation damage on the light pipe would be expected.

## Summary

It is clear from the above review that, except for the activation method, there is no commercially developed neutron detector available for fast reactor applications. The activation method has many disadvantages. In thermal reactors the fission chambers and the self-powered detectors are the two detectors that operate successfully. Improvement of these detectors to suit the fast reactor environment does not seem to be promising. Improving cable properties will not solve the problem. The new ideas introduced to eliminate in-core or close-to-core cables by

either a light pipe or a microwave guide do not seem to be very successful. The Cerenkov gas detector using the light pipe has a large scintillation background and it is unable to detect localized neutron flux. The gas scintillation detector has a strong sensitivity to a gamma-ray field. Radiation damage is expected to change the properties of the light pipe as well. The detectors using microwave guides are only in the early stage of development and it seems unlikely that they will have any application in the near future. Another more successful means is required to transfer the information from the reactor core to the region where this information is evaluated. The medium carrying the information should be completely insensitive to radiation damage and high temperature. For this reason the work described here resulted in the development of a method where the electrons generated by an incident neutron flux were transported into a low-radiation region by means of magnetic focusing before being detected and counted.

# CHAPTER III

# A NEW NEUTRON DETECTOR USING MAGNETICALLY FOCUSED ELECTRONS

## Introduction

The objective of this work is to design a detector with a better means of transferring the information from the reactor core or a position close to the core to a point outside the core where this information can be evaluated without undue interference. The detector should be insensitive to the intense gamma-ray field and to high temperatures. It is important too that the detector have a linear response for ease of evaluation. The detector should have a reasonable range of neutron flux values so that only a few detectors of different ranges have to be used. The life time of the detector should be relatively long in order to avoid replacing the detector. This is affected highly by the burn-up characteristics. Fast response time is important in the detector to meet reactor control requirements. The detector should have a small size so that it will not interfere with the reactor design or produce flux depression. Good signal reproducibility is important for reliable detectors. Other factors that are considered in designing a new detector are its cost, simplicity, and low maintenance.

The new detector that was designed to meet the above requirements depends on the use of a neutron-sensitive converter material that will emit conversion electrons when exposed to neutrons. It utilizes a long

evacuated pipe along which the electrons are focused onto a distant electron detector, which is located in a low-flux location. A solenoid coil is wound on the tube to produce a coaxial magnetic field. The neutron-sensitive material is put at one end of this tube, which is placed inside of the reactor, and an electron detector is put at the other end well outside the reactor or the high-flux region. Electrons are emitted by the process of internal conversion or beta decay when the neutron-sensitive material is exposed to the neutron flux. Under the influence of the magnetic field these electrons will follow a spiral path and will reach the electron detector at the other end. The rate of electrons reaching the electron detector is proportional to the neutron flux at the converter end.

## Description of the Detector

The detector as shown in Figure 5 consists of a long solenoid inside of which a vacuum or low pressure is maintained. Close to the output end of the detector there is a larger diameter curved section 11) to minimize gamma-ray and neutron streaming. At the input end a disk containing a neutron converter 1) is mounted. At the other end of the tube there is a plastic scintillator electron detector 3) followed by a long enclosed light pipe 4) which is attached to a photomultiplier 10). The reason for the long light pipe is to keep the photomultiplier away from the magnetic field and outside any damaging radiation field. The signal from the photomultiplier is fed into the electronic counting system (9,12). The electrons emitted by the interaction of the neutron flux with the neutron converter will follow a spiral path 2) within the magnetic field.

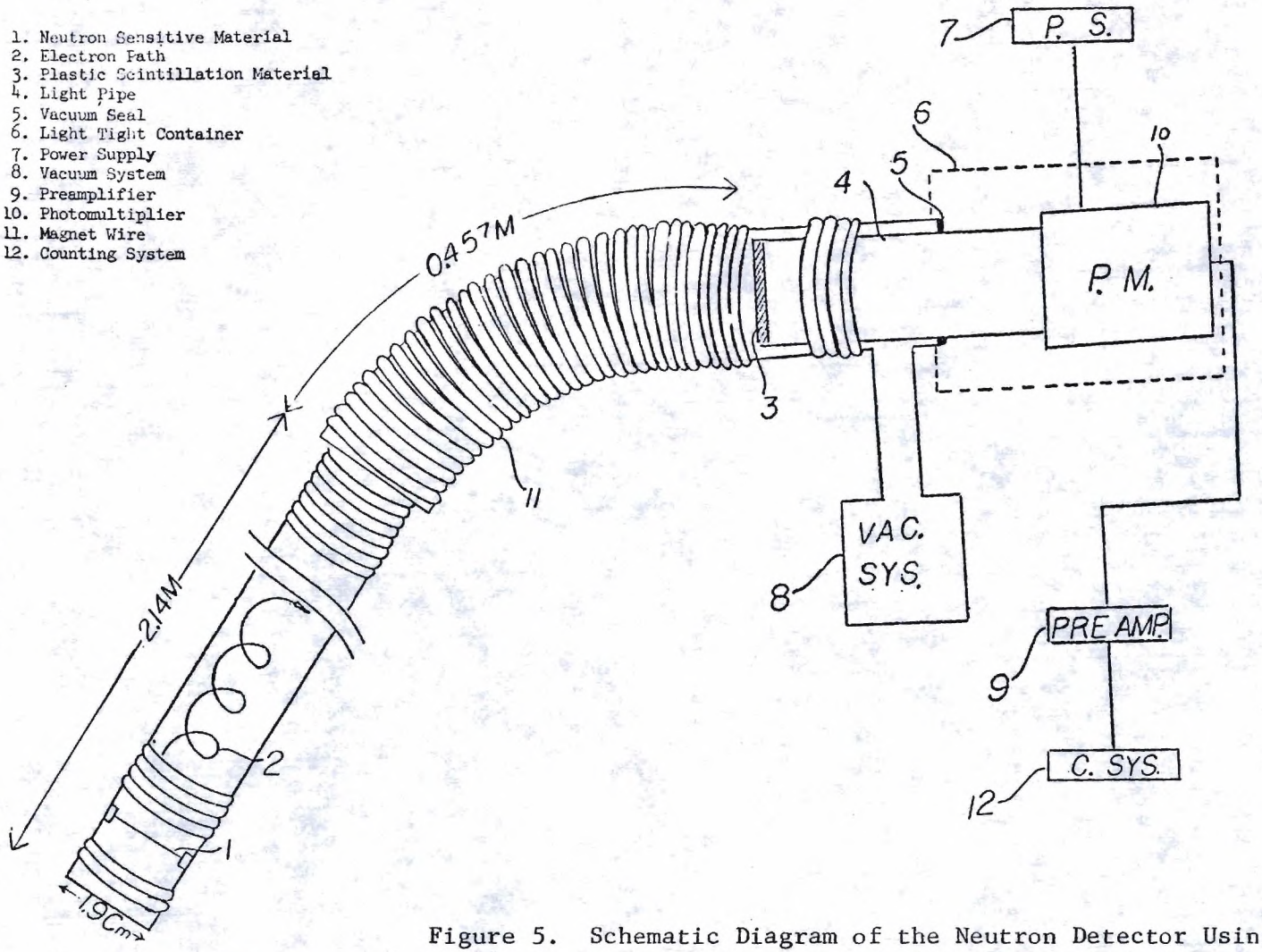


Figure 5. Schematic Diagram of the Neutron Detector Using Magnetically Focused Electrons

When these electrons reach the curved section they will continue this spiral path about the magnetic field but will acquire a velocity component perpendicular to the plane containing the magnetic field and the radius of curvature. To prevent some of these electrons from hitting the wall, the diameter of the curved tube was made larger than the straight section. When the electrons reach the electron detector they will be counted. The rate of arrival of electrons is proportional to the neutron flux. The system has to be calibrated in a known neutron flux or against other detectors of known sensitivity.

## The Magnetic Field

The magnetic field at the center of a solenoid whose length L is much greater than its radius is

$$B = \mu_0 \frac{Ni}{L} \tag{3-1}$$

where

$\mu_0$ = the magnetic permeability of free space ($12.57 \times 10^{-7}$ in the MKS system)

N = the total number of turns

i = the current in amperes

At the face of the solenoid the central magnetic field is

$$B = \mu_0 \frac{Ni}{2L} \tag{3-2}$$

At any other point inside the solenoid at a distance L' = aL from the face, the magnetic field for a solenoid of radius R is

$$B = \mu_0 \frac{Ni}{2} \left[ \frac{(1-a)}{\{R^2+(1-a)^2L^2\}^{1/2}} + \frac{a}{\{R^2+a^2L^2\}^{1/2}} \right] \tag{3-3}$$

In our system, N/L was 4200. This value was chosen in consideration of the available power supply and the magnetic field strength needed. The magnetic field inside the solenoid is

$$B = 52.794 \times 10^{-4} \; i \; Wb/m^2$$

where

i = the current in the solenoid in amperes

If an electron is ejected at an angle $\phi$ with the magnetic field direction, its trajectory will be a circular helix of radius r, in meters, such that

$$r = \frac{mv}{eB} \sin\phi \tag{3-4}$$

where

m = mass of the electron in kilograms

v = velocity in meters per second

e = electron charge in coulombs

In our system the radius is

$$r = 6.392 \times 10^{-4} \frac{\sqrt{E}}{i} \tag{3-5}$$

where

E = electron energy in electron volts

If i = 15 amperes, then all electrons having energy of 55 keV emitted at any angle $\phi$, all electrons having an energy of 69 keV and emitted at an angle $\phi \leqq 63^\circ$, and all electrons having an energy of 100 keV emitted

at angle $\phi \leqq 48^{\circ}$ will be focused.

The pitch h (the distance traveled by the electron along the tube per one revolution) is

$$h = 2\pi \frac{mv}{eB} \cos\phi \tag{3-6}$$

In our system h, in meters, is

$$h = 40.16 \times 10^{-4} \frac{\sqrt{E}}{i} \cos\phi \tag{3-7}$$

## The Electron Trajectory

To find the electron trajectory, we determine the force $\vec{F}$ acting on the electron in the magnetic field, given by

$$\vec{F} = e\,\vec{v} \times \vec{B} \;;$$

therefore, the acceleration $\vec{a} = \frac{e}{m}\vec{v} \times \vec{B}$.

In Cartesian coordinates

$$\vec{a} = \vec{i}\ddot{x} + \vec{j}\ddot{y} + \vec{k}\ddot{z}$$

$$\vec{v} = \vec{i}\dot{x} + \vec{j}\dot{y} + \vec{k}\dot{z}$$

$$\vec{B} = \vec{k}B$$

$$\vec{i}\ddot{x} + \vec{j}\ddot{y} + \vec{k}\ddot{z} = \frac{e}{m}\left[(\vec{i}\dot{x} + \vec{j}\dot{y} + \vec{k}\dot{z}) \times \vec{k}B\right]$$

$$\therefore \quad \vec{i}\ddot{x} + \vec{j}\ddot{y} + \vec{k}\ddot{z} = \vec{i}\,\frac{e}{m}B\dot{y} - \vec{j}\,\frac{e}{m}B\dot{x} + \vec{k}(0)$$

$$\ddot{x} = \frac{eB}{m}\dot{y} = w\dot{y} \qquad \text{where} \qquad w = \frac{eB}{m} \tag{3-8a}$$

$$\ddot{y} = - w\dot{x} \tag{3-8b}$$

$$\ddot{z} = 0 \tag{3-8c}$$

From equation (3-8c):

$$\frac{d\dot{z}}{dt} = 0 \qquad \dot{z} = C_1 = v\cos\phi \qquad z = vt\cos\phi + C_2$$

where $C_1$ and $C_2$ are constants.

Assuming the electron is initially at the origin, then $C_2 = 0$; therefore,

$$z = vt\cos\phi \tag{3-9}$$

We define a complex variable $u = x + iy$:

$$\dot{u} = \dot{x} + i\dot{y} \qquad \ddot{u} = \ddot{x} + i\ddot{y}$$

Using equations (3-8a) and 3-8b) we have:

$$\ddot{u} = w\dot{y} - iw\dot{x} = -wi(\dot{x} + i\dot{y}) = -wi\dot{u} \tag{3-10}$$

From equation (3-10):

$$\frac{d\dot{u}}{dt} + iw\dot{u} = 0$$

Multiplying by exp(iwt) we have:

$$\exp(iwt)\,\frac{d\dot{u}}{dt} + \dot{u}\,iw\,\exp(iwt) = 0$$

$$\frac{d}{dt}\left[\dot{u}\,\exp(iwt)\right] = 0$$

Solving this equation we have:

$$\dot{u} = C_3\,\exp(-iwt)$$

at $t = 0$ $\quad \dot{u} = \dot{u}_0 \quad \therefore C_3 = \dot{u}_0$ or

$$\dot{u} = \dot{u}_0\,\exp(-iwt)$$

Solving this equation we have:

$$u = \frac{i\dot{u}_0}{w}\,\exp(-iwt) + C_4$$

At $t = 0$ $\quad u = 0$ (the particle initially at the origin)

$$\therefore C_4 = -i\,\frac{u_0}{w}$$

$$u = \frac{iu_0}{w}\left[\exp(-iwt)-1\right] \qquad (3\text{-}11)$$

If the electron moves originally along the negative y-axis with a velocity equal to $v\sin\phi$ and along the z-axis with a velocity equal to $v\cos\phi$, then:

$$\dot{u}_0 = -i\dot{y} = -i\,v\sin\phi$$

and

$$u = \frac{v\sin\phi}{w}\,(\cos wt - 1 - i\sin wt)$$

$$x = r(\cos wt - 1) \qquad (3\text{-}12a)$$

$$y = -r \sin wt \tag{3-12b}$$

where

where $r = \frac{v\sin\phi}{w}$

If the electron is moving initially along the positive y-axis, then:

$$x = r(1 - \cos wt) \tag{3-13a}$$

$$y = r \sin wt \tag{3-13b}$$

To find y as a function of z, we eliminate t in equations (3-9), (3-13b):

$$y = r \sin \frac{wz}{v\cos\phi}$$

or

$$y = \frac{mv}{eB} \sin\phi \sin\left(\frac{eB}{m} \frac{z}{v\cos\phi}\right) \tag{3-14}$$

It is clear from equation (3-9) that electrons travel along the z-axis in steady motion. From equations (3-12a) and (3-12b) we can see that the electron motion in the y-direction and the x-direction is sinusoidal. At their maximum values, $x_{max} = y_{max} = r$, the radius of the spiral path. To focus an electron emitted from the center of the source, this radius should not exceed the radius of the tube. If all electrons of energy 38.7 keV emitted at angle $\phi \leq 45^{o}$ with the magnetic field direction from $^{156}Gd$ are to be focused in a one cm radius tube, then from equation (3-5) the minimum magnetic field required is 0.0455 $Wb/m^2$ while in focusing the 69 keV conversion electrons from $^{114}Cd$ emitted at $\phi \leq 45^{o}$ a minimum magnetic field of 0.0626 $Wb/m^2$ is required. Since our source

is an extended source, a larger magnetic field is required to focus electrons emitted from points other than the center of the source. If the radius of the spiral path is 0.7 of the tube radius, then focusing all 38.7 keV electrons emitted at $\phi \leq 45^{\circ}$ with the magnetic field, then a field strength of 0.067 $Wb/m^2$ is required, and focusing all 69 keV electrons emitted at the same angle requires a magnetic field of 0.089 $Wb/m^2$. If the spiral radius is 0.5 of the value of the tube radius, then the magnetic field strength needed is 0.094 $Wb/m^2$ and 0.125 $Wb/m^2$ for the $^{156}Gd$ and $^{114}Cd$ conversion electrons emitted at $\phi \leq 45^{\circ}$.

## Neutron Converter

In choosing the neutron converter the neutron capture cross section is a very important factor. Large cross-section materials give good counting efficiency but the burn-up of the material is so high that the sensitivity will change rapidly with time and will limit the lifetime of the detector. Large cross-section materials may cause a significant neutron flux depression in the reactor which would be unacceptable. Low cross-section material leads to low-sensitivity detectors with a longer life. Intermediate cross-section materials (10-200 barns) may be the best compromise if a wide range of flux values is anticipated.

In the detector studied here one of the neutron converter materials used was gadolinium. The reactions $^{155}Gd(n,\gamma)^{156}Gd$ and $^{157}Gd(n,\gamma)^{158}Gd$ have high cross sections for thermal neutrons but much smaller cross sections for higher energy neutrons. The internal conversion coefficient is relatively high and many low-energy electrons are emitted due to closely separated energy levels (208-212). Relatively high intensity electrons

whose energy is of the order of 38.7 keV were emitted from the transition of the $^{156}Gd$ 88.7 keV level and electrons of about 29 keV from the transition of the $^{158}Gd$ 79 keV level. These electrons are easy to focus due to their soft energy spectrum but many of them are stopped in the source layer. This is one reason for making the Gd foil very thin. The other reason is that the large cross section of the element may cause a large flux depression in the reactor core in which it is located. If Gd is used in a reactor with a fast neutron flux this problem does not exist.

Cadmium has also been used. Cadmium-114 has closely separated energy levels and a conversion electron of 69 keV with relatively high intensity which arises from the transition of the 95.9 keV excited level (213,214). Of each 100 neutrons absorbed in $^{113}Cd$, only 1.18 contribute to this level.

Indium has an intermediate absorption cross section and has been tried as well. It emits several groups of beta particles when exposed to a thermal neutron flux. Those that contribute to the detector signal are the beta particle of 1.988 MeV maximum energy and the positron of 0.42 MeV maximum energy from the 72-second half life $^{114}In$; also the beta particle of 3.3 MeV from the 13.4-second half life $^{116}In$ and the conversion electrons of 0.138 MeV and 0.160 MeV from 2.16-second $^{116m2}In$. The product $^{116m}In$ is undesirable since it has a 54-minute half life. The particles emitted have a high energy which makes them difficult to focus unless the magnetic field is very high. This problem can be solved by allowing them to lose part of their energy in the source before being emitted. This can be accomplished by choosing thicker foils. Thick foils are generally undesirable in in-core detectors since they produce a neutron

flux sink and cause foil heating. In out-of-core detectors this is not so important. The thick-source problem can be solved easily by using a thin converter on which a low cross-section material such as beryllium has been deposited that will provide an absorber film where electrons can lose part of their energy.

Silver was the fourth element used. It shares many of the characteristics of the indium converter but it has the advantage over indium of not having a product of long half life. The nuclides that contribute to the detector signals are the $^{108}Ag$ of 2.42-minute half life, which emits beta particles of 1.64 MeV maximum energy and positrons of 0.90 MeV, and $^{110}Ag$ of 24.4-second half life which emits beta particles of 2.87 MeV. Silver-110m has a very long half life of 255d but the cross section of $^{109}Ag$ to produce this product is fairly small (3 barns).

It should be mentioned here that in both the internal conversion process and the beta decay processes, Auger electrons are emitted which contribute to the detector count rate. Their energy is relatively low which makes them easy to focus. Internal conversion electron converters are preferred over beta decay converters since the half life of the latter makes for a slow response detector. Some elements that can be used as neutron converters are listed in Table 1.

## Electron Detector

The electron counter is an important element in this neutron detector. Electron multipliers form the most direct detection system. In the present work the scintillation method was preferred over other methods for low energy counting since it is sensitive to electron energies down

Table 1. Potential Converter Materials

| Element | Parent Nuclide | Parent Abundant (%) | Absorption Cross Section (barns) Thermal | 2 MeV per Element | Isotopes Contributing to Signal | Half-life | Type of Process* |
|---|---|---|---|---|---|---|---|
| In | $^{115}In$ | 95.77 | 45 | 0.15 | $^{116}In$ | 13.4 s | $\beta$ |
| | $^{115}In$ | 95.77 | 4 | | $^{116m2}In$ | 2.16 | $\beta$,ce |
| | $^{113}In$ | 4.23 | 4 | | $^{114}In$ | 72 s | $\beta^-,\beta^+$ |
| Cd | $^{113}Cd$ | 12.26 | 20,000 | 0.07 (1 MeV) | $^{114}Cd$ | stable | ce |
| Ag | $^{109}Ag$ | 48.65 | 89 | 0.08 | $^{110}Ag$ | 24.4 s | $\beta^-$ |
| | $^{107}Ag$ | 51.35 | 35 | | $^{108}Ag$ | 2.42 m | $\beta^-,\beta^+$ |
| Gd | $^{155}Gd$ | 14.7 | 58,000 | 0.11 | $^{156}Gd$ | stable | ce |
| | $^{157}Gd$ | 15.68 | $2.4 \times 10^5$ | | $^{158}Gd$ | stable | ce |
| Al | $^{27}Al$ | 100 | 0.235 | 0.002 | $^{28}Al$ | 2.31 m | $\beta^-$ |
| Ti | $^{50}Ti$ | 5.25 | 0.14 | 0.003 | $^{51}Ti$ | 5.8 m | $\beta^-$ |
| V | $^{51}V$ | 99.75 | 4.9 | 0.003 | $^{52}V$ | 3.75 m | $\beta^-$ |
| Co | $^{59}Co$ | 100 | 19 | 0.003 | $^{60}Co$ | 5.2 y | ce |
| | $^{59}Co$ | 100 | 18 | | $^{60m}Co$ | 10.5 m | $\beta^-$,ce |
| Ge | $^{74}Ge$ | 36.74 | 0.2 | 0.007 | $^{75m}Ge$ | 48 s | ce |
| | $^{76}Ge$ | 7.67 | 0.1 | | $^{77m}Ge$ | 54 s | $\beta^-$,ce |
| Rh | $^{103}Rh$ | 100 | 144 | 0.05 | $^{104}Rh$ | 43 s | $\beta^-$ |
| Nb | $^{93}Nb$ | 100 | 1 | 0.01 | $^{94m}Nb$ | 6.29 m | ce |
| Sm | $^{149}Sm$ | 13.82 | 41,500 | 0.03 | $^{150}Sm$ | stable | ce |

Table 1. Concluded

| Element | Parent Nuclide | Parent Abundant (%) | Absorption Cross Section (barns) Thermal | 2 MeV per Element | Isotopes Contributing to Signal | Half-life | Type of Process* |
|---|---|---|---|---|---|---|---|
| Hg | $^{199}Hg$ | 16.84 | 2,000 | | $^{200}Hg$ | stable | ce |
| Tl | $^{205}Tl$ | 70.5 | 0.11 | 0.005 | $^{206}Tl$ | 4.19 m | $\beta^-$ |
| Th | $^{232}Th$ | 100 | 7.4 | | $^{233}Th$ | 22.4 m | $\beta^-$,ce |

*
$\beta^-$ = beta decay

$\beta^+$ = positron decay

ce = conversion electron

to 5 keV (215) and can be designed to be insensitive to the magnetic field by using long light pipes or effective magnetic screening of the photomultiplier. The detector can also be used as an electron spectrometer where undesirable pulses can be discriminated against.

Gaseous chambers can be used for electron detection as well, but they should have very thin windows to allow the passage of low energy electrons. Special support for the window is needed since there will be a vacuum on one side of it. Semiconductor detectors can be useful in counting electrons of 50 keV energy or above due to their dead layer thickness. Channeltrons can detect electrons of energy down to 100 eV but this device has to have very good vacuum ($10^{-5}$ torr or less) and its sensitivity drops drastically in a magnetic field (216). Only a special, more expensive, low-efficiency type can be used directly in high magnetic fields.

Plastic scintillators are preferred over NaI(Tl) or anthracene, since those two are not stable in a vacuum, though they have a slightly higher detection efficiency.

## Possible Gamma-ray Interference

Gamma-ray interference is undesirable since it is not necessarily proportional to the reactor power. In our system gamma photons cause the emission of electrons from the neutron converter and from the walls of the solenoid by photoelectric, Compton, and pair-production effects. Those coming from the neutron-sensitive material due to the gamma-ray interaction are fewer in number than those emitted due to the neutron interaction owing to the much smaller cross section for the gamma-ray

interactions for low-Z materials and thin layers. They also have much higher energy (an order of MeV) than those emitted after internal conversion, hence the diameter of their helix is much larger than the total diameter of the solenoid and only a small fraction, whose direction makes a small angle $\phi$ with the magnetic field, will be focused. These high energy electrons also cannot survive the curved section of the solenoid. In that region the electrons will acquire a velocity component perpendicular to both the magnetic field B and the radius of curvature R. This drift velocity $v_D$ is given by

$$v_D = \left(\frac{\vec{R} \times \vec{B}}{R^2 B^2}\right) \frac{m}{e} v^2 \cos^2\phi \qquad (3\text{-}15)$$

Since $v_D$ is proportional to $v^2\cos^2\phi$, where v is the velocity of the electron, the higher energy electrons will drift towards the wall much faster than the slower electrons. In any case, undesirable electrons can be discriminated against electronically.

Electrons emitted from the wall of the solenoid due to gamma-ray interaction will make a spiral path and return back to the wall. If the z-axis is taken parallel to the wall of the solenoid as shown in Figure 6 and if $\vec{v}$ is the initial velocity of the electron coming from the wall and $v_{xy} = v\sin\phi$ is the component of the velocity in the x-y plane, then the projection of the electron path in this plane will be as shown in Figure 7a. The two continuous lines are for two electrons having the same velocity $v_{xy}$ but different angles $\theta$. The two solid lines in Fibure 7b are for two electrons having larger $v_{xy}$. To find an expression for the distance d that an electron coming from the wall can travel along the

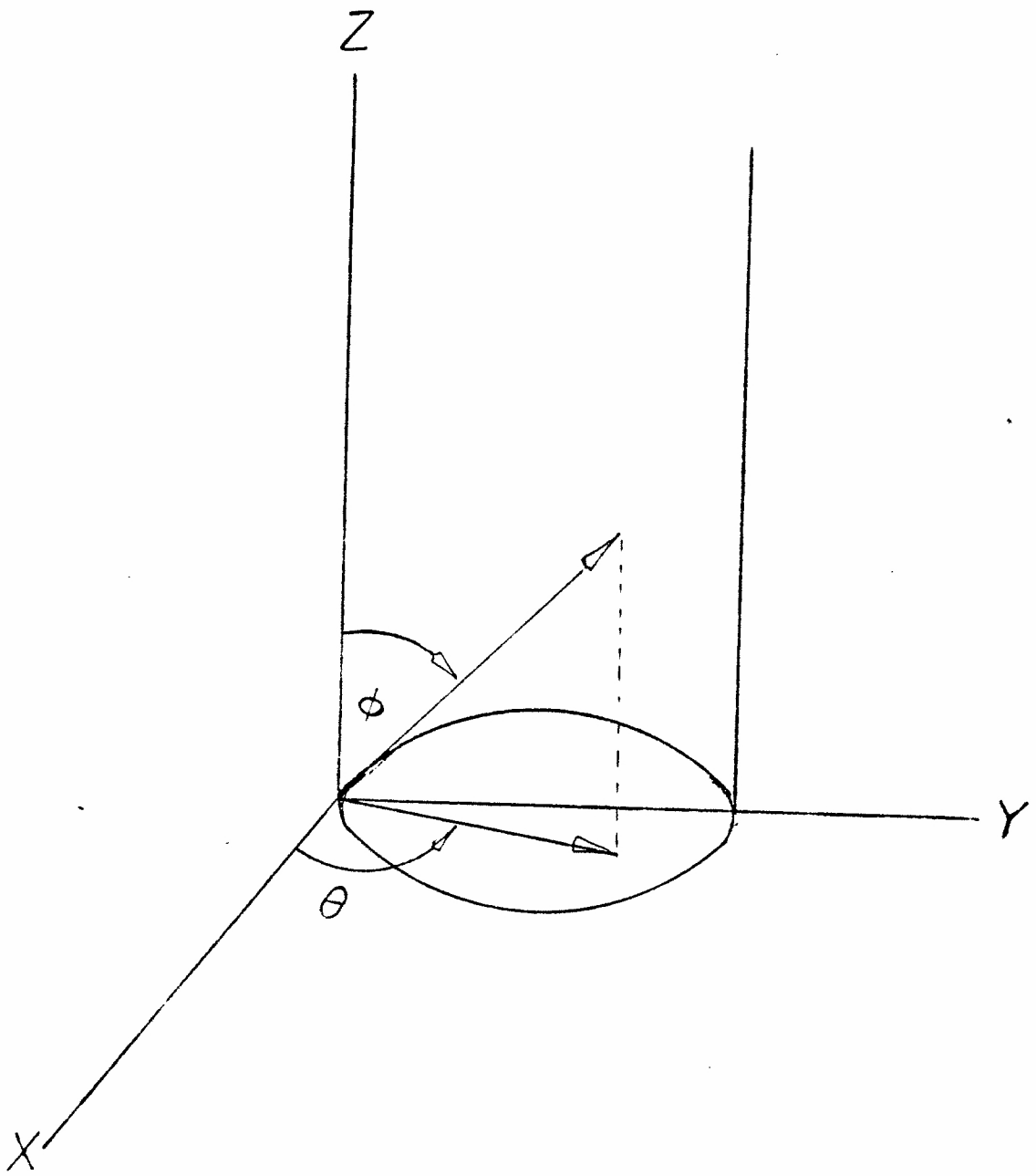


Figure 6. Solenoid Position with Respect to the x,y,z Coordinates

z-axis, the direction of focusing, before hitting the wall again we have in Figure 8 the circle $O_2$ which is the trajectory of this electron while circle $O_1$ is the cross section of the solenoid. The electron is emitted from point B, due to gamma-ray interaction, and hits the wall again at point A where the arc segment BHA is

$$BHA = 2r\delta$$

If the electron spends a time t in traveling this arc then

$$t = \frac{2r\delta}{v \sin\phi}$$

and

$$d = tv\cos\phi = \frac{2m\delta}{eB} v \cos\phi \qquad (3\text{-}16)$$

To relate $\delta$ to $\theta$ it can be proved that

$$R \sin(\theta + \delta) = r \sin \delta \qquad (3\text{-}17)$$

## Other Properties of the Detector

The time response of the detector depends on the time elapsed between the absorption of a neutron and the prompt emission of an electron, the time the electron spent in traveling the tube, and the time response of the associated counting system. In the internal conversion process the electron emission is prompt, while in beta decay it depends on the half life of the decaying radionuclide. The time required to

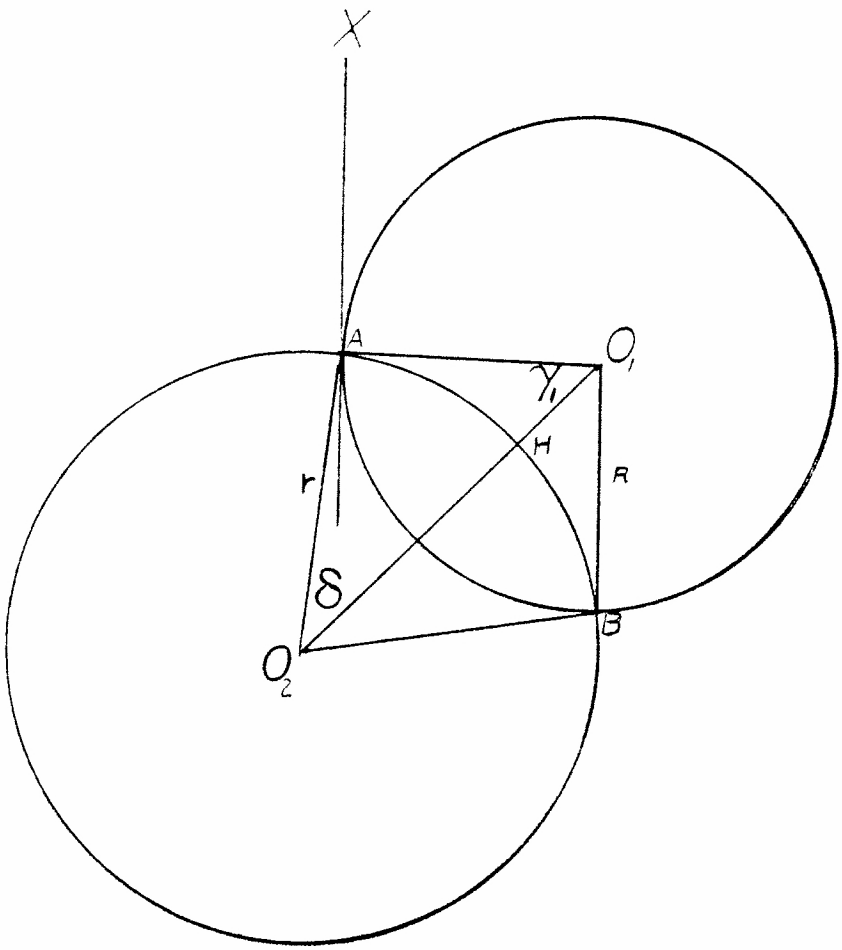


Figure 8. Cross Section of the Solenoid $O_1$ and the Circle of Electron Trajectory $O_2$

travel down the tube depends on the energy of the electron and the angle $\phi$ that its path makes with the magnetic field. The 69 keV internal conversion electron of $^{113}Cd$, emitted at an angle $\phi$ between 0-17 degrees, will travel one meter of the tube in $(0.324 - 0.91) \times 10^{-8}$ sec (3-9 nanoseconds).

The time response of the electronic counting system used in this experiment was of the order of microseconds, mainly governed by the pulse rise time in the photomultiplier. Faster electronic systems can be obtained if necessary.

Residual gas particles in the tube can attenuate the focused electrons by changing their direction in elastic collision, changing their direction and energy by inelastic collision, or attaching them to themselves and becoming negative ions. If we assume the pressure inside the solenoid is $10^{-6}$ torr and the total removal cross section Q of the residual air particles is $10^{-15}$ $cm^2$, then the relative electron beam transmitted $I/I_0$ is

$$\frac{I}{I_0} = \exp(-NQX)$$

where N is the number of the residual particles per cubic cm and X is the distance traveled in centimeters. In one meter the relative electron beam intensity transmitted is 0.99.

# CHAPTER IV

# EXPERIMENTAL DETAILS AND PROCEDURE

## General

A practical detector must meet a number of practical objectives and specifications. It must be thin enough to represent detectors that could ultimately be inserted into a reactor and long enough to remove effectively all radiation-sensitive components from the intense radiation field surrounding the converter. The converter material must be selected from among those listed in Table 1 in a low enough concentration to minimize flux depression. For a given tube diameter the magnetic field must meet the limiting conditions set by equation (3-5) on page 57. The tube material itself must have a low neutron capture cross section and all other components, such as sealants, gaskets and insulators must be capable of withstanding long-term irradiation.

To test the conceptual design, a 2 cm I.D. aluminum tube, 2.14 m long, was selected; this implies that the magnetic field strength for a Gd converter must be at least 600 gauss (0.06 $Wb/m^2$).

The detector system shown diagramatically in Figure 9 consisted of the following components: 1) aluminum cap, 2) magnet wire, 3) quartz converter holder, 4) aluminum tube, 5) O-ring, 6) neutron-converter material, 7) scintillation material, 8) aluminum tube connector, 9) light pipe, 10) light tight container, 11) photomultiplier and base, 12) preamplifier, 13) amplifier, 14) single channel analyzer, 15) ratemeter,

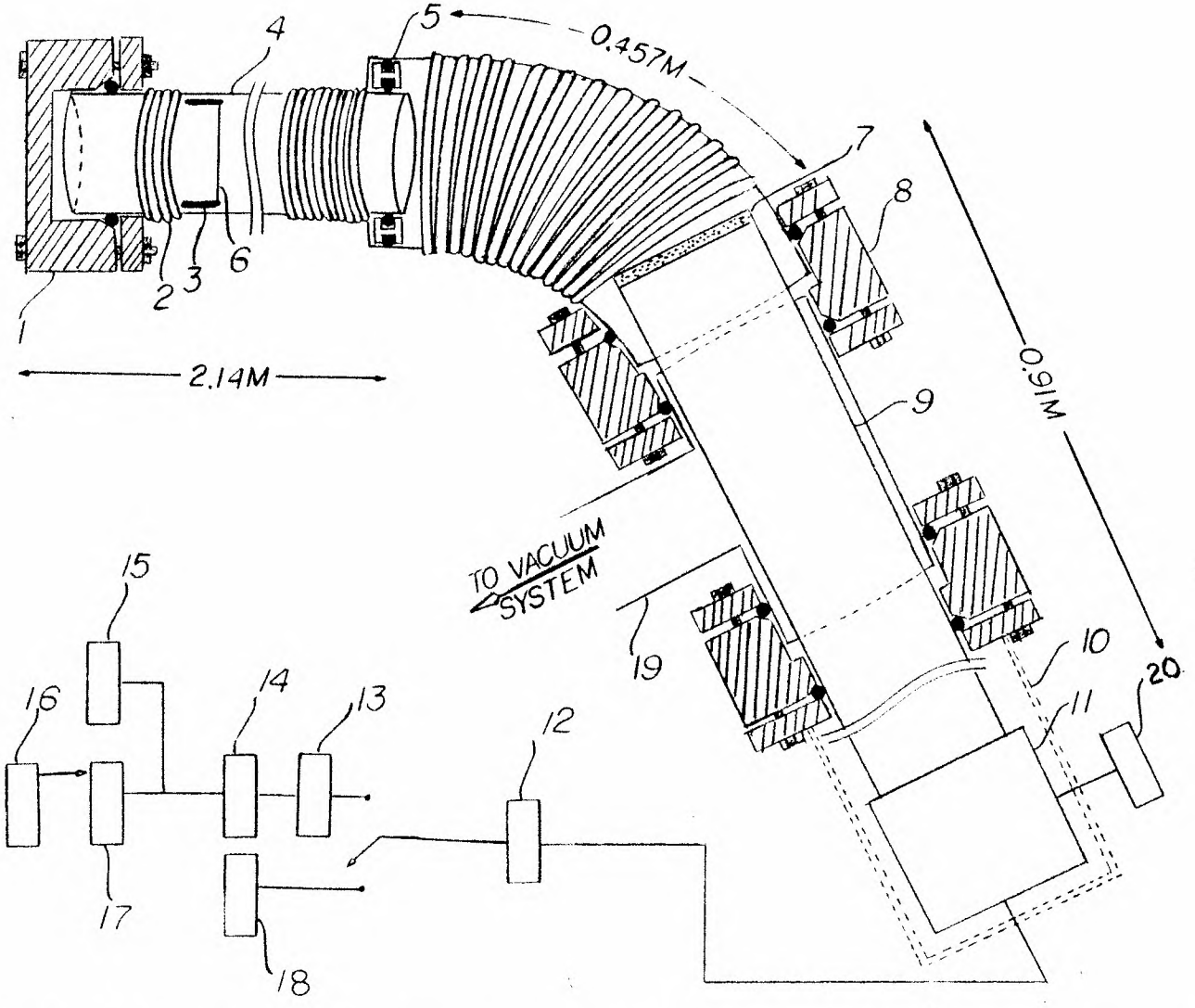


Figure 9. Schematic Diagram of the Neutron Detector Assembly and Electron Counting System

16) timer, 17) scaler, 18) multichannel analyzer, 19) T-shaped tube, and 20) power supply.

The straight section of the solenoid was made of high purity aluminum, type 1100, to avoid residual induced activities when exposing the tube to the neutron flux. The curved section was made of 45.7 cm long, less-pure aluminum tube since it will be far from the intense neutron flux, with a coil having the same number of turns per meter (4200), a radius of curvature of 45.7 cm and a 4-cm diameter. That is large enough that most focused electrons will traverse it without hitting the wall due to drift velocity, and the angle is enough to avoid neutron and gamma-ray streaming. The straight tube was sealed at one end by the cap 1), also made of aluminum and six stainless steel screws, with a conical-shaped groove for the O-ring. This design was useful when the neutron-sensitive material had to be changed. The straight and curved tubes were connected together as shown, using a relatively thick gasket which has outside and inside rectangular grooves where two O-rings were mounted. The smaller tube was inserted first into the connector fitting and on it the larger tube was then pushed. The other end of the curved tube is connected to a T-shaped tube 19) by the connector 8) made of aluminum and six steel screws using the same design as for the cap. The T-tube couples to the light pipe 9) using a similar connector. All the connectors were designed such that they can be disassembled and form a good demountable seal (207). The system was machined at the School of Nuclear Engineering shop by W. Jeter. The light-tight container 10) was made of a wooden box enclosing the photomultiplier 11), and its base. The electric feed-through of the photomultiplier was made using a silicone

rubber cement.

The light pipe was covered by several layers of thin aluminum sheet and entered the box through a hole which was sealed very well by Apiezon-Q seal.

The power supply for the solenoid current, made by Eastern Scientific Instrument Corp., was operated to give an output voltage from 0-50 volts and output current from 0-60 amperes.

## Magnetic Field Measuring Device

To measure the magnetic field inside the tube a small size magnetic fluxmeter is needed. A two-ohm resistance Hall generator type 803, made by Westinghouse Corporation, was utilized. The Hall probe (202-206) is essentially a thin-plate rectangular semi-conducting material which has four perpendicular terminals. A current is allowed to pass through two opposite terminals and when the probe is put in a magnetic field perpendicular to the direction of the current, electrons will drift in a direction perpendicular to both the magnetic field and the initial direction of charge flow. The electric field will build up until it balances the force induced by the magnetic field and the charges will retain their initial direction of flow. The induced voltage is proportional directly to the product of the electric current and the magnetic field and inversely to the thickness of the crystal. Therefore, for the same probe and constant current the resulting voltage which is measured at the other two terminals is proportional directly to the magnetic field.

In our probe an electric current was obtained from a transistorized power supply model 1020 build by Electric Instrument Company and the volt-

age was measured using a Fairchild multimeter model 7050. The probe was calibrated in a known magnetic field. The magnetic field as a function of the induced voltage for different values of current is shown in Figure 10.

## The Neutron Converters

Four types of neutron-converter materials were used, Gd, Cd, In, and Ag. A gadolinium film was prepared by vacuum deposition on 0.0063 cm thick stainless steel. A tantalum crucible boat obtained from R. D. Mathis Company was used. The Gd metal, Ta boat, and the stainless steel disk were carefully cleaned before the deposition occurred. The steel was immersed in 2% concentrated $HNO_3$ with 25% HCl of equal amount at about 65°C; the Ta was cleaned in hot HF while the Gd was cleaned in 20% concentrated $HNO_3$. The three metals were then washed in a solution of sodium carbonate (30 g/ℓ) with soap at about 70° C (207). The steel disk was positioned about 45 cm over the Gd in the crucible in the vacuum system inside the bell jar. The crucible was heated slowly at $10^{-6}$ torr pressure for about 15 minutes by allowing a current to flow in it and increasing it gradually. The Gd film obtained was a few $mg/cm^2$ thick weighed by a sensitive balance. The cadmium foil, 0.0025 cm thick, was obtained from Ventron Corporation and was used without backing material. The indium foil, 0.076 cm thick, and the silver, 0.038 cm thick, could also be used without backing material.

All of the foils 6) were cemented on the base of a one cm long, 1.9 cm diameter quartz cylinder 3) using epoxy. The wall of the cylinder was painted with a special type of electric conductive paint to maintain

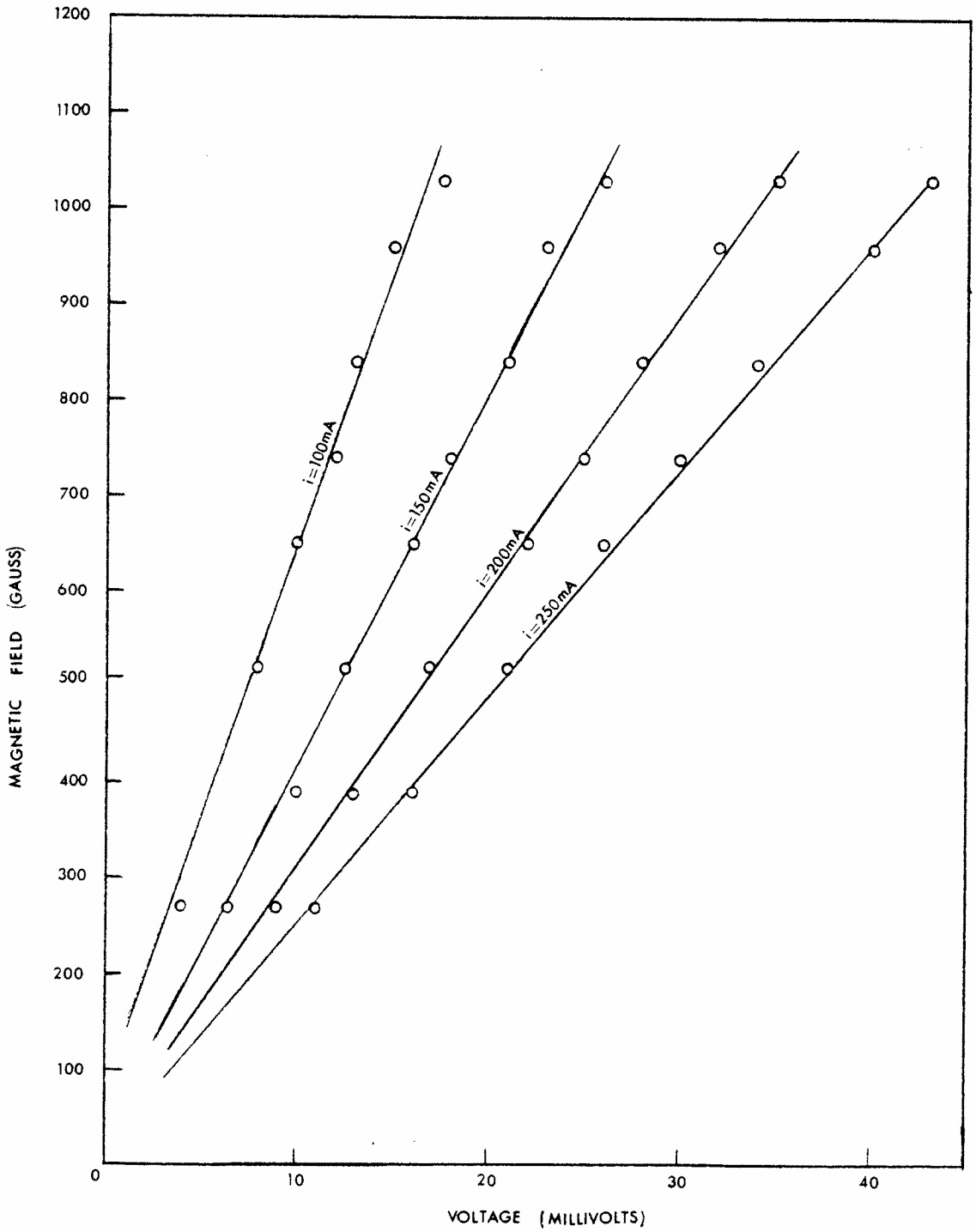


Figure 10. Magnetic Field vs Induced Voltage in the Hall Probe

good contact between the neutron converter and the wall of the focusing channel to avoid electric charge accumulation in the converter when exposed to the neutron flux.

## The Counting System

A plastic scintillator 7), 0.023 cm thick type Pilot B, obtained from Nuclear Enterprises, Inc., was used for the electron detector. This material contains 68% anthracene in polyvinyltoluene, has a decay time of 1.8 n sec and has a maximum fluorescence spectrum around 410 nm. The range of 100 keV electrons in it is about 0.015 cm.

The scintillator is mounted on two feet of Plexiglas light pipe, 3.8 cm in diameter, to keep the photomultiplier away from the magnetic field. The ends of the Plexiglas rod were smoothly polished and its surface was very well cleaned. Scratches on the surface effectively attenuate the light transmission through the pipe. The scintillator was attached to the light pipe using Dow-Corning high-vacuum silicon grease. The same grease is used to attach the pipe to the photomultiplier.

A photomultiplier type RCA 6342 was used. This multiplier has a spectral response that covers the range from 3000-6500 Å with a maximum response at approximately 4400 Å. Therefore, it matches spectral emission from the Pilot B scintillator very well. The multiplier gave the best signal-to-noise ratio when operated at 1000-1250 volts. In our experiment the voltage used was always 1000 volts. This multiplier is stable up to 250 microamperes. At higher values of anode current the sensitivity drops and recovers after a period of idleness. The tube is metallically coated for light and electrostatic shielding. It is very sensitive to magnetic

fields, it loses 98% of its sensitivity in a magnetic field of only two gauss (0.0002 $Wb/m^2$) parallel to the dynode-cage axis.

The signal from the photomultiplier was fed into an Ortec type 113 preamplifier 12). This type is designed mainly for use with photomultipliers; it has an adjustable output impedance from 40-140 ohms and was operated at an input capacitance of 45 pF. Its input is 0 to ± 7 volts and its output saturation level is ± 10 V into open circuit. Its rise time is less than 60 nsec.

From the preamplifier the signal was fed into an Omega-1 multichannel analyzer 18) manufactured by Canberra Industries. This unit has a built-in power supply for the photomultiplier, an amplifier, and a single channel analyzer. It has 1024 channels with a count capacity of 999999 per channel. The power supply varies from 0-3000 V with a ripple of 10 mV peak to peak. The amplifier is of bipolar type with a pulse width of 10 μsec. Its input impedance is 300 ohms, maximum input six volts, and it has a gain factor of 10-1000. Its integral nonlinearity is less than 0.1% of full scale.

An alternative counting circuit was also used which substituted for the Omega-1 multi-units. It consisted of a power supply 20) (Figure 9 ), an amplifier 13), a single channel analyzer 14), a ratemeter 15), a scaler 17), and a timer 16). The power supply was a Fluke Electronics model 415A which gives an adjustable output voltage from 0-3100 V dc with a ripple of less than one millivolt peak to peak, and positive or negative polarities. The amplifier was Ortec type 485. It has less than 0.25 μsec rise time for best filter action and 40 μsec minimum decay time for pole-zero cancellation. The input impedance is 1000 ohms and output

impedance is 0.5 ohm. The output pulse is 0-10 volts linear with 11.5 V saturation into 1000 ohms. The maximum gain is 640 of 0.15% linearity. It has less than 0.5% gain shift and 0.25% resolution spread full width at half maximum for a pulse above a 50 K count/sec $^{137}Cs$ background. The ratemeter was Ortec type 441; it covers a range up to $10^5$ counts/second. The input pulse needs 2 V to operate and ∓ 100 V maximum pulse amplitude. The single channel analyzer was Ortec model 406A which can operate in a window or normal integral fashion with a nonlinearity of less than 0.25% of full scale. The scaler 17) was Ortec model 430 which has a count capacity of 999999 and a typical, continuous counting rate of 16 MHz. The timer 16) was a Nuclear-Chicago model T1 dual timer.

## Preliminary Test Arrangements

Before the actual detector was constructed, a preliminary test system was set up to check the focusing using a tungsten filament as a source of electrons. The filament 10) (Figure 11) was connected to 6.3 volts ac for heating purposes. The electric feedthrough was made using Duro-Steel filler epoxy. This type makes a good bond with aluminum and can withstand high electric fields without breakdown. To improve the bond, the aluminum was etched with 10% solution of NaOH saturated with NaCl at 80°C for about 30 seconds, immersed in 20% $HNO_3$ and in 10% HCl, and then washed in a solution of 30 g/ℓ $Na_2CO_3$ with soap at about 70°C. After heating the tungsten filament it was noticed that an electric contact between the tube 8) and the power supply 13) took place which short circuited the power supply. The reason for this was the deposition of a tungsten film on the epoxy making a conductive layer. This problem was

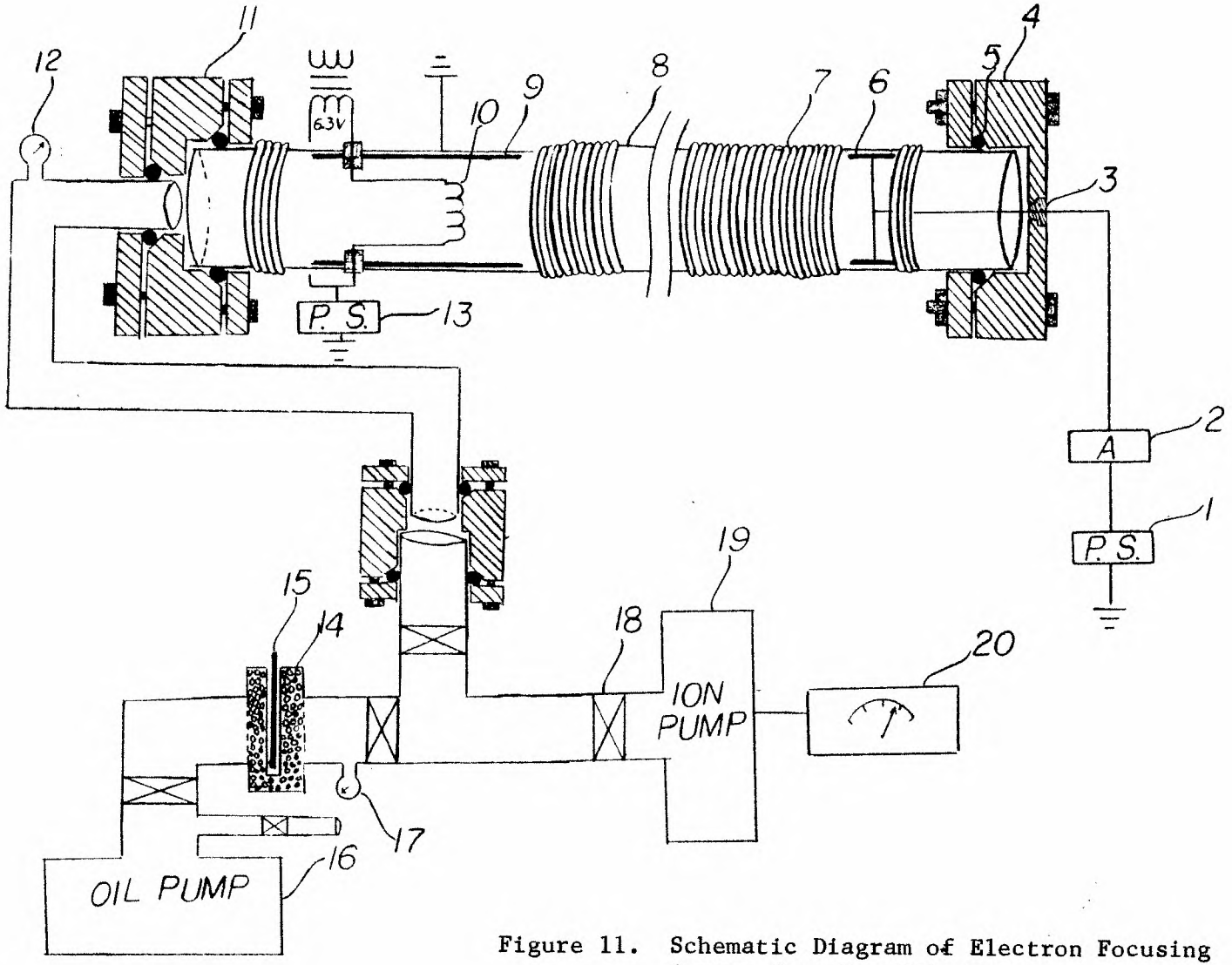


Figure 11. Schematic Diagram of Electron Focusing System from Hot Filament

solved using a quartz cylinder 9) encapsulating the filament. The collector was a stainless steel cup cemented by epoxy inside a one-cm long quartz cylinder 6). The feedthrough 3) made in the cap 4) was again epoxy. The current collected was measured using a Keithley 615 digital electrometer 2) which covers a range of $10^{-13}$ to $10^{-1}$ amperes. The power supply 1) was a Fluke model 415A usually put at a positive voltage to attract back the secondary electrons emitted from the collector surface when bombarded by the incoming electrons.

## The Vacuum System

The vacuum system shown in Figure 11 consisted of a roughing pump 16), several vacuum valves 18), a Versa trap molecular sieve 14), and its heater 15), a thermocouple vacuum gauge 17), hot cathode ionization vacuum gauge 12), ion vacuum pump 19), and ion pump control unit 20).

The roughing pump is an oil rotary pump. The pump was able to reduce the pressure in the system to 15 microns in a few minutes. The molecular sieve 14) was heated once every two weeks using the heater 15) for degassing. The thermocouple gauge 17) is NRC type 0531 and was connected to an NRC type 804 indicator. The hot cathode ionization gauge 12) was a Veeco Instrument Inc. type RG 75K connected to a Veeco type RG-3A indicator. The ion pump 19) was an Ultek type 100 L/S which uses electrical and chemical cleaning in reducing the pressure. The control unit of the ion pump 20) provides the high voltage (4750 V) to the ion pump and gives an indication on the voltage, current, and vacuum in the pump.

## The Georgia Tech Research Reactor (GTRR)

The GTRR (Figure 12) is a CP-5 type highly enriched (93% $^{235}U$), heavy-water-moderated and -cooled heterogeneous reactor. The core forms a right cylinder about two feet (61 cm) long and two feet (61 cm) in diameter. The fuel consists of fully enriched aluminum-uranium alloy plates, and when fully loaded the core contains 19 fuel assemblies spaced six inches apart in a triangular array where each assembly contains 16 fuel plates making approximately 3.2 kilograms of uranium-235. The fuel is located at the center of a six-foot diameter aluminum vessel and is surrounded by two-foot thick $D_2O$. The vessel is mounted in a graphite cylinder which provides two feet of reflector to the sides and beneath the core. The graphite is surrounded by a biological shield consisting of a 1/4 inch (0.63 cm) boral, 3 1/2 inch (8.9 cm) thick layer of lead and by heavy concrete and steel about one meter and 15 centimeters thick. The reactor is controlled by four cadmium shim-safety blades and one cadmium regulating rod.

The experimental facilities used were the biomedical facility and the H-3 and H-8 horizontal beam tubes. The biomedical facility beam is fitted with a bismuth gamma shield, water for neutron thermalization, a collimator, and a shutter. Its opening is four inches (10 cm) I.D. to a shielded room 10 x 12 feet in size. The side walls are made of two-foot barytes concrete and the back wall which is subject to beam impingement is made of four feet of concrete, 1/4 inch (0.63 cm) boral, and 1/2 inch (1.27 cm) lead.

Beam ports H-3 and H-8 are four-inch openings that look directly toward the fuel elements. They open through a stopcock shutter. The

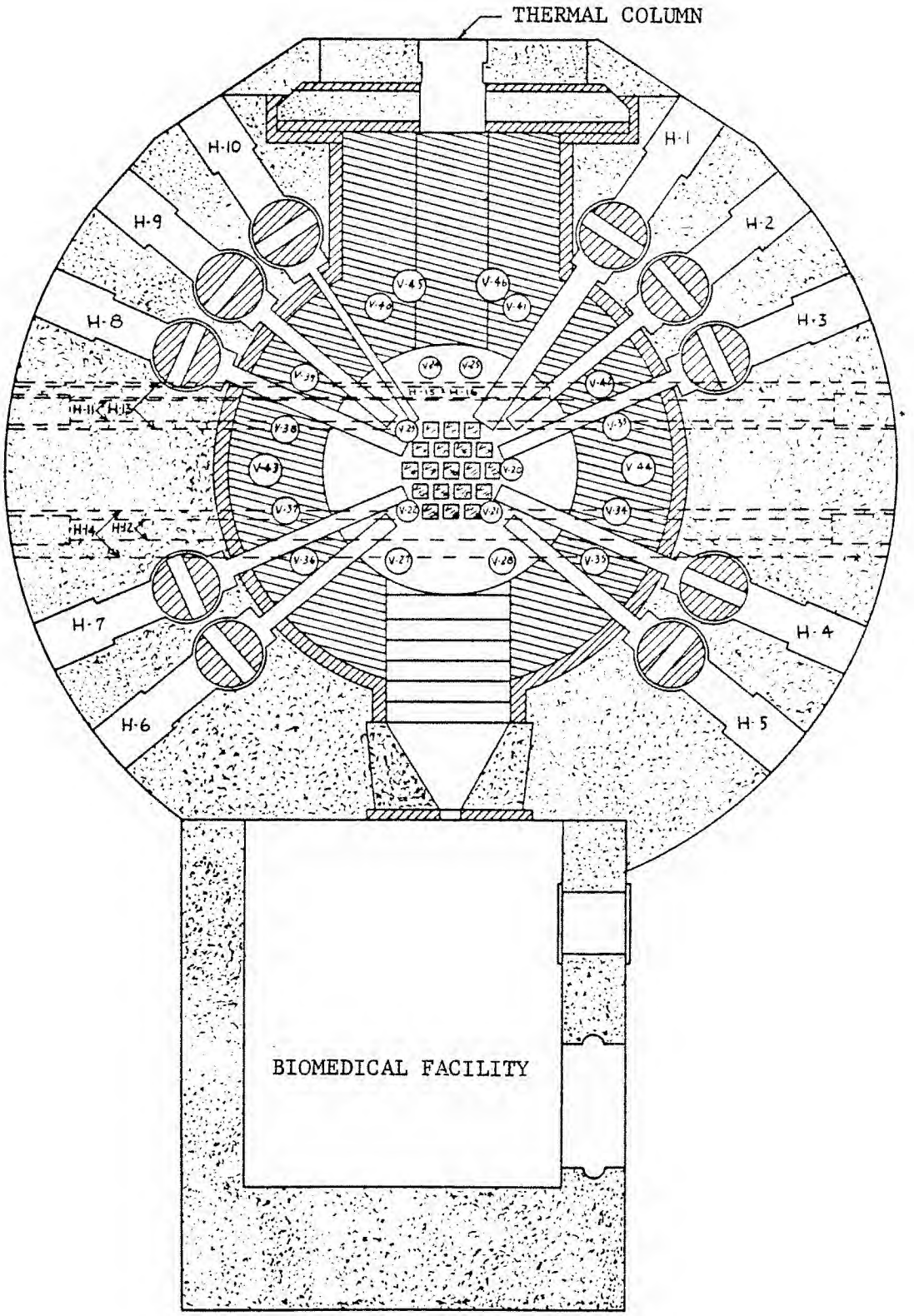


Figure 12. Mid-plane Section of the Georgia Tech Research Reactor

neutrons are brought out through a filtered and collimated tube. Port hole H-3 is fitted with a neutron diffractometer which gives about $1.4 \times 10^5$ nv at about five inches (12.7 cm) from the diffractometer face at 1000 kW reactor power.

During our experiment the device has simply been placed in front of the beam hole of H-3 and the biomedical facility. The tube direction was perpendicular to the reactor face in H-3 experiments and slightly rotated in the biomedical facility such that the scintillator would not be exactly in front of the beam. In experiments using H-8 the arrangement was set up as shown in Figure 13. A steel plug 3) was used with a 10-cm diameter hole into which the focusing tube was inserted. The plug was followed by a 46-cm long barrel-shaped shield made of 10 cm borated epoxy resin 5) and 10 cm paraffin 4) with a 6-cm hole. This was followed by a layer of 25-cm thick lead 6). In Figure 13 item 1) is the beam shutter, 2) is the reactor, 7) is the vacuum system 8) is the power for the solenoid current, 9) is the counting system, and 10) is the photomultiplier. A big barrel of paraffin 11), backed by cadmium, is used as a beam catcher.

Figure 14 shows a photograph of the experimental assembly.

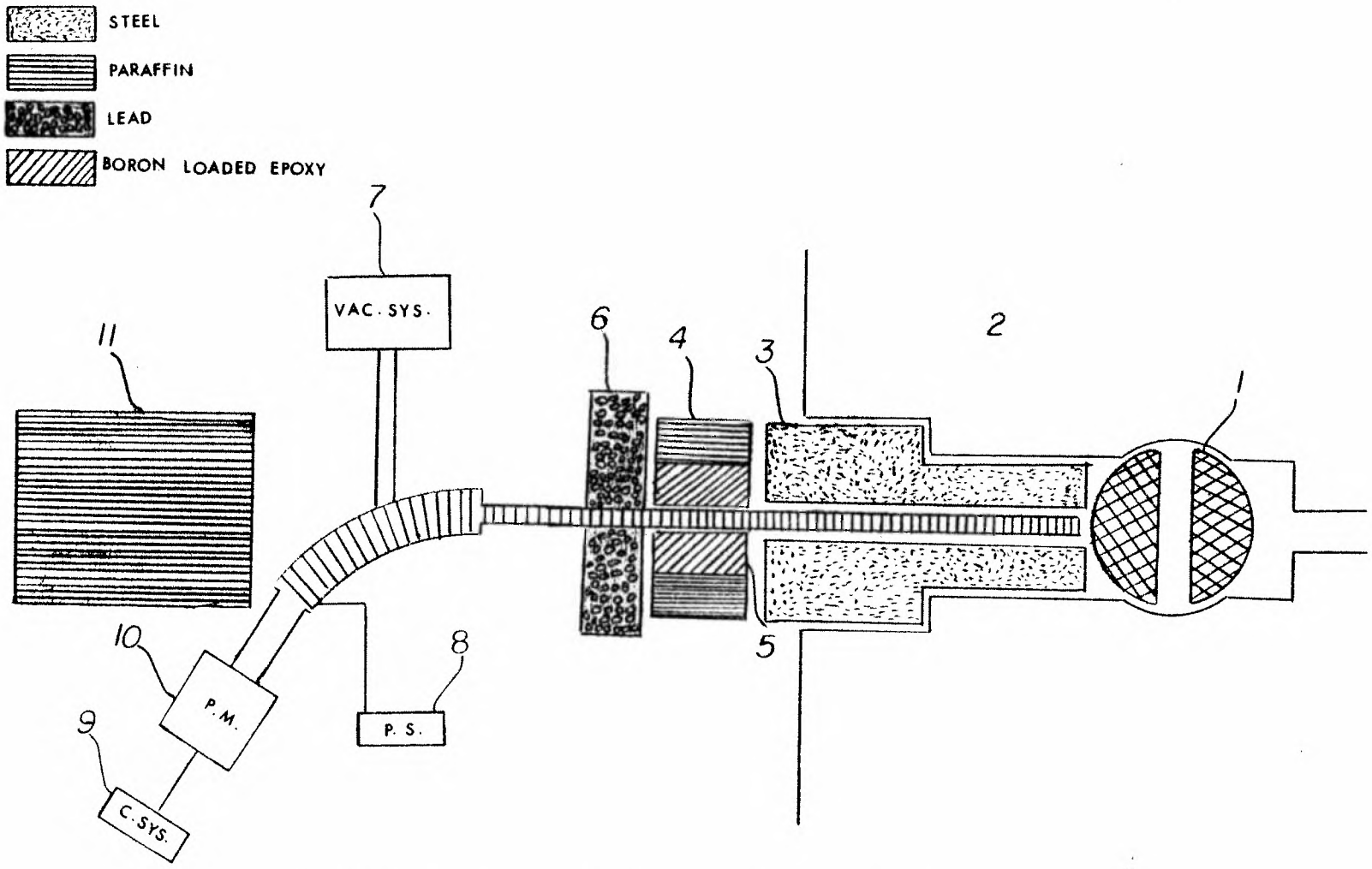


Figure 13. Schematic of Detector Position Inside H-8 Beam Hole

Figure 14. Photograph Showing the Detector Outside the Beam Hole with the Paraffin Catcher Removed

# CHAPTER V

# RESULTS

## Hot Filament Electron Focusing

To test the focusing effect of the magnetic field a heated tungsten filament was used as shown in Figure 11. A simplified circuit is shown in Figure 15. $V_1$ was kept negative with respect to the tube to accelerate the electrons emitted from the filament. This voltage will be called the focusing voltage. The anode voltage, V, was kept positive most of the time to attract back secondary electrons emitted from the anode surface when it is hit by focused electrons from the filament. In Figure 15, B indicates the magnetic field. The electrons emitted from the filament follow a spiral path and are collected by the anode. The current is measured by the electrometer, A. First a 30-cm long solenoid was used. Both the filament and the anode were placed 3 cm from the ends of the tubes. When -100 volts focusing voltage $V_1$ was applied, giving an energy of 100 eV to the electrons emitted from the filament, a magnetic field of 250 gauss (0.025 $Wb/m^2$), and a pressure inside the tube of $8 \times 10^{-8}$ torr, the anode current reached a saturation value of about $2 \times 10^{-4}$ amperes at an anode voltage of about 100 volts.

The long solenoid (2.14 cm) was then used in the same arrangement. When the focusing voltage $V_1$ was zero, the pressure $2.6 \times 10^{-6}$ torr, the anode current varied as a function of the anode voltage as shown in Figure 16 at zero, 70 (0.007 $Wb/m^2$), and 190 gauss (0.019 $Wb/m^2$) magnetic field.

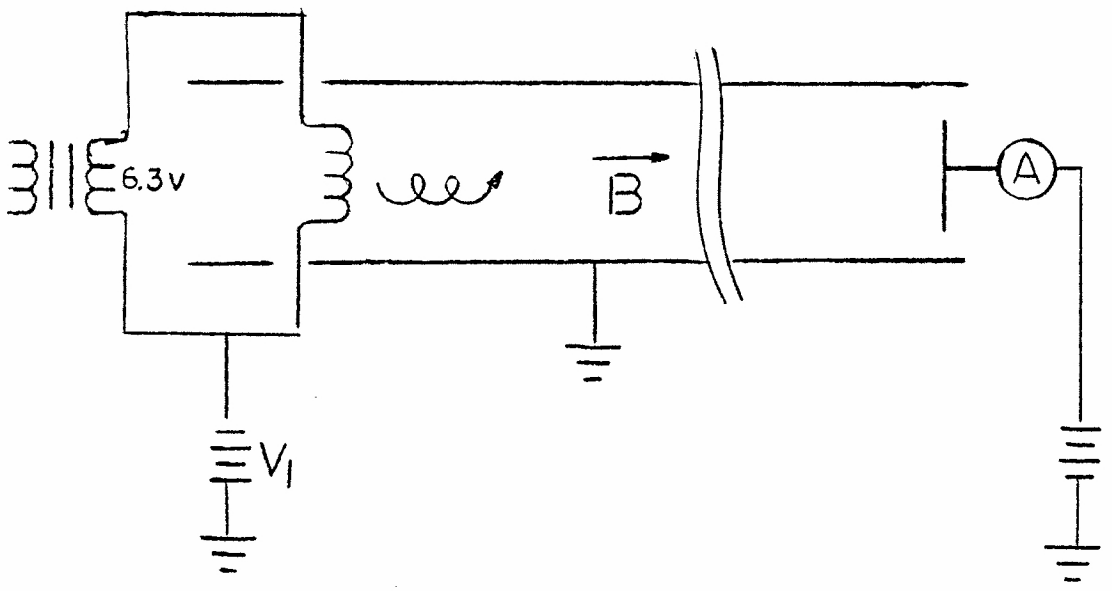


Figure 15. Simplified Circuit of Electron Focusing from Hot Filament

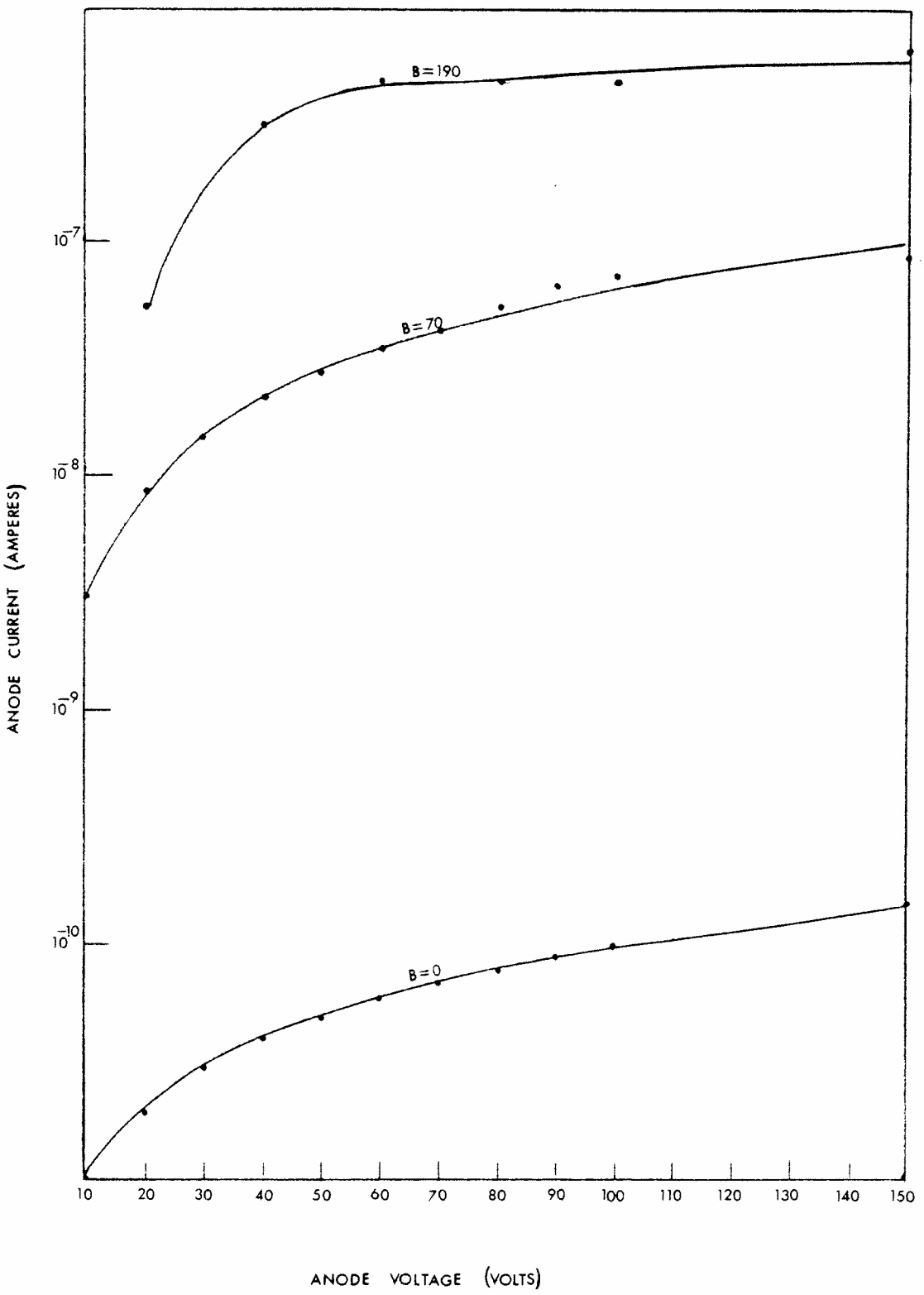


Figure 16. Anode Current vs Anode Voltage at Focusing Voltage $V_1 = 0$ and Three Different Values of Magnetic Field

When the focusing voltage $V_1$ was -2000 volts, giving each electron an energy of 2000 eV, the result of Figure 17 was obtained in zero and 70 gauss (0.007 $Wb/m^2$) magnetic field. The current is higher than that of Figure 16 of the same magnetic field. These electrons have much higher energy than those of Figure 16 and they are not lost by attachment in the residual air molecules. In contract, the electrons of Figure 16 would attach themselves to the residual gas molecules and they were very easily scattered and lost. The anode current as a function of the focused electron energy (or $V_1$) at a pressure of $1.8 \times 10^{-6}$ torr is shown in Figure 18 at 0, 70, and 190 gauss. More electrons are focused at higher magnetic field strengths. As the electron energy is increased they become more difficult to focus. This is the reason for the decrease in the current at higher electron energy.

## Focusing $^{35}S$ Beta Particles

A sulfur foil, 3.851 grams in weight, 1.30 cm in diameter, was irradiated in the nuclear reactor using the V21 vertical experimental facility at 1000 kW reactor power (neutron flux ~ $10^{13}$ $n/cm^2 \cdot sec$) for eight hours. Sulfur-35 was produced by the reaction $^{34}S(n,\gamma)^{35}S$. The parent $^{34}S$ has 0.0422 abundance and a 0.27 barn thermal absorption cross section. The product $^{35}S$ has an 88-day half life and is a soft beta emitter of average energy, 0.0488 MeV. This energy is suitable for a preliminary check of focusing since it is close to the gadolinium conversion electron energy, 0.038 MeV, and the cadmium conversion electron energy of 0.069 MeV. The radioactive disc was put 3 cm inside the long coil; only the straight section was used. A 1.9 cm diameter Pilot B scintillator

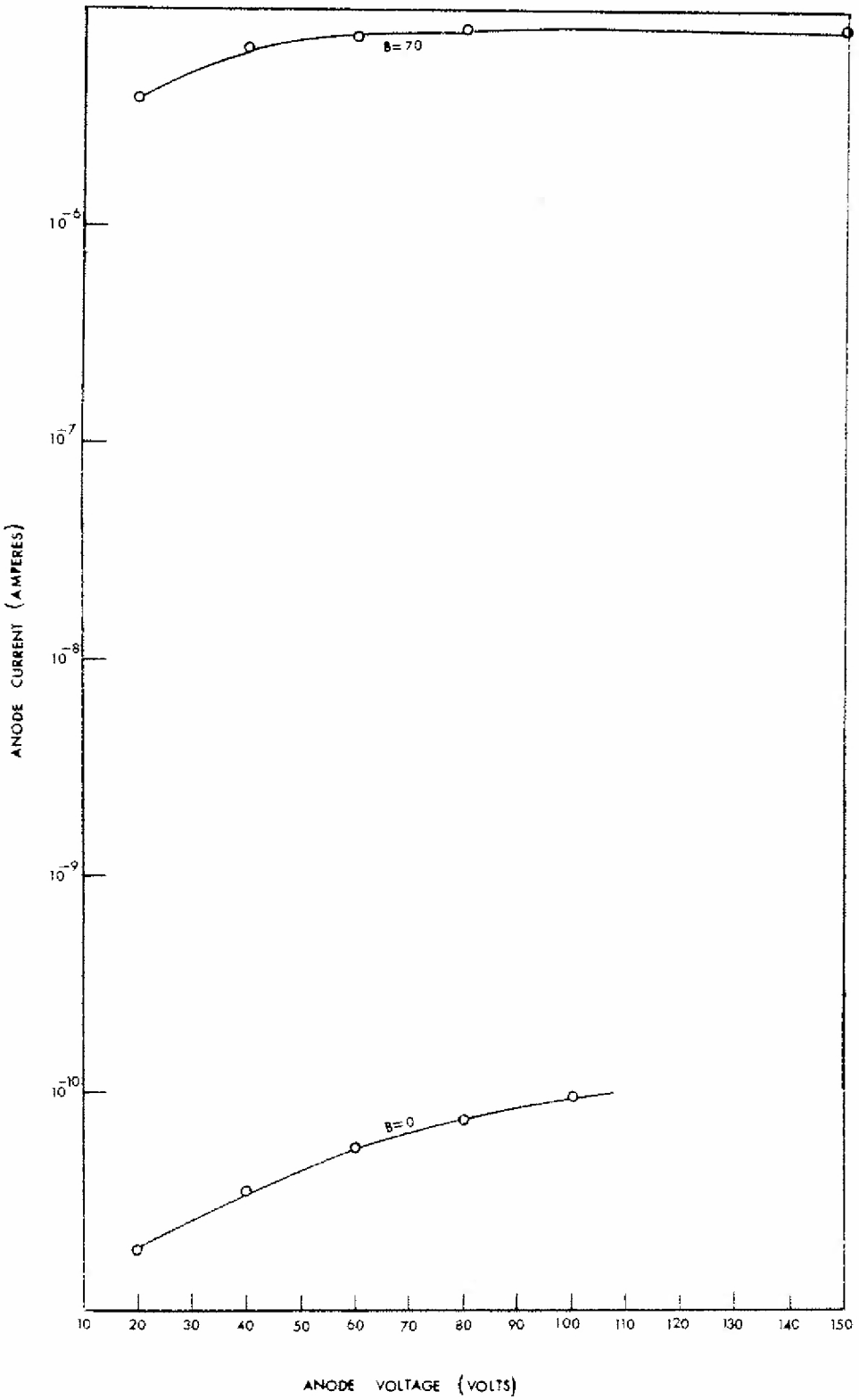


Figure 17. Anode Current vs Anode Voltage at Focusing Voltage $V_1$ = -2000 Volts (electron energy = 2000 eV) and Two Values of Magnetic Field

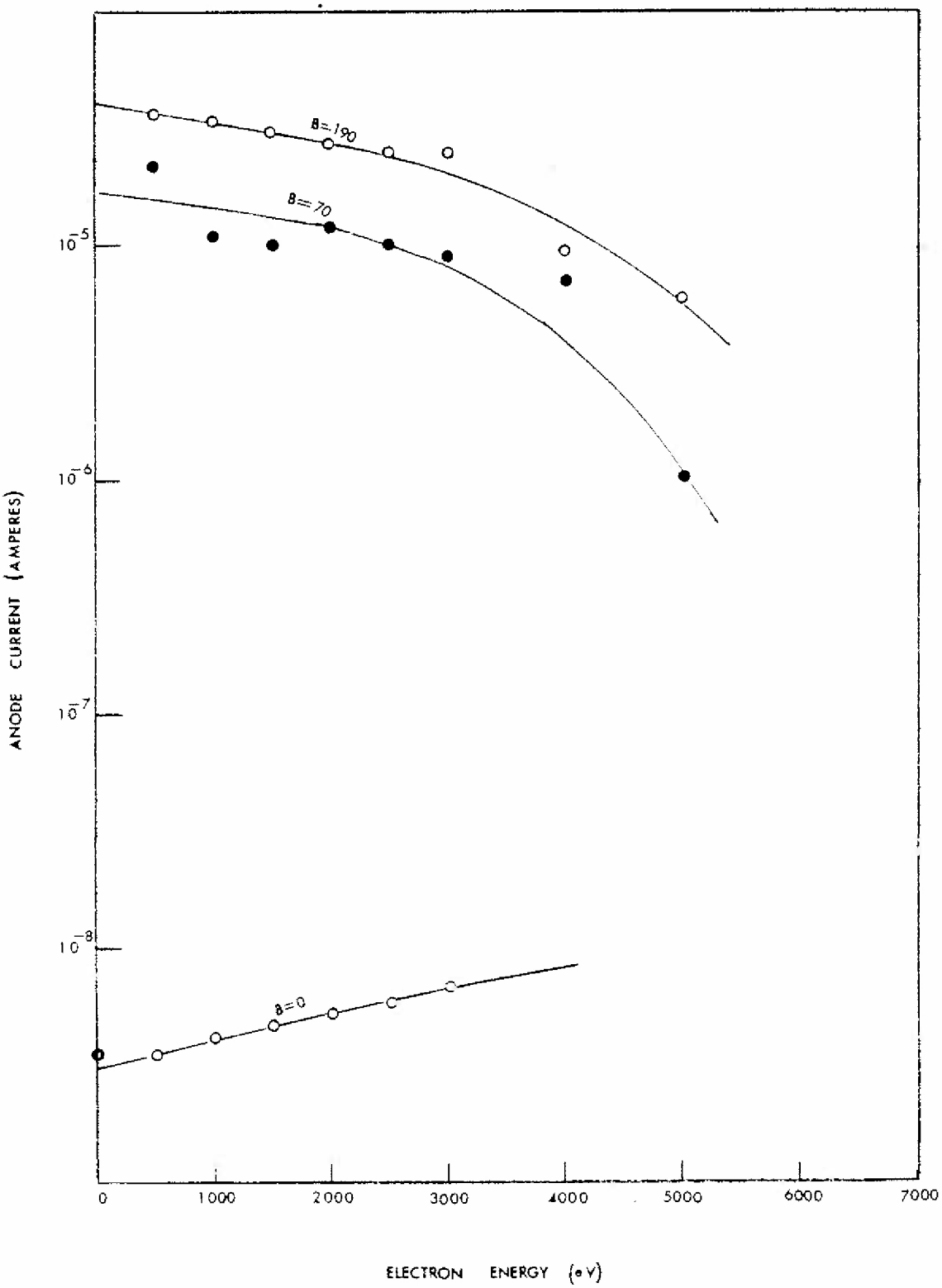


Figure 18. Anode Current vs Electron Energy at Three Values of Magnetic Field and Anode Voltage V = 67 Volts

and a 1.9 cm diameter Plexiglas light pipe were inserted at the other end followed by the rest of the counting system. The pressure in the system was $4 \times 10^{-6}$ torr. The count rate on the Omega-1 pulse height analyzer as a function of the magnetic field is shown in Figure 19, together with the statistical standard deviation. The line was drawn by a best visual fit. It is clear that the sensitivity of the device can be varied by changing the magnetic field, and conversely its consistency depends on the stability of the solenoid current.

## Detector Response Using Gadolinium, Cadmium, Silver, and Indium Converters in the Biomedical Facility

The detector, without the curved section, was put in the Biomedical facility of the Georgia Tech Research Reactor. The Gd foil was used first and was put 3 cm inside the coil and this end was put in front of the beam at a distance of 10 cm from the beam port. The other end of the coil, containing the scintillation material, was moved about two feet from the beam direction and was shielded by 5.1 cm thick lead bricks. The neutron flux at the converter position was measured using a 0.1239 gram, 1.3 cm diameter gold foil at different power levels. The Cd ratio was 86. The count rate as a function of the reactor power and neutron flux is shown in the upper curve of Figure 20 at a pressure of $2 \times 10^{-6}$ torr and 530 gauss (0.0530 $Wb/m^2$) magnetic field. Above $2.7 \times 10^7$ $n/cm^2 \cdot sec$ the detector counting system saturated and no reliable value could be obtained. In the lower curve for zero magnetic field, the response was due only to gamma-ray photons hitting the scintillator directly.

A cadmium foil, 0.0025 cm in thickness, was then used as a converter.

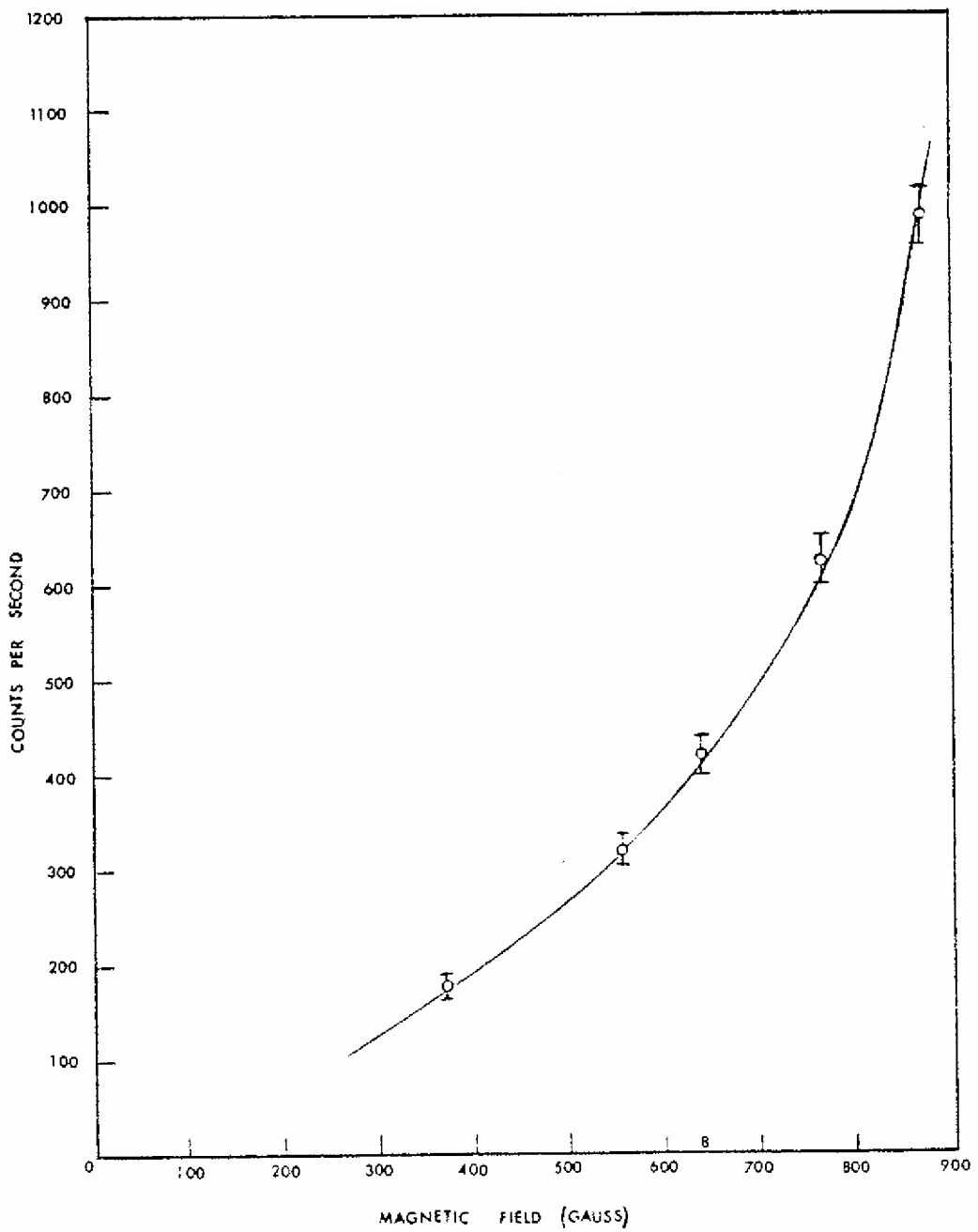


Figure 19. Count Rate vs Magnetic Field of Sulfur-35 Beta Source

The response at 800 gauss (0.08 $Wb/m^2$) magnetic field and the same pressure was obtained and is shown in Figure 21. The gamma-ray contribution shown in the lower curve of Figure 20 was subtracted.

When the silver foil, 0.038 cm thick, was used, the count rate was measured at each power level 10 minutes after the neutron flux stabilized to allow for the saturation of the 2.42-minute half life $^{108}Ag$ and the 24.4-second half life $^{110}Ag$ activities to be reached. The detector response is shown in Figure 22 at the same pressure and magnetic fields as above.

The indium foil, 0.076 cm thick, was then tested at the same pressure and with 440 and 800 gauss (0.044 and 0.08 $Wb/m^2$) magnetic field strengths. The response obtained is shown in Figure 23. The readings were taken three minutes after the flux was stabilized to allow for the saturation of the 72-second half life $^{114}In$, the 13.4-second half life $^{116}In$, and the 2.16-second half life $^{116m_2}In$ activities to be reached The gamma-ray background counts shown in the lower curve of Figure 20 were subtracted in all the cases. The straight lines in Figures 20, 21, 22, and 23 were drawn by visual fit and the standard deviation is shown.

## Effect of Solenoid Curvature

To minimize the streaming of neutrons and gamma rays down the tube the detector curved section was tested to see the effect of bending the magnetic field on the movement to the wall. To see this effect clearly, it was important to work in a gamma-free neutron flux; therefore, the H-3 horizontal beam was chosen. Only the curved section of the tube was used at first. To see the effect of electrons on count rate at the point of

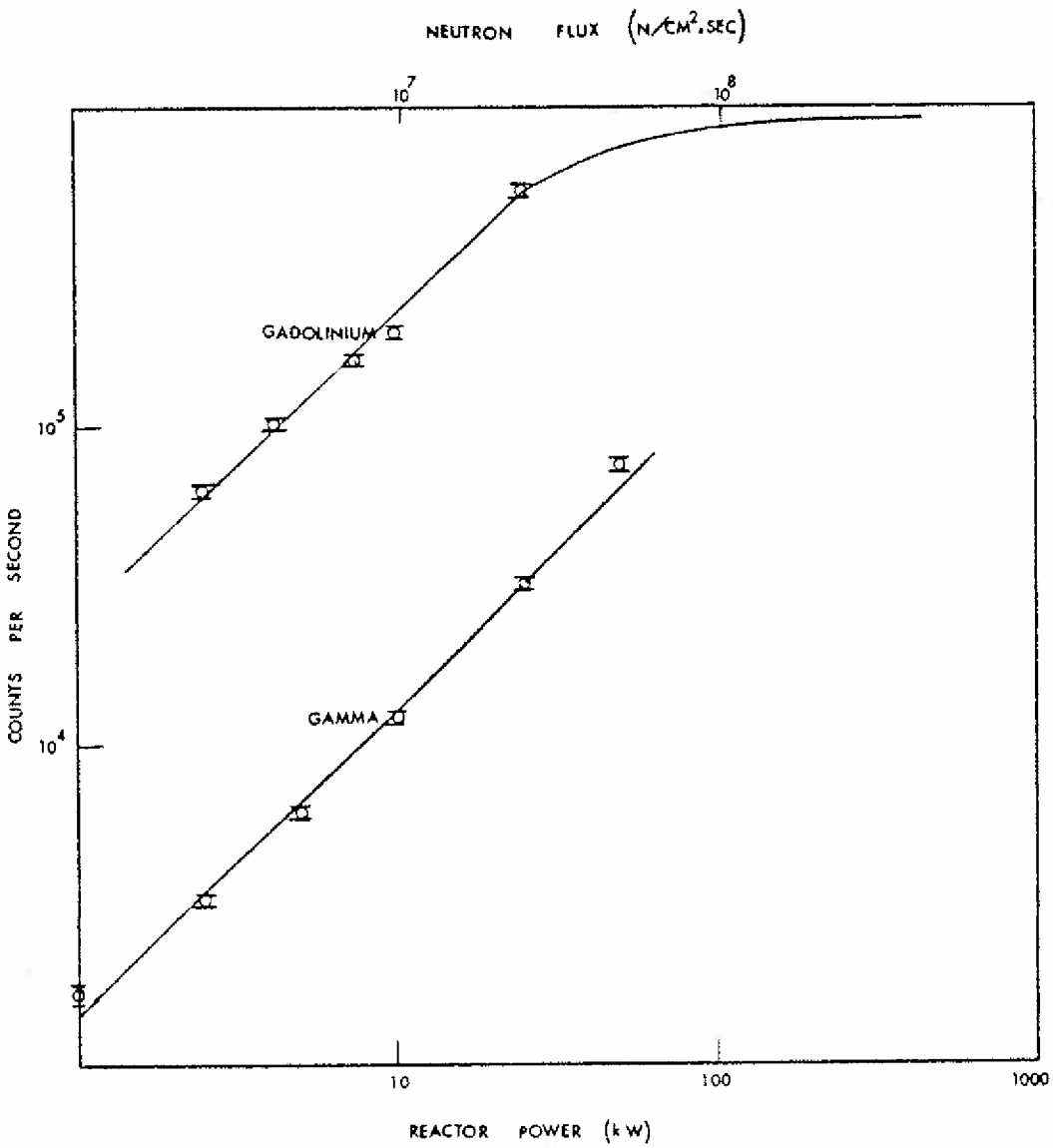


Figure 20. Count Rate vs Reactor Power and Neutron Flux of Gadolinium Converter and Gamma-ray in the Biomedical Facility

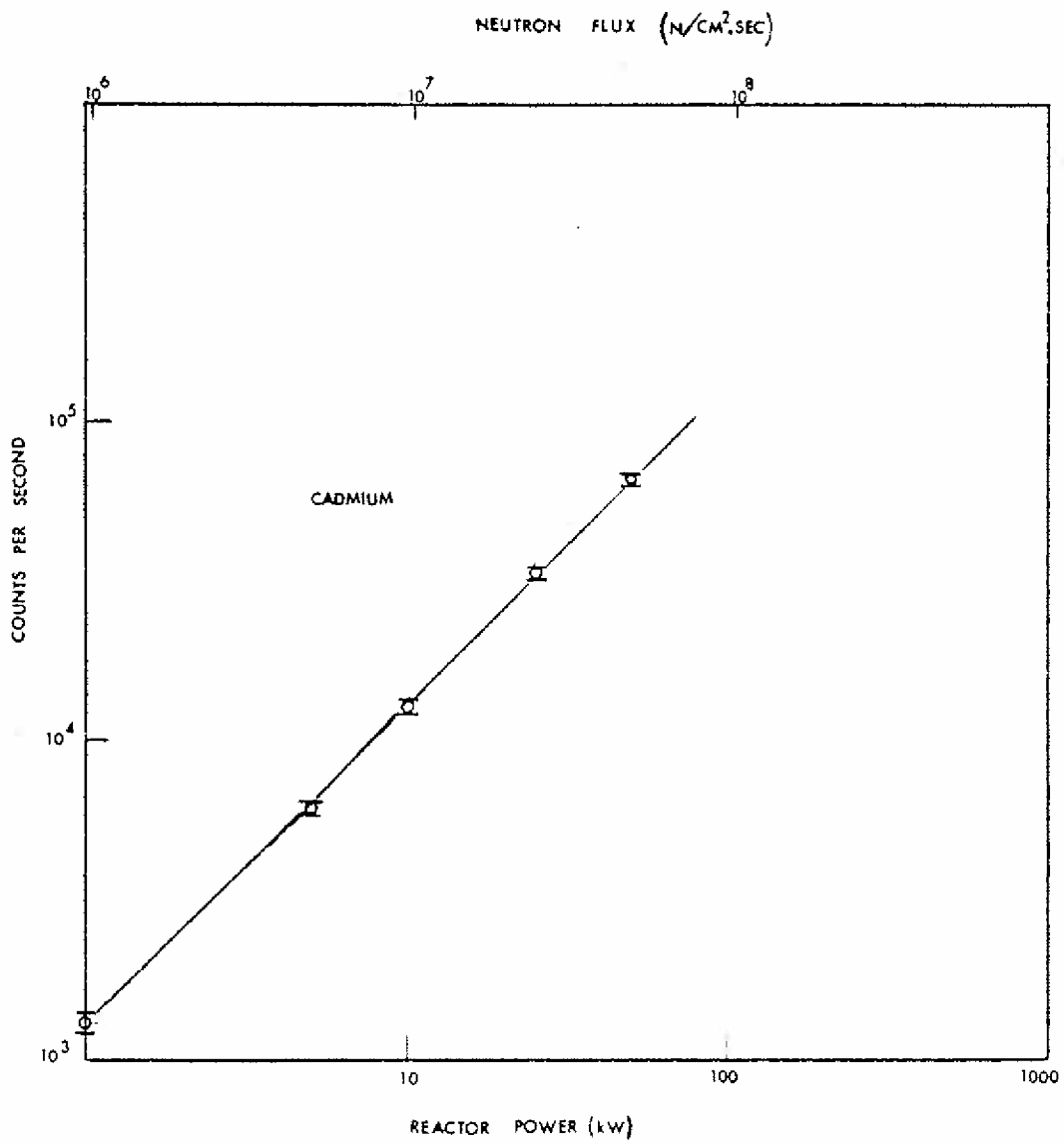


Figure 21. Count Rate vs Reactor Power and Neutron Flux of Cadmium Converter in the Biomedical Facility

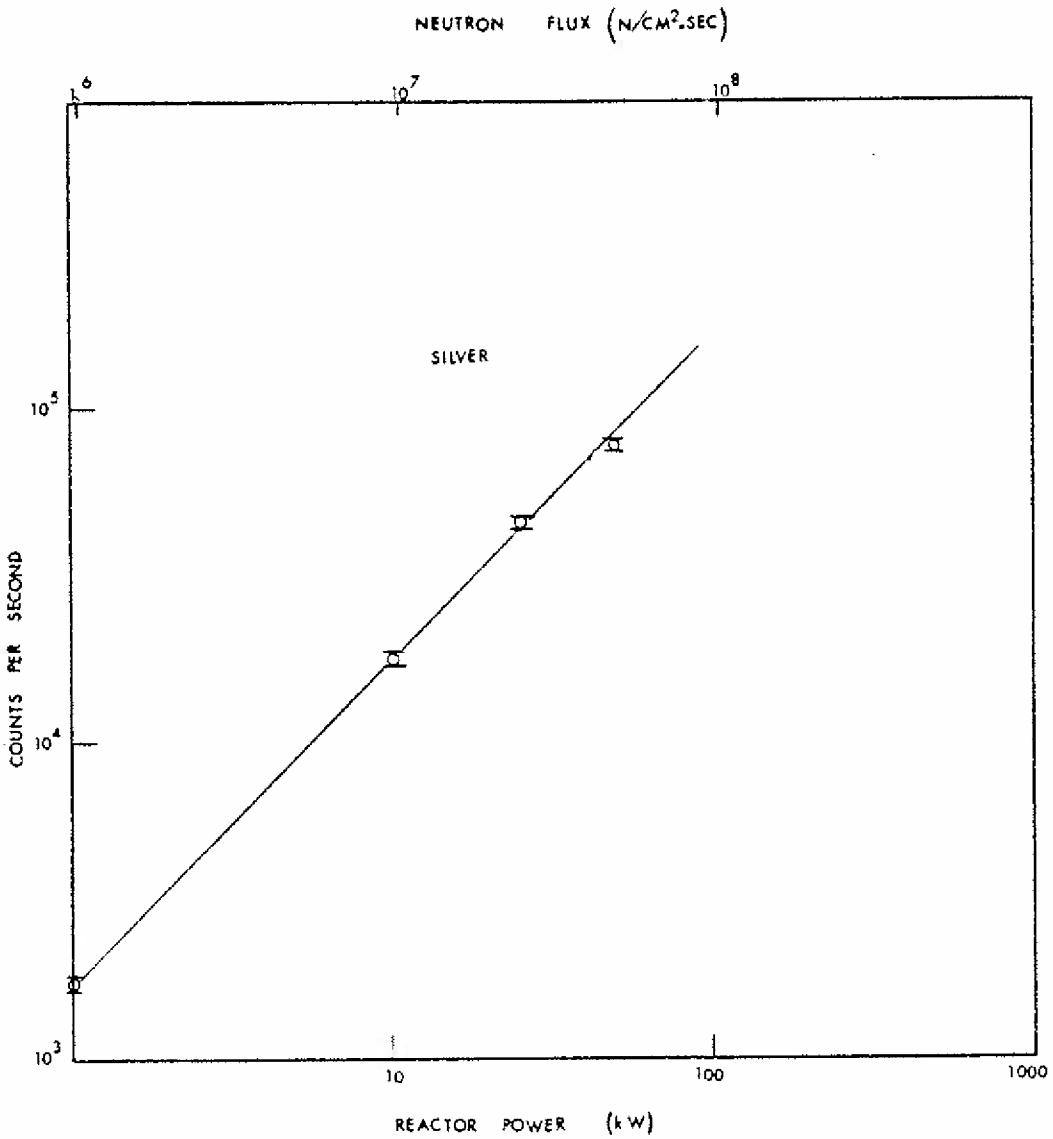


Figure 22. Count Rate vs Reactor Power and Neutron Flux of Silver Converter in the Biomedical Facility

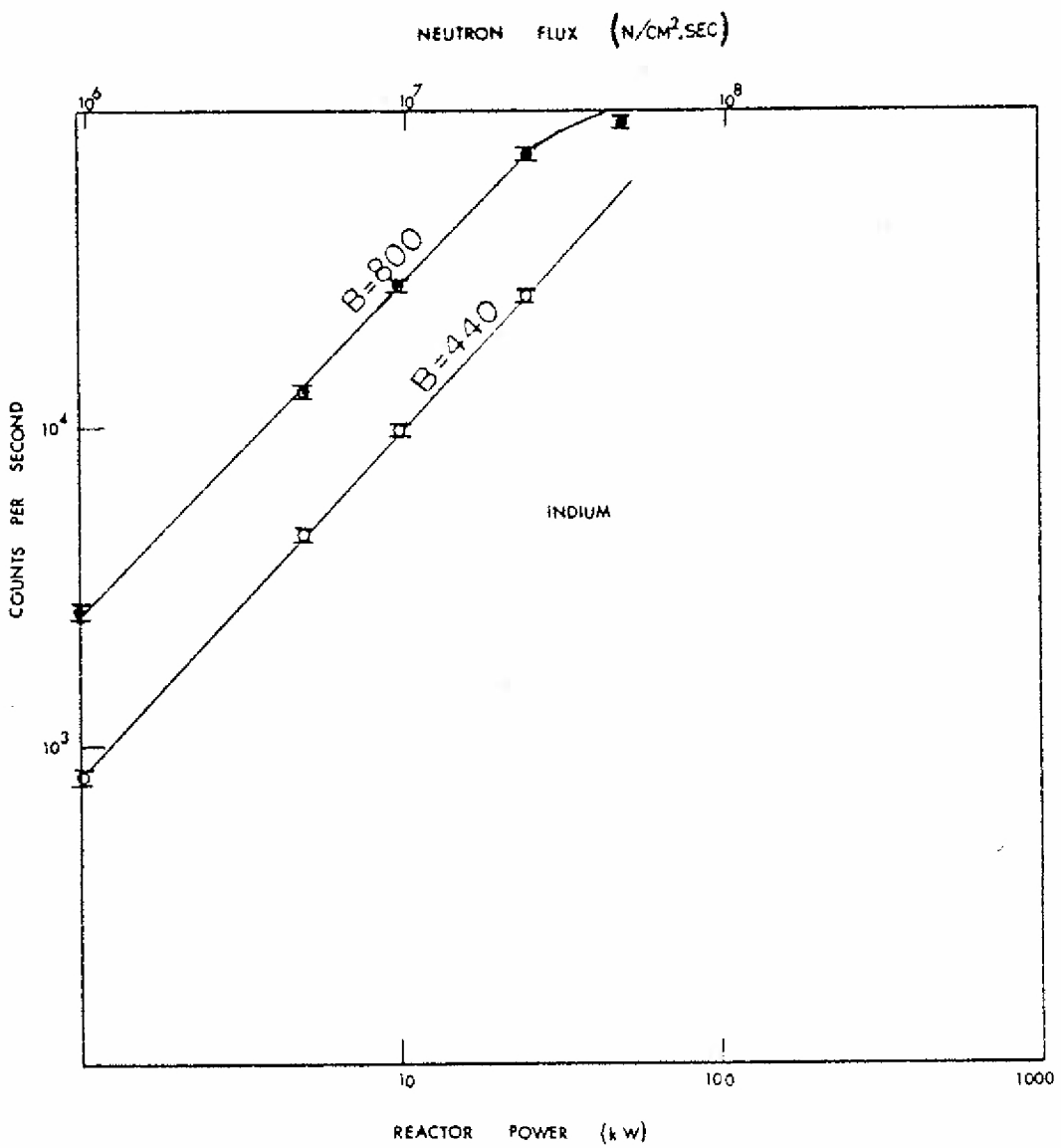


Figure 23. Count Rate vs Reactor Power and Neutron Flux of Indium Converter in the Biomedical Facility at Two Values of Magnetic Field

entry, the Gd converter (1.9 cm diameter) was placed at position A of Figure 24. This detector end was exposed to the diffracted neutrons from the H-3 beam hole at 1000 kW reactor power. The count rate was measured at magnetic fields of 600 and 1130 gauss (0.06 and 0.1130 $Wb/m^2$). The converter was then put at position C of the curved solenoid. The count rate was measured at the same two values of the magnetic fields. It was found that at 1130 gauss the counting efficiency dropped to 0.7 and at 600 gauss to 0.4 of the previous values. The magnetic field was then reversed and the counting increased to the first value again. This behavior is consistent with equation (3-15) for the drift velocity, $v_D$. The magnitude of this velocity is inversely proportional to the magnetic field and its direction is reversed when reversing the magnetic field. When the Gd foil was put in position B of the curved solenoid the count rate was 0.8 and 0.6 of the value when the converter was in position A at the two values of the magnetic fields.

The Gd converter was then put at the end of the long, straight solenoid and the electron detector system was put at the other end. The count rate was taken. The curved section was then added and the count rate was measured again. The efficiency dropped to 0.8 and 0.9 of the previous value when the curved section was removed at 600 and 740 gauss (0.074 and 0.06 $Wb/m^2$), respectively.

It can therefore be concluded that a loss in efficiency, of the order of 10% at 740 gauss, occurred which is acceptable in view of the other benefits to the performance of the system resulting from the use of the bent tube.

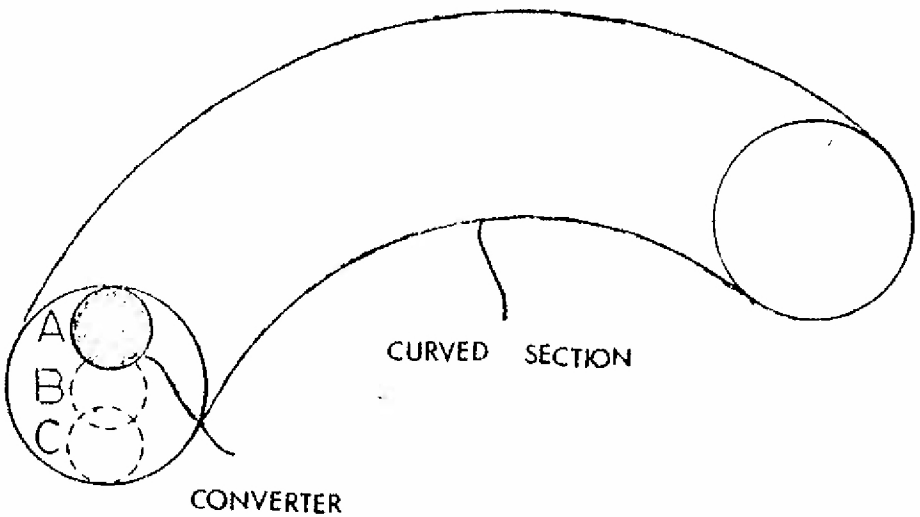


Figure 24. Position of Converter in the Curved Section of the Solenoid

## Effect of Pressure on the Count Rate

To test for the effect of gas pressure inside the device the gadolinium converter was used in the H-3 horizontal beam facility at 1000 kW. The complete device including the curved section was used. The response at 740 gauss is shown in Figure 25 together with the standard deviation. As expected there was some loss of output at higher gas pressures.

## Use of the H-8 Horizontal Beam Facility

The detector was now put into the H-8 horizontal beam facility to test the system in more realistic conditions since the H-8 looks directly toward the fuel element. A 120 cm long, 10.16 cm diameter graphite rod was placed in the beam. The detector shielding shown in Figure 13, as described before, was used. In spite of the shield, gamma photons were still able to reach the scintillator and give counts when the magnetic field was turned off. These gamma-rays were found to come from $^{41}Ar$ activity in the air and from leakage from the reactor through the focusing channel where they scatter at the curved section and hit the scintillator. The gamma-ray dose rate at the detector end where the neutron-sensitive material was mounted was measured using TLD-200 $CaF_2$:Dy thermoluminescent dosimeters. The results are shown in Table 2.

The count rate at different reactor power levels with zero magnetic field and at 740 gauss, at a pressure of $12 \times 10^{-3}$ torr, is shown in Table 3. The net count rate as a function of the reactor power and neutron flux is shown in Figure 26. The straight line was drawn using a least squares method. The neutron flux at the converter position was measured using

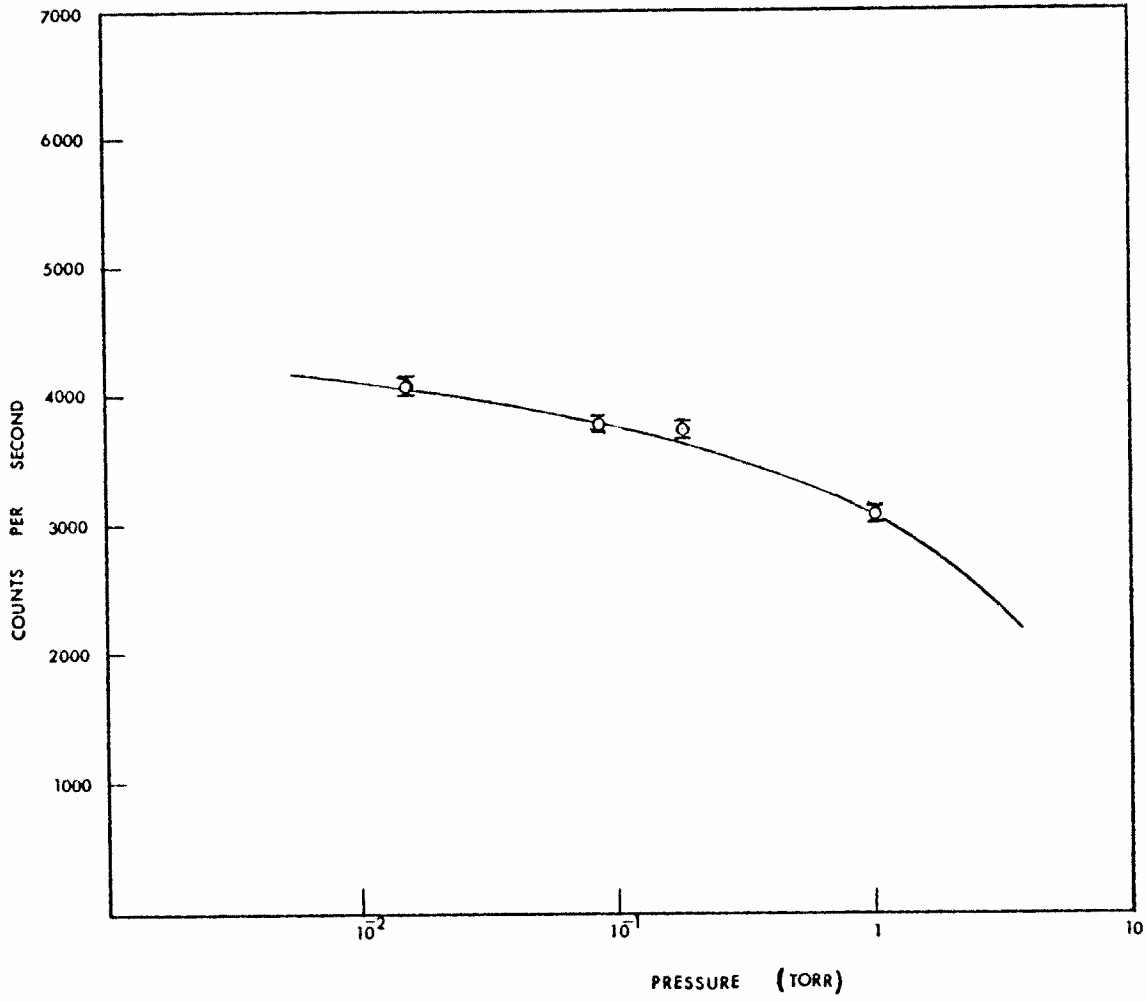


Figure 25. Count Rate vs Pressure of Gadolinium Converter in H-3 Beam Hole at 1000 kW

Table 2. Gamma-ray Background Fields: Beamport H-8 with Graphite Rod Inserted

| Reactor Power (kW) | Gamma Dose (R/hr) |
|---|---|
| 1 | 3 |
| 10 | 4.8 |
| 100 | 19.8 |
| 1,000 | 48 |

Table 3. Detector Count Rate at Different Power Levels with and without Magnetic Field

| Reactor Power (kW) | Neutron Flux ($n/cm^2 \cdot sec$) | Count Rate (c/s) | | | Standard Deviation |
|---|---|---|---|---|---|
| | | No Field | B = 740 Gauss (59 mT) | Net c/s | |
| 10 | $1.78 \times 10^4$ | 123 | 803 | 680 | 30 |
| 25 | $4.5 \times 10^4$ | 323 | 1,790 | 1,467 | 46 |
| 50 | $8.9 \times 10^4$ | 617 | 3,384 | 2,767 | 63 |
| 100 | $1.78 \times 10^5$ | 1,162 | 6,474 | 5,315 | 87 |
| 250 | $4.5 \times 10^5$ | 2,929 | 16,267 | 13,338 | 139 |
| 500 | $8.9 \times 10^5$ | 6,095 | 32,152 | 26,057 | 196 |
| 1,000 | $1.78 \times 10^6$ | 11,422 | 62,764 | 51,342 | 272 |

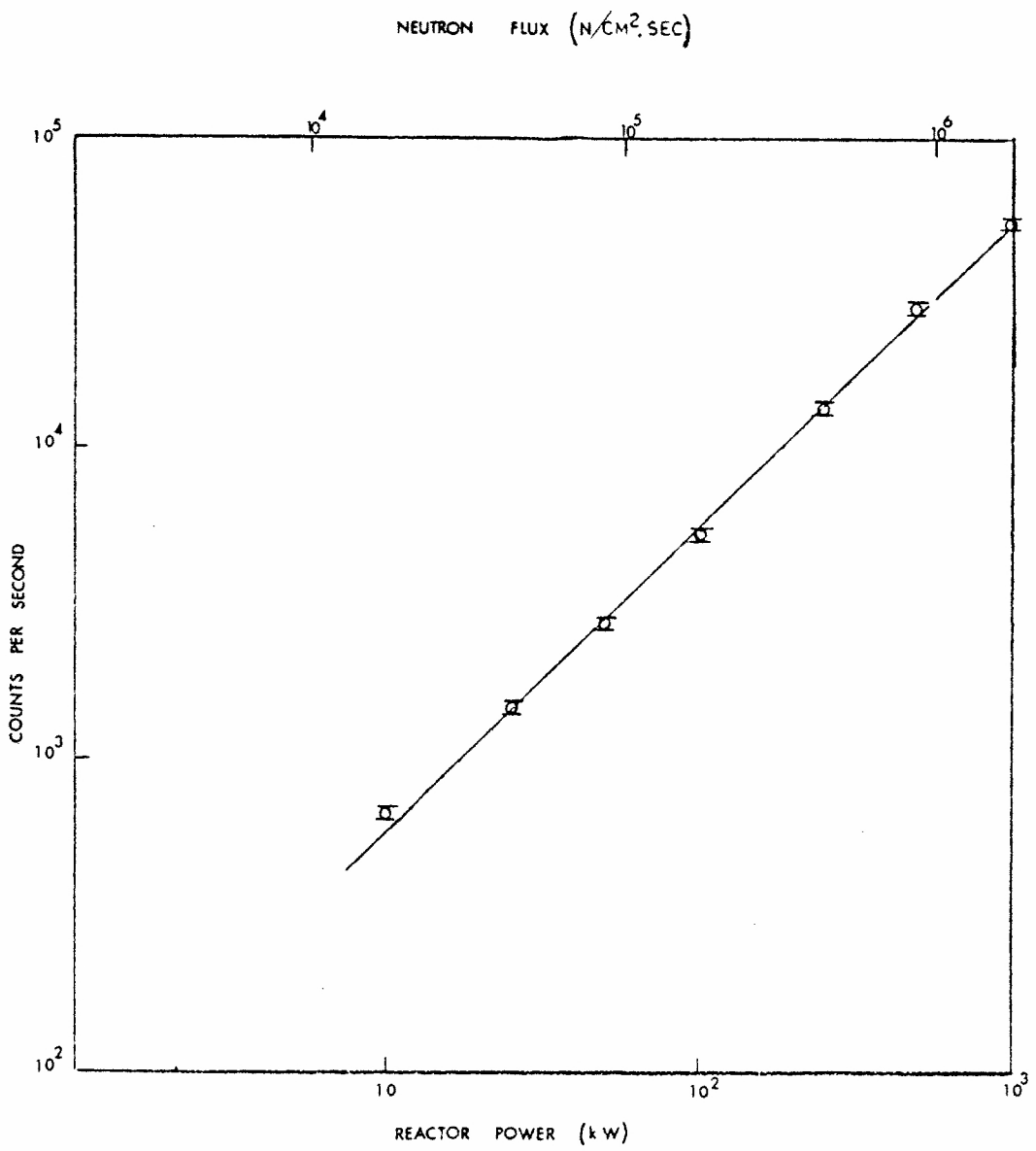


Figure 26. Count Rate vs Reactor Power and Neutron Flux of Gadolinium Converter in H-8 Beam Hole

gold foil, 0.1239 gram weight and 1.3 cm diameter. The cadmium ratio was eight. The standard deviation is also shown in the figure.

## Detector Time Response

To test the detector time response the count rate as a function of time was measured during reactor start up. The reactor power was increased by a factor of e (2.71828) per 100 seconds. The net detector count rate (gamma interference subtracted) is shown in Figure 27 and it is seen that a true exponential rise in count rate resulted (linear in a semilog plot). This indicates that the time response of a Gd converter detector is prompt. Since it takes a few nanoseconds for an electron to travel the tube, the time limiting factors are those associated with the electron counting system. The standard deviation is shown in the figure.

## Detector Sensitivity to Gamma-ray Interference

To test the effect of gamma-ray interference on the detector response, the graphite was removed from the beam. The neutron flux was $5.6 \times 10^8$ $n/cm^2 \cdot sec$ and the Cd ratio was measured as 5.5 using gold foil. The detector was then put across the beam direction as shown in Figure 28 where 1) is the beam shutter, 2) is the reactor, 3) is the beam plug, 4) is the boral sheet, 5) is the Cd sheets, 7) is the vacuum system, 8) is the power supply for the coil, 9,10) are the electron counting system, and 11) is the paraffin beam catcher. The reason for covering the beam catcher is that fast neutrons are thermalized in the paraffin and diffuse back to the detector position. The gamma-ray intensity in front of the beam then was 2000 R/hr at 1000 kW measured by a Nuclear-Chicago Cutie-Pie

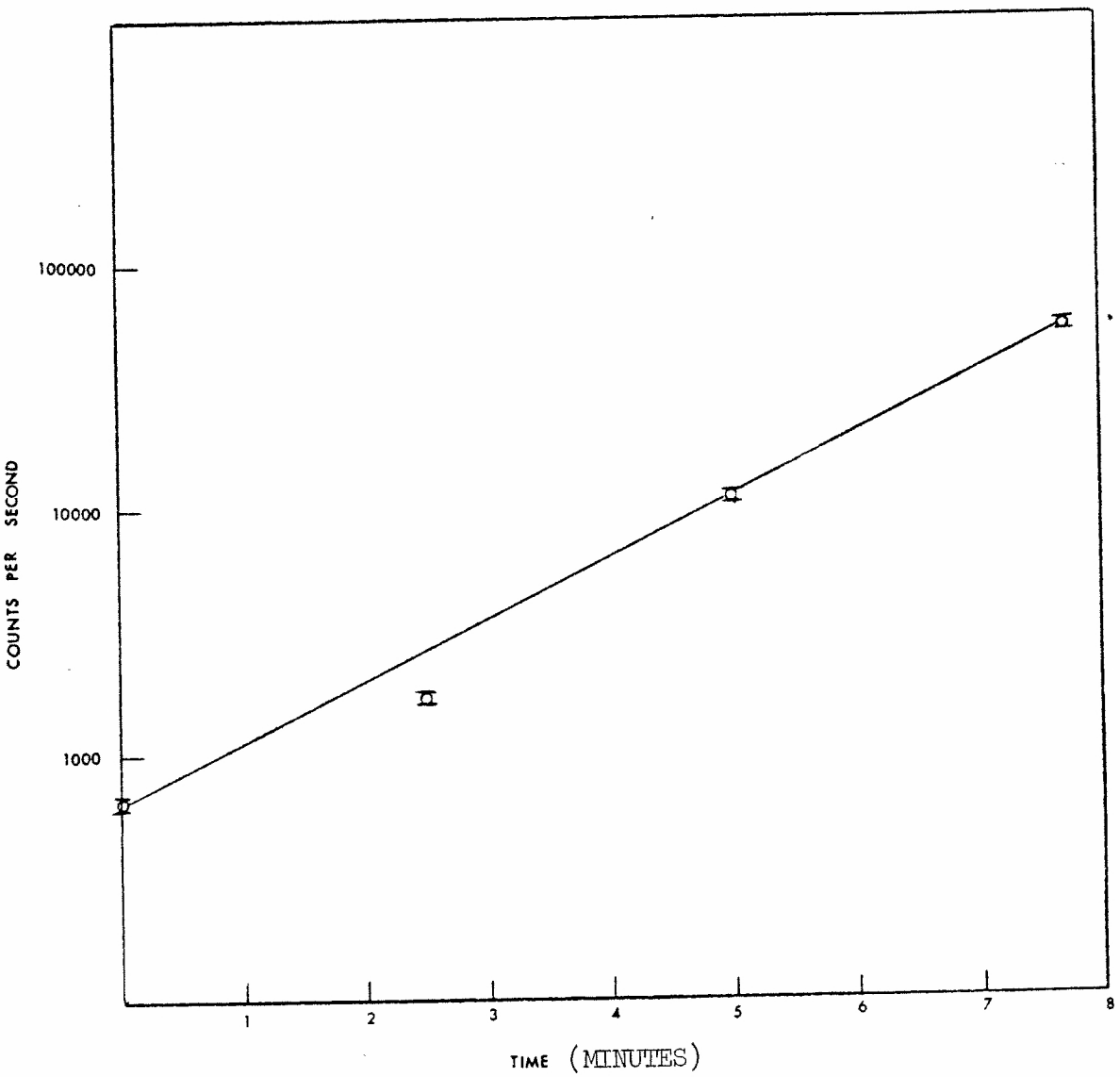


Figure 27. Count Rate vs Time During Reactor Start Up Using Gadolinium Converter

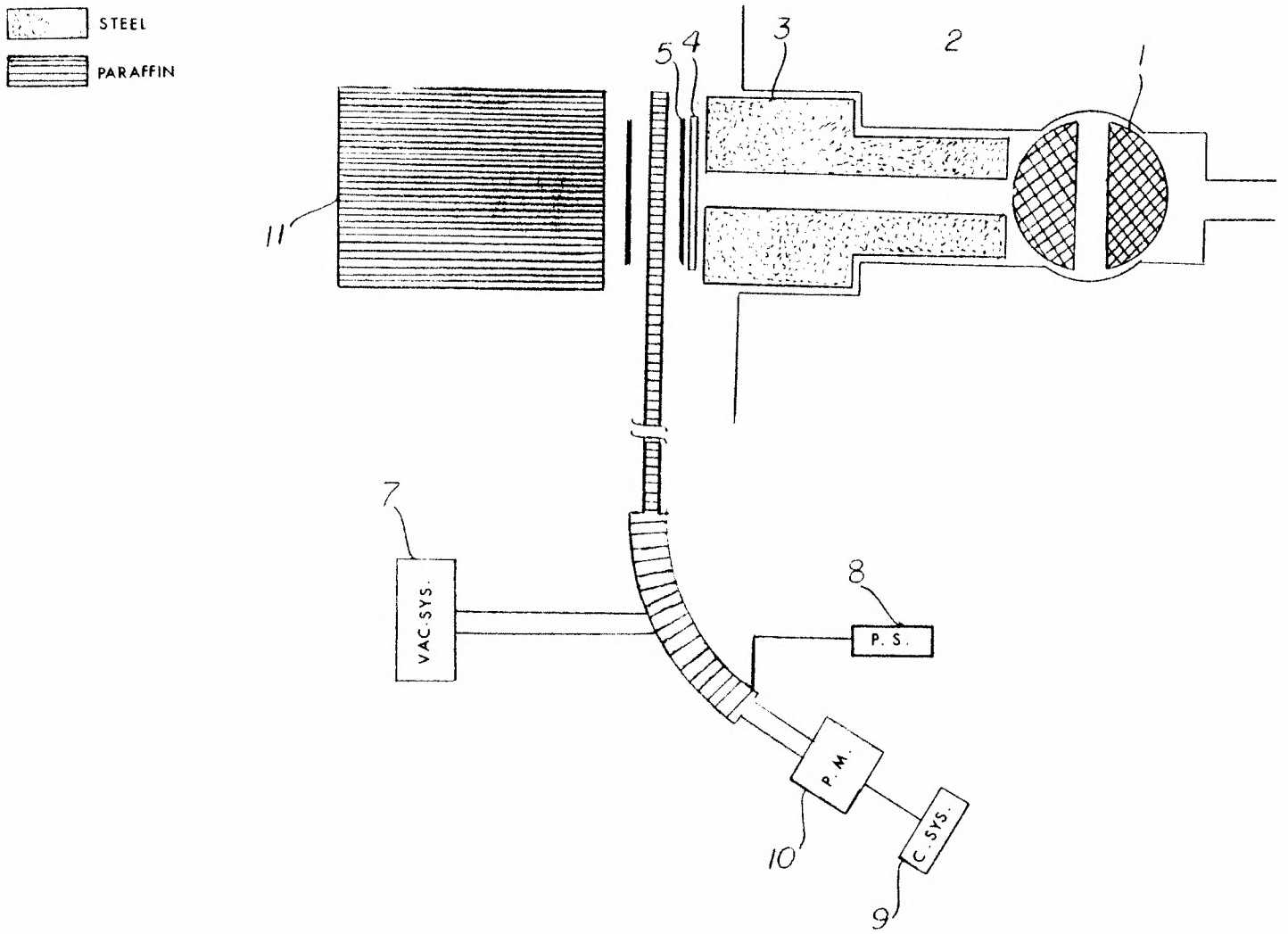


Figure 28. Schematic of Detector Solenoid Position for Intense Gamma Irradiation from H-8 Beam Hole

six-foot rigid-extension survey meter, model PC43. The gamma-ray intensity at the scintillation material position was 200 mR/hr at two meters away from the beam. The count rate at zero magnetic field was 26,051 c/s when the section of the detector containing the scintillator was shielded by 5-cm thick lead. When the magnetic field was set at 740 gauss no increase in the count rate was observed, indicating the insensitivity of the detector to gamma-rays hitting the tube walls. Different sections of the tube were exposed up to 120 cm from the curved section with no increase in the count rate when the magnetic field was applied.

When the section of the tube containing the neutron-sensitive material was in front of the beam, the count rate increased to 62,381 c/s at a magnetic field of 740 gauss. This increase is assumed to be mainly due to the effect of fast neutrons since gadolinium has a 1000 barn resonance peak at 2.5 eV and several hundred barn resonance peaks above 2.5 eV. This is just above the cadmium cut-off value.

# CHAPTER VI

# DISCUSSION OF RESULTS

## Detector Performance

### Linearity

Figures 20, 21, 22, 23, and 26 show that the detector response for all the converters is linear up to $5 \times 10^7$ $n/cm^2 \cdot sec$. The gadolinium converter detector was able to cover about five decades. In the upper margin the detector count rate is limited by the saturation of the electron counting system as shown in the upper curve of Figure 20. In our counting system reliable count rates were below $10^6$ counts per second. Using a faster counting system can extend this upper limit of the detector. The upper counting rate can also be extended by using a smaller amount of the converter material or using a smaller cross-section material. Both of these methods produce less flux depression but the latter method is preferred since the detector will have a longer life in the reactor. In these last two methods the detector sensitivity will be reduced thereby increasing the upper range, but it becomes more difficult to measure low neutron fluxes. Reducing the tube diameter will also reduce the sensitivity, increasing the upper limit of the detector and affecting the lower limit. This approach is desirable since it will lead to a thinner detector that will interfere less with the reactor design. An alternative method could be used which can extend the upper limit to any value desired. It is clear from Figure 19 that the detector sensitivity depends strongly

on the magnetic field. At a higher counting rate, reducing the magnetic field will prevent the detector from being saturated. Another way of reducing the sensitivity is by increasing the pressure, but this will be less practical since the gamma-ray can then ionize the residual gas and release electrons which can be focused; therefore, adjusting detector response by controlling the pressure is more difficult than by controlling the magnetic field.

In the lower range the detector count rate is limited by the pulse height distribution, the photomultiplier noise, and the background radiation. The pulse height distribution in scintillation detectors can affect the counting efficiency especially at low electron energies where a discrimination level has to be set against photomultiplier dark current. If the pulse distribution is close to the discrimination level, then a fraction of the pulse counts is lost. The statistical behavior of the system is the main reason for the pulse distribution. This is associated with the production of light in the scintillator, collecting the light at the cathode, secondary electron emission at the photocathode, collecting the electrons at the first dynode, and in multiplication of electrons (217). This statistical nature is more pronounced at lower energies since the number of light flashes per incident electron is low. In our system, less than one fourth of the light produced in the scintillator reached the photocathode, because of light collection geometry. Light beams hitting the light pipe at an angle less than the critical angle ($45^{o}$ in Plexiglas) will be lost. A small fraction of the light will be lost in transmission through the light pipe by internal absorption.

The back scattering of the incoming electrons also contributes to

the pulse distribution. Most scintillation materials have longer, less intense excited states which tend to produce more than one peak for single energy incident particles. At low energies the full energy peak is close or merges with the low amplitude section. This behavior can also widen the pulse distribution. In Pilot B plastic scintillators the long-lived states are more intense than in NaI(Tl) or anthracene.

The photomultiplier noise highly affects the lower limit of the counting rate (33,218). In our system, operated at room temperature, about 150 counts per second were measured at an amplification factor of 300 and a lower discrimination setting set at channel 5 in the Omega-1 multichannel analyzer. This leads to a practical, lower flux-measuring limit of the Gd converter detector operated with a magnetic field of 740 gauss and a pressure of $12 \times 10^{-3}$ torr to about $10^4$ nv where the count rate was 680 at $1.78 \times 10^4$ nv, about four times the detector noise. At an amplification factor of 1000 the noise level above channel 5 was very high and reached about 13,000 counts per second. All of the experimental measurements were made at an amplification factor of 300. It was also noticed that this noise differs from one type of photomultiplier to another and from one unit to another of the same type.

The thermal emission of electrons from the photocathode produces higher pulses than those coming from the dynodes since the former receive more amplification. This thermal noise problem can be reduced in theory by cooling the photomultiplier; this is not usually practical at the reactor face.

The ions produced by ionization of the residual gas in the tube can be accelerated toward the photocathode or the dynodes and eject elec-

trons that produce pulses. The photocathode has very high resistance and any leakage of current in the glass envelope produces non-negligible noise especially at higher voltage. Nonuniformity of the photocathode sensitivity over its surface will also produce nonuniform pulses.

In this experiment a high counting rate was usually obtained. A relatively high current will pass through the photomultiplier. In this case a redistribution of voltage will occur which tends to lower the pulse height and reduces the sensitivity and makes the detector nonlinear.

Sensitivity

The principal parameters of interest in any detector are its sensitivity and linearity. For an in-core detector one does not want or need an over-sensitive detector, since the incident flow of neutrons is so high that it would overwhelm a highly sensitive device. It is more important to maintain consistency of detection and linearity over the desired range of neutron flux values, and long-life performance considering that such devices usually have to operate unattended and in inaccessible locations.

The detector sensitivity obtained for the Gd converter detector was $2.9 \times 10^{-2}$ counts per second per unit flux at 740 gauss magnetic field (Figure 26), with indium, 0.076 cm thick, a sensitivity of $2.6 \times 10^{-3}$ counts per second per unit flux was obtained in a magnetic field of 800 gauss (Figure 23), whereas 0.038 cm of silver foil resulted in a value of $1.8 \times 10^{-3}$ counts per second per unit flux (Figure 22) and cadmium, 0.025 cm thick, resulted in a value of $1.3 \times 10^{-3}$ counts per second per unit flux (Figure 21). The reason for the relatively low

sensitivity of cadmium is that only 1.8 in each 100 neutrons absorbed contribute to the 95.7 keV separated level from which the 69 keV conversion electron is emitted.

In the gadolinium, 0.4 of the incident neutron beam is transmitted through the foil while it is 0.57 in the indium, 0.75 in the cadmium, and 0.87 in silver. These values were obtained by calculation. The thickness of these foils does not contribute to the detector sensitivity. The additional thickness is provided to allow electrons emitted to lose part of their energy in the source so that they can be focused easily. Thinner foils on which a low cross-section material is deposited can produce better results. The reason for the high sensitivity of the gadolinium converter detector is its high cross section. Since the cross section of the neutron-converter material depends on the neutron energy spectrum, the above mentioned values of the sensitivity will be different in a field of fast neutrons. For this reason some converter that may be unsatisfactory in a thermal neutron flux, like Gd, may not be so in a fast neutron flux.

The detector sensitivity does not depend only on the converter. Factors such as the electron counter sensitivity, magnetic field, diameter of the tube, and pressure inside the tube highly affect the detector sensitivity.

The plastic scintillator detector has good sensitivity for detecting low-energy electrons down to about 5 keV (215). Below this energy the photomultiplier noise interferes with the counting. The Channeltron electron multiplier with its high counting efficiency of 95% for electrons of energy down to 100 eV may be a good substitute for the scintillation

detector and may make a higher sensitivity neutron detector if good magnetic shielding is provided. It has the disadvantage of being unable to be used as a spectrometer.

As mentioned before, the magnetic field is an important factor in determining the detector sensitivity. The effect of the magnetic field on focusing beta particles from sulfur-35 is shown in Figure 19. Above about 550 gauss (0.055 $Wb/m^2$) the graph has a slope of 1.6 counts per second per gauss. If the count rate is 800 c/s, then a change of 0.2% will result from a change of one gauss in the magnetic field. It is also clear from the figure that at higher magnetic fields the count rate change per unit magnetic field change is more effective than that at lower magnetic field values.

The other factors which affect the sensitivity have been discussed before.

Sensitivity to Gamma-ray Field

The gamma-ray field is the largest source of interference in most existing detectors. In gas-filled detectors it may ionize the gas to saturation. It produces noise mainly in the cables, the means of transferring the information to the outside of the core. In this detector the magnetic focusing is used to carry the information to the outside. As was shown experimentally, this mean is completely insensitive to the gamma-rays. The detector was exposed to a gamma-ray dose rate of 2000 R/hr as described in the preceding chapter with no increase in the count rate above the background. Electrons emitted from the wall of the tube will make a tight spiral path and return back to the wall. The only important design feature here is to keep the electron scintillation detector and the photo-

multiplier away from any gamma-ray background since both of them are sensitive to gamma-ray photons. Using a solenoid of one or more curved sections prevents the gamma-ray streaming in the tube from reaching the electron counting system. Since this counting system is outside of the reactor, shielding it will not constitute a design problem but will reduce its sensitivity to the background.

Time Response

It is clear from Figure 27 that the response time of the Gd converter detector is prompt. All conversion electron converter detectors are expected to behave the same way. This is very important for safe control of the reactor. A time response of a few milliseconds or less is desired. Slower time response in detectors such as the self powered detector limits their use to flux mapping only. The fast response time of this detector makes it desirable for reactor control and monitoring subject only to avoid excessive burst effects. If a converter material with a half life of seconds is found, such as In or Ge, this will determine the approach to equilibrium; in general this will be more rapid than neutron-induced core transient response. If the detector response is of the order of minutes, a time lag would be introduced losing a major advantage over other detectors.

Reproducibility

Excellent reproducibility is obtained in this detector. Using the H-8 port the experiment was repeated every day for five days. No more than 1.5% deviation from the average value occurred. Only one time a small increase in the detector background was noticed with no magnetic field applied. The background was about 400 c/s, compared to 150 c/s

measured on other days. This is still much below the signal from the reactor. This increase was due to an increase of argon-41 in the air where the reactor was operating at 1000 kW until 2:00 a.m. in the morning and when the experiment was performed at 8:00 a.m. on the same day, the argon-41 activity was still in the air.

## Design Features

### Magnetic Coil

Since the solenoid may have to function in a high temperature region (about 700°C in an LMFBR), the melting point of the internal conductor and the insulator of the coil wire should be high. The internal conductor should also have a small temperature coefficient of resistivity. Copper has a temperature coefficient of resistivity equal to 0.00393/°C. A temperature rise of 50°C will reduce the current to 0.836 of its previous value. The magnetic field will be reduced by the same fraction. A change of 100°C will reduce the current to 0.72 of its initial value. Such a large variation in temperature is not expected at constant reactor power level. When a change in temperature accompanies a change in reactor power level, the detector response, using copper wire, will be slightly curved downward. This problem can be solved easily by using a power supply with a current regulator to give a steady output current or by using a material with a smaller temperature coefficient of resistivity. Constantan with a temperature coefficient of resistivity of $2 \times 10^{-6}/°C$ can be used. A change in temperature of 100°C will decrease the current and the magnetic field then to only 0.9998 of their initial value and a 700°C rise in temperature would reduce them to 0.9986 of their initial value.

The insulator used should have good thermal conductivity such that the heat generated by the coil will be dissipated easily. It should be thin enough not to add to the volume of the solenoid. Thick insulators are not needed since there is no electric field across these insulators and a small leakage current is not important.

In choosing the material of the coil attention should be paid to the change in magnetic properties with increased temperature such as the change in magnetic susceptibility and the Curie temperature. The coil material should also have a low neutron absorption cross section so that it will not affect the neutron flux being measured.

Tube System

The material of the tube, like the coil conductor, should have a high melting point, small absorption cross section, and small and stable magnetic susceptibility under increased temperature. In addition, it should have good mechanical strength to withstand the high pressure of the core. Aluminum has a small neutron absorption cross section (0.235 barn for thermal neutrons) but its melting point is low (659$^{o}$C). It can be used only in thermal reactors. Materials such as stainless steel, nickel, or some refractory alloys, e.g. Ti or Mo alloys, can make good materials for the tube. A tube made of a ceramic insulator material of high melting point cannot be used. The electric charge deposition on such materials with time will disturb the focusing of the electrons.

Instead of O-rings used in our experiment, welding or soldering the different parts would make the detector stable at high temperature and under high irradiation and would help to produce a better vacuum.

The inside diameter of the detector used was two centimeters. This size is practical for out-of-core detectors, but a smaller diameter is preferred for in-core detectors. A smaller diameter tube reduces the sensitivity as discussed earlier. Since the detector proved to have a relatively high sensitivity, a decrease in sensitivity may not be important. The reduction in sensitivity can be compensated by increasing the magnetic field strength.

Effect of Tube Curvature

It was shown that the detector lost about 10% of its count rate when the curved section was added to the straight detector at a magnetic field of 740 gauss (0.074 $Wb/m^2$). The fraction of the count rate lost depended on $v_D$, the drift velocity. This velocity depends on $v\cos\phi$, the component of the electron velocity parallel to the magnetic field, on the radius of curvature, and on the magnitude of the magnetic field. If it takes a time t for the electron to travel a curved tube making an angle of curvature $\Omega$, then

$$t = \frac{R\Omega}{v\cos\phi}$$

where R is the radius of curvature, v is the electron velocity, and $\phi$ is the angle between the magnetic field direction and the electron initial direction upon emission. The distance D that the electron will travel toward the tube wall is

$$D = tv_D$$

$$D = \frac{R\Omega}{v\cos\phi} \cdot \frac{m}{e} \frac{v^2\cos^2\phi}{RB} = \frac{m}{e} \frac{\Omega}{B} v\cos\phi$$

An electron having an energy of 100 keV emitted at $\phi = 45^{\circ}$ will drift 0.01 cm toward the wall if the angle of curvature $\Omega$ is $60^{\circ}$ and the magnetic field is 0.07 $Wb/m^2$.

D in the above equation is independent of R. This is not strictly true in an actual situation because the drift velocity was derived assuming that the radius of curvature is much larger than the radius of the spiral path of the electron. The distance D will be independent of R only when R is much larger than the electron radius of revolution. From the above equation we see that electrons of higher velocity drift faster to the wall. This is an advantageous characteristic since higher energy electrons emitted due to gamma-ray interaction will drift faster to the wall and will not survive passing the curvature. To reduce the fraction of electrons lost in the curvature either the magnetic field or the tube diameter should be increased in this section. The increase in the diameter will not interfere with the reactor component since it will be outside of the reactor.

## Possible Sources of Error in the Experiment

It was noticed that the temperature of the coil increased during the experiment. This behavior was expected. The resistance of the copper wire due to increase in the temperature reduced the current in the coil and decreased the count rate. A decrease in the count rate down to 0.95 of the initial value was observed at an elevated coil temperature. The solution to this problem was discussed earlier.

The power supply that provides the voltage to the solenoid was fairly stable. A stability of 0.1% was reported. This means that at a

magnetic field of 740 gauss (0.074 $Wb/m^2$) a variation of 0.74 gauss (0.000074 $Wb/m^2$) exists. It is clear from Figure 19 that the effect on the counting rate is negligible; therefore, no great error was expected from the power supply of the coil.

A negligible error was expected from the variation in pressure. The increase in the coil temperature may increase the tube degassing but, as we have seen before, the detector is fairly insensitive to pressure variation if the pressure is below about $10^{-2}$ torr. In Figure 25 the count rate of the Gd converter detector dropped 1.1 count per second per micron. This corresponds to a fraction of the $2.6 \times 10^{-4}$ drop of the initial count rate. No more than a few microns of change in pressure was observed at a pressure of $12 \times 10^{-3}$ torr.

The power supply that provided the voltage to the photomultiplier had fairly good stability, as previously reported. At a high count rate the current in the tube will be relatively high and this tends to produce a change in the distribution of the voltage in the tube. The magnitude of error introduced by this variation is not expected to be high.

The background radiation due to gamma-ray photons hitting the scintillation detector and producing counts depends on the power level of the reactor. This background was measured at zero magnetic field where no focusing effect is produced and was subtracted from the total count rate.

The burn-up effect caused negligible changes in the experiment since the experiment occurred over a time short compared with that needed for such a correction to become significant. The burn up of the foil ma-

terial is governed by the equation

$$\frac{N}{N_0} = e^{-\sigma\Phi t}$$

where N is in the number of the target atoms at any time t after exposing the target to the neutron flux $\Phi$, $N_0$ is the initial number of atoms, and $\sigma$ is the absorption cross section.

We can conclude that the systematic error is small in this experiment. The pressure stability was good and only a negligible error might be introduced. The magnetic field stability depends on the stability of the current in the coil. No more than 5% reduction in the value of the current was allowed; therefore, a maximum error of 5% occurred at elevated temperatures. This error and the statistical standard deviation are the main two sources of the resulting fluctuation.

## Stability

The short term performance of the detector depended mainly on the stability of the current in the coil and the gamma-ray background reaching the scintillator directly. Impurities in the neutron converter may produce some interfering signals as well.

The long term performance may be affected by increased pressure inside the tube due to the high temperature environment. For this reason the tube should be baked in vacuum for a long time before being used. Aging of the electron counting system, especially the photomultiplier and the scintillator, may reduce the sensitivity with time. Radiation damage is not likely to produce instability in the system. The coil conductivity may change slightly under irradiation but the high temperature of the reactor anneals the damage. The burn-up effect also changes the sensitivity with time as discussed before.

# CHAPTER VII

## CONCLUSIONS

It is felt that the research described in this dissertation has indicated the basic feasibility of the proposed device over the range of flux values and fluences employed. The detector insensitivity to gamma-ray interference, its linearity, good neutron sensitivity, wide range, reproducibility, and expected stability in a high temperature environment are the bases for this conclusion. The detector may become a successful neutron flux measuring device in fast and thermal reactors.

Further study on this detector is needed to make it more suitable for practical applications. Decreasing the tube diameter is important in order that the detector will not interfere with other reactor components. A study of the detector response as a function of the tube diameter and magnetic field will help to obtain a better understanding of the detector characteristics.

Further studies are needed on the effect on the electron focusing of bending the magnetic field. This can be done using a photographic emulsion at different positions inside the tube and tracing the electron beam. The effect of the radius of curvature on the electron focusing can be observed by using several curved sections of different radii of curvature in turn at various solenoid currents. An alternative way of bending the electron path can be obtained by using a combination of electric and magnetic fields.

An alternative way of using an electron counting system could be tried using a magnetically shielded Channeltron or other direct electron multiplier.

In this research the detector behavior was studied mainly in thermal neutron fluxes. A study of the detector response in fast neutron fluxes is important since the detector was basically designed to detect fast neutrons.

The detector characteristics should be studied using more favorable tube and coil materials which were suggested in earlier chapters.

# BIBLIOGRAPHY


1. Liquid Metal Fast Breeder Reactor Program Plan, USAEC Rept. WASH-1104, August 1968, Task 4-7.1, 4-7.2.

2. B. B. Rossi and H. H. Staub, "Ionization Chambers and Counters," McGraw-Hill, New York, 1949.

3. "Feasibility Study of In-Core Flux Monitoring with Regenerating Detectors," USAEC Rept. HW-73335, June 1962.

4. J. Shaw, "Reactor Operation," Pergamon Press, Oxford, 1969.

5. A. Goodings and D. L. Roberts in "Neutron Dosimetry," IAEA, Vienna, 1963.

6. L. Satyanaraya and E. V. R. Rao in "Nuclear Electronics," IAEA, Bombay, 1965.

7. D. P. Roux, J. C. Gundlach, and S. H. Hanauer, Trans. Amer. Nucl. Soc. 7, 54 (1964).

8. R. Aves, D. Barnes, and R. B. MacKenzie, J. Nucl. Energy 1, 110 (1954).

9. W. Bear and R. T. Bayard, Rev. Sci. Inst. 24, 138 (1953).

10. W. D. Allen and A. T. G. Furguson, J. Nucl. Energy 2, 138 (1953).

11. W. R. Loosemore, R. P. Henderson, and G. Knill in "Neutron Dosimetry," IAEA, Vienna, 1963.

12. R. C. Rohr, E. R. Rohrer, and R. L. Macklin, Rev. Sci. Inst. 23, 595 (1952).

13. S. H. Hanauer, Third Int. Conf. on Peaceful Uses of Atomic Energy 8, 395 (1965).

14. R. A. DuBridge, "In-Core Power Monitoring of Nuclear Reactors," Atomic Power Equipment Department, General Electric Company Rept. GEMP-3914, April 15, 1962.

15. D. Harrison, I. Wilson, and R. J. Cox in "Nuclear Electronics," IAEA, Bombay, 1965.

BIBLIOGRAPHY (Continued)

16. A. Goodings in "Radiation Measurement of Nuclear Power," Inst. Phys. and Physical Soc. Conf. 2, London, 1966.

17. R. J. Cox, D. Harrison, and A. Goodings in "Nuclear Electronics," IAEA, Bombay, 1965.

18. C. C. Scott, chapter 9 in "Fast Breeder Reactor," J. G. Yevick, Editor, M.I.T. Press [c 1966].

19. P. B. F. Evans, p. 765, "Fast Breeder Reactor," P. V. Evans, Editor, Proc. of the London Conf. on Fast Breeder Reactors, May 17-19, 1966.

20. N. C. Hoitink and D. C. Thompson, USAEC Rept. HEDL-TME-47, 1971.

21. N. C. Hoitink and D. C. Thompson, USAEC Rept. HEDL-SA-192, September 21, 1971.

22. N. C. Hoitink and M. R. Wood, Trans. Amer. Nucl. Soc. 15, No. 2, 851 (1972).

23. D. P. Roux, USAEC Rept. ORNL-TM-3959, December 1972.

24. D. P. Roux, J. T. DeLorenzo, and C. W. Ricker, Nucl. Appl. Tech. 9, 736 (1970).

25. M. Hara in "Nuclear Power Plant Control and Instrumentation," IAEA, Vienna, 1972.

26. G. J. Dau and M. V. Davis, Nucl. Sci. Eng. 25, 223 (1966).

27. K. G. Kerris, C. C. Berggvan, D. B. Carter, and G. G. Spehar, Trans. IEEE NS-16(6), 264 (December 1969).

28. Argonne National Laboratory Reactor Development Progress Report, April-May, 1969.

29. F. E. Terry, "Effects of Transient Radiation on Transducers and Electrical Cables," IDO-16914, November 1963.

30. F. E. Terry, "Transient Radiation Effects on Transducers, Devices, and Electrical Cables," IDO-17103, November 1965.

31. J. L. Stringer and R. R. Bourassa, USAEC Rept. BNL-749.

32. R. W. Levell, USAEC Rept. AEEW-M-369.

BIBLIOGRAPHY (Continued)


33. Y. K. Akimov, chapter 1 in "Scintillation Counters at High Energy Physics," Academic Press, New York, 1965.

34. A. Pearson in "Nuclear Power Plant Control and Instrumentation," IAEA, Vienna, 1972.

35. W. Bastl in "Nuclear Power Plant Control and Instrumentation," IAEA, Vienna, 1972.

36. H. L. Olesen, "Radiation Effects on Electronic Systems," Plenum Press, 1966.

37. R. A. Wullaert, R. J. Burian, J. B. Melehan, M. Kangilaski, and J. E. Gates, chapter 6 in "Effect of Radiation on Materials and Compounds," J. F. Kircher and R. E. Bowman, Editors, Reinhold Publishing Co., New York, 1964.

38. Y. Plaige and R. Quenee, Trans. IEEE NS-14, No. 1, 247 (February 1967).

39. R. M. Lichtenstein, U. S. Patent #2,903,591.

40. R. A. Dubridge, Trans. IEEE NS-14, No. 1, 241 (February 1967).

41. J. P. Neissel, Trans. Amer. Nucl. Soc. 8, 64 (1965).

42. J. P. Neissel, "Theory of Campbell System of Reactor Instrumentation," Quarterly Progress Report, General Electric Co. Rept. GEAP-4747, 1964.

43. W. D. Allen, "Neutron Detectors," George Newnes, Ltd., 1960.

44. A. J. Lockwood, F. R. Woods, and E. F. Bennett, Rev. Sci. Inst. 25, 446 (1954).

45. R. K. Soberman and S. A. Korff, Rev. Sci. Inst. 24, 1058 (1953).

46. A. Milojevic, M. Kurepa, and S. Ribnikar, Second United National International Conference on the Peaceful Uses of Atomic Energy, Geneva 14, 325 (1958).

47. P. G. Salmon and S. Pyrah, Proc. Inst. Elect. Eng., Part 105B, 349 (1958).

48. W. Abson, R. J. Cox, and A. L. Gray, Second U.N. Int. Conf. on the Peaceful Uses of Atomic Energy 11, 298 (1958).

BIBLIOGRAPHY (Continued)


49. D. Roux, "Nuclear Electronics," IAEA, Bombay, November 22-26, 1965.

50. J. W. Hilborn, Nucleonics 22, No. 2, 69 (February 1964).

51. M. G. Mitelman, R. S. Erofeev, and N. D. Rozenblyum, Soviet Atomic Energy 10, 70 (1961).

52. W. R. Loosemore and G. Knill in "Radiation Measurement in Nuclear Power," Institute of Physics and Physical Soc. Conf. 2, London, 1966.

53. J. F. Boland, "In-Core Instrumentation," Gordon and Breach Science Publishers, New York, 1970.

54. H. Stevens in "Nuclear Power Reactor Instrumentation System Handbook," Edited by J. M. Harrer and J. G. Beckerley, TID 25952-P.1, Argonne National Laboratory, 1973.

55. H. J. Worsham and R. M. Ball, Trans. Amer. Nucl. Soc. 8, 579 (1965).

56. J. Kinzer, Trans. Amer. Nucl. Soc. 8, 579 (1965).

57. H. D. Warren, Nucl. Sci. and Eng. 48, 331 (1972).

58. W. W. Hudritsch, Nuclear Tech. 18, 25 (April 1973).

59. M. N. Baldwin and J. E. Rogers, Trans. IEEE NS-16, No. 1, 171 (1969).

60. O. Strindehag and B. Söederlund, Nucl. Inst. Meth. 78, 173 (1970).

61. C. C. Price and J. R. Karvinen, Trans. Amer. Nucl. Soc. 15, 366 (1972).

62. A. G. Edward in discussion in "Nuclear Measurement in Reactor Power," Institute of Physics and Physical Soc., London, 1966.

63. G. Casarelli, B. Chinaglia, L. Ciuffolotti, M. Coli, E. Denti, A Drago, G. Fogagnolo, M. P. Luboz, A. Massaglia, P. Pizzi, A. Rossi, and R. Somigliana in "Neutron Dosimetry," IAEA, Vienna, 1963.

64. R. F. Byars, USAEC Rept. DPSPU-30-5, 1967.

65. K. Mochizuki, K. Matsuno, S. Shirayama, A. Sekiguchi, and A. Toraishi in "Nuclear Power Plant Control and Instrumentations," IAEA, Vienna, p. 757, 1973.

BIBLIOGRAPHY (Continued)

66. R. C. Hawkings, "Neutron Flux Monitors and Thermocouples for In-Core Measurements," AECD-2033, CRL-85, 1964.

67. J. W. Hilborn, Trans. Amer. Nucl. Soc. 6, Supp. 1, 33 (October 22, 1963).

68. G. Ramirez and L. David, Nucl. Inst. Meth. 85, 279 (1970).

69. C. N. Jackson, Jr., USAEC Rept. BNWL-395, Battelle Northwest Laboratory, April 1967.

70. R. Cervalloti, R. Gislon, and B. Rispoli, Nucl. Inst. Meth. 45, 221 (1966).

71. G. Barbaras, "The Design and Construction of Boron Coated Thermopile for Use in Neutron Field," AECU-2975, June 2, 1950.

72. A. C. Lapsley, Nucleonics 11, No. 5, 65 (May 1953).

73. J. M. Harrer, Nucleonics 11, No. 6, 35 (June 1953).

74. L. Labno, W. Dabeck, and W. Byszewski, Nukleonika 5, 685 (1960).

75. T. S. Gray, W. M. Grim, Jr., F. S. Replogle, Jr., and R. H. Spencer, Trans. Amer. Inst. Elec. Engineer 76, Part 1, 678 (1957).

76. D. Robertson, "Neutron Sensitive Thermopile for Reactor Applications," Progress Report No. 1, Rept. AECU-3416, 1956.

77. K. E. Watkins, "Performance of Miniature High Temperature High Level Neutron Sensitive Thermopile," USAEC Rept. KAPL-M-KEW-1, December 9, 1968.

78. T. R. Herold, Nucleonics 13, No. 5, 64 (May 1955).

79. A. C. Lapsley, Nucleonics 16, No. 2, 106 (February 1958).

80. Y. K. Guskov and A. V. Zvonarev, Inst. and Exp. Tech. 5, 821 (1959).

81. R. G. Morrison, "Application of Miniature Intrinsic Thermocouples for Reactor Transient Diagnostics," Los Alamos Scientific Lab. Rept. LA-3313, 1965.

82. Advanced Reactor Technology Quarterly Report for Period Ending April 30, 1967, Loa Alamos Laboratory Rept. LA-3708 (Pt. 1), 1967.

BIBLIOGRAPHY (Continued)


83. R. A. DuBridge in "Neutron Dosimetry," IAEA, Vienna, 1963.

84. J. E. Kinzer and E. L. Bobble, Trans. Amer. Nucl. Soc. 11, 336 (1968).

85. R. G. Morrison and D. B. Stillman, "Fission Couple Application Toward Reactor Diagnostics Safety," Los Alamos Laboratory Rept. LA-3470-MS, 1966.

86. R. G. Morrison in "Fast Burst Reactors," Proc. of National Topical Meeting Held at Albuquerque, New Mexico, January 28-30, 1969, CONF. 690102, p. 519.

87. D. B. Stillman and R. L. Chaney, "Recent Advances in Fast-Response Miniature Neutron Flux Monitors," Los Alamos Scientific Laboratory Rept. LA-4126, 1969.

88. C. K. Fairchild, J. P. Berting, W. C. McCreary, and P. G. Salgade, "Vapor Deposition in the Fabrication of Fission Thermocouples," 1966.

89. L. D. Posey and J. V. Walker, Trans. Amer. Nucl. Soc. 11, 342 (1968).

90. D. F. Paddleford, A. Weitzberg, J. O. Zane, and L. I. Moss, Trans. Amer. Nucl. Soc. 7, 384 (1964).

91. G. R. Dittbenner, "Development and Application of the Intrinsic Thermocouple for Fast Response," Lawrence Radiation Laboratory Rept. UCRL-14593, 1966.

92. E. Lewis, "Nuclear Reactor Detection and Measurement Devices," USAEC Rept. KAPL-M-6961, October 1968.

93. R. G. Morrison, "Instrument Development Branch Annual Report--1967," Phillips Petroleum Co., Idaho Atomic Energy Division Rept. IDO-17269, 1968.

94. L. S. Mins, U.S. Patent #2,997,587.

95. P. D. Wickersham, D. L. Rall, and W. H. Giedt, U.S. Patent #3,028,494.

96. L. J. Gee, "Design and Developments of Fast Response Thermopile-type Neutron Sensitive Device," Advanced Technology Lab. Div. of Division of American Standard Rept. ATL-124, 1962.

BIBLIOGRAPHY (Continued)


97. Z. P. Azary, J. R. Burnett, and C. W. Sandifer, TCC Control Systems Transducer Evaluation, Wire Evaluation, and Calorimetric Detector Development, Edgerton, Germechausen and Grier, Inc. Rept. EGG-1183-2019, 1964.

98. G. G. Eichholz, Nucl. Inst. Meth. 94, 131 (1971).

99. J. L. Bloom, U.S. Patent #3,226,547.

100. D. J. Hughes, "Pile Neutron Research," Addison-Wesley, Reading, Mass., 1953.

101. "Standard Method for Measuring Neutron Flux by Radioactivation Techniques," Annual ASTM Part 30, p. 795, 1973, E261-70.

102. W. Zobel, "Experimental Determination of Correction to the Neutron Activation in Gold Foil Exposed in Water," ORNL-3407, April 4, 1963.

103. E. D. Klema and R. H. Ritchie, Phys. Rev. 87, 167 (1952).

104. T. L. Gallagher, Nucl. Sci. Eng. 3, 110 (1958).

105. A. Sola, Nucleonics 18, No. 3, 78 (March 1960).

106. M. W. Thompson, J. Nuclear Energy 2, 286 (1965).

107. G. S. Stanford, Trans. Amer. Nucl. Soc. 5, 33 (1962).

108. D. Ilberg and Y. Segal, Nucl. Inst. Meth. 61, 93 (1968).

109. R. H. Ritchie and R. B. Eldridge, Nucl. Sci. Eng. 8, 300 (1960).

110. G. R. Dalton and R. K. Osborn, Nucl. Sci. Eng. 9, 198 (1961).

111. K. H. Beckurtz and K. Wirtz, "Neutron Physics," Springer-Verlag, 1964.

112. B. Burtt, Nucleonics 5, No. 8, 28 (August 1949).

113. M. A. Greenfield, Nucleonics 15, No. 3, 57 (March 1957).

114. B. L. Cohn, Phys. Rev. 81, 184 (1951).

115. G. K. Schweitzer and R. B. Stien, Nucleonics 7, 65 (September 1950).

116. F. J. Jankowski, Trans. Amer. Nucl. Soc. 6, 205 (1963).

BIBLIOGRAPHY (Continued)


117. C. W. Title, Nucleonics 9, No. 1, 61 (July 1951).

118. M. A. Greenfield, R. L. Koontz, and A. A. Jarrett, Nucl. Sci. Eng. 2, 246 (1957).

119. C. W. Tittle, Nucleonics 8, No. 6, 5 (June 1951).

120. "Standard Method for Measuring Thermal Neutron Flux by Radioactivation Techniques," Annual ASTM, Part 30, p. 806, 1973, E262-70.

121. "Standard Method for Measuring Fast Neutron Flux by Radioactivation of Iron," Annual ASTM, Part 30, 0. 814, 1973, E263-70.

122. "Standard Method for Measuring Fast Neutron Flux by Radioactivation of Nickel," Annual ASTM, Part 30, p. 814, 1973, E264-70.

123. "Standard Method for Measuring Fast Neutron Flux by Radioactivation of Sulfur," Annual ASTM, Part 30, p. 825, 1973, E265-70.

124. "Standard Method for Measuring Fast Neutron Flux by Radioactivation of Aluminum," Annual ASTM, Part 30, p. 830, 1973, E266-70.

125. "Standard Method of Test for Fast Neutron Flux by Analysis of Molybdenum-99 Produced by Uranium-238 Fission," Annual ASTM, Part 30, p. 1251, 1973, E393-69T.

126. "Tentative Method for Measuring Fast Neutron Flux for Analysis for Barium-140 Produced by Uranium-238 Fission," Annual ASTM, Part 30, p. 1251, 1973, E393-69T.

127. R. A. Wiesmann and S. N. Ehrenpreis, U.S. Patent #3,263,081.

128. B. V. Hatcher, U.S. Patent #3,598,996.

129. J. P. Spaa, U.S. Patent #3,140,396.

130. J. W. Knapp, Trans. Amer. Nucl. Soc. 6, 3 (1963).

131. A. Danis, F. Rebigan, N. Savu, and M. Sandue, Rev. Roum. Phys. 16, No. 10, 1213 (1971).

132. R. H. Sardina, H. Plaza, and D. S. Sasscer, Trans. Amer. Nucl. Soc. 15, Supp. 1, 18 (1972).

133. M. R. Melendez, Thesis, Puerto Rico Nuclear Center, PRNC-166.

BIBLIOGRAPHY (Continued)

134. C. Papastergiou and J. H. Swanks, "Neutron Flux Measurements Using Monitor Pairs," Oak Ridge National Laboratory Rept. CONF 730819-2, 1972.

135. F. F. Fritzen and W. A. Jester, Trans. Amer. Nucl. Soc. 10, 450 (1967).

136. E. M. Page, R. E. Horne, and J. Montfort, Trans. Amer. Nucl. Soc. 8, 244 (1965).

137. W. Kohler, Atomkernenergie 15, 263 (1970).

138. D. A. McCune, U.S. Patent #3,125,678.

139. A. Withop, B. A. Hutchins, and G. C. Martin, General Electric Company Rept. GEAP-5744, January 1969.

140. E. M. Page and R. E. Horne, Trans. Amer. Nucl. Soc. 10, 267 (1967).

141. A. Hins, Proc. Third International Symposium on Material for Nuclear Measurements, USAEC Rept. CONF-711002, 1971.

142. J. L. Jackson and B. L. Combs, Trans. Amer. Nucl. Soc. 15, 767 (1972).

143. E. E. Drucker, Nucl. Sci. Eng. 3, 215 (1958).

144. H. P. Spracklen, Trans. IEEE NS-14, No. 1, 271 (February 1967).

145. P. G. Mallory, Trans. IEEE NS-17, No. 1, 520 (1970).

146. S. A. Scott and A. Notea, Trans. Amer. Nucl. Soc. 8, 70 (1965).

147. J. Moteff, chapter 21 in "Radiation Dosimetry," Edited by F. H. Attix and E. Tochilin, Academic Press, New York, 1968.

148. P. R. Byerly, Jr., chapter in "Fast Neutron Physics," Edited by J. B. Marion and J. L. Fowler, Inter-Science Publishers, 1960-1963.

149. B. L. Cohn, Nucleonics 8, No. 2, 29 (February 1951).

150. G. Dearnaley and D. C. Northrop, "Semiconductor Counter for Nuclear Radiation," London SPON, 1966.

151. J. M. Taylor, "Semiconductor Particle Detectors," Butterworths, London, 1963.

BIBLIOGRAPHY (Continued)


152. J. B. Birks, Proc. of Symposium on Nuclear Instruments, IAEA, 1966.

153. D. N. Poenaru and N. Vilcov, "Measurement of Nuclear Radiation with Semiconductor Detectors," Chemical Publishing Company, New York, 1969.

154. S. Deme, "Semiconductor Detectors for Nuclear Radiation Measurements," Wiley-Inter-Science, New York, 1971.

155. J. Weisman, Editor, "Miniature Neutron Detector Development," Repts. WCAP 1929, 1989, 2053, 2117, 2128, 2175, and 2666; 1961-1963.

156. R. V. Babcock and H. C. Chang, "Neutron Dosimetry," IAEA, Vienna, 1963.

157. "Solid State Detector," Quarterly Report No. 1, EURAEC-51, A. Anelinckx, Supervisor, 1960.

158. P. C. Canepa, P. Malinaric, R. B. Campbell, and J. Ostroski, Trans. IEEE NS-11, 3, 262 (June 1964).

159. R. R. Ferber and G. N. Hamilton, Trans. Amer. Nucl. Soc. 8, 72 (1965).

160. R. R. Ferber and G. N. Hamilton, Nucl. Appl. 2, 246 (1966).

161. D. S. Billington and J. H. Crawford, Jr., "Radiation Damage in Solids," Princeton University Press, 1971.

162. R. Babcock, Trans. IEEE NS-12, 6, 43 (December 1965).

163. L. M. Epstein and R. R. Ferber, Trans. Amer. Nucl. Soc. 9, 483 (1966).

164. L. M. Epstein and R. R. Ferber, Nucl. Appl. 3, 692 (1967).

165. V. Ajdacic and B. Lavic in "Neutron Dosimetry," IAEA, Vienna, 1963.

166. V. Ajdacic, M. Kurepa, and R. Lalovic, Nucleonics 20, Part 1, 47 (February 1962).

167. G. G. Eichholz, Nucl. Inst. Meth. 87, 181 (1970).

168. G. G. Eichholz, "Spark Counter Neutron Detector for High Temperature Applications," Georgia Institute of Technology, USAEC Rept. TID-25164, June 1969.

BIBLIOGRAPHY (Continued)

169. B. J. Moyer, chapter 3 in "Nuclear Instrumentation and Their Uses," Edited by A. H. Snell, Wiley, New York, 1962.

170. S. E. Rippon, Nucl. Inst. Meth. 21, 192 (1963).

171. "Heavy Water Lattice Project, Final Report," T. J. Thompson, I. Kaplan, and M. J. Driscoll, Editors, Rept. MIT-2344-12, September 30, 1967.

172. R. Madey and D. Duffey, Trans. Amer. Nucl. Soc. 6, 307 (1963).

173. H. Weiss, "Nuclear Electronics," IAEA, Bombay, 1965.

174. D. A. Herbst, L. G. Kuncl, and J. H. Talboy, Trans. Amer. Nucl. Soc. 10, Supp. 2 (July 1967).

175. O. Strindehag, Nucl. Inst. Meth. 33, 314 (1965).

176. C. M. Gordan, J. H. Miller, and R. E. Larson, Nucl. Inst. Meth. 27, 69 (1964).

177. S. E. Rippon, Nucl. Inst. Meth. 21, 185 (1963).

178. O. Strindehag, Kerntechnik 9, 194 (1967).

179. O. Strindehag, "Cherenkov Detectors for Fission Products Monitoring in Reactor Coolant Water," Aktiebolaget Atomeriergi Rept. AE 294, Sweden.

180. C. D. Baumann, Nuclear Safety 12, 90 (1971).

181. K. G. Porgess, R. Gold, and W. C. Corwinn, Trans. IEEE NS-17, 501 (1970).

182. K. G. Porgess and R. Gold, U.S. Patent #3,600,578.

183. J. T. Russell, U.S. Patent #3,130,307.

184. D. P. Brown in "Nuclear Electronics," IAEA, Bombay, 1965.

185. D. P. Brown and N. S. Porter, BNWL-38.

186. T. R. Billeter and D. P. Brown, BNWL-SA-1314.

187. D. P. Brown and T. R. Billeter, Trans. Amer. Nucl. Soc. 10, 637 (1967).

BIBLIOGRAPHY (Continued)

188. D. P. Brown, T. R. Billeter, and W. G. Spear, Trans. IEEE NS-17, 486 (1970).

189. R. L. Staples, R. R. Warnken, Jr., and C. H. Gleason, U.S. Patent #3,137,792.

190. General Electric Reactor Instrumentation and Control, Reports GEMP 71, 72, 73, 74, 75, 76, 77, 78, 79, 80, 81, 82, 83, 84, 85, 87, 1962-1965; also Third Annual Report on High Temperature Materials and Reactor Component Program, GEMP 270c, Vol. III, February 28, 1964.

191. Y. Fujiie and T. Suita, J. Nucl. Sci. Tech. 3(2), 83 (February 1966).

192. W. H. Todt, Nucl. Appl. 5, 173 (1968).

193. W. H. Todt, Nucl. Appl. 6, 422 (1969).

194. J. H. Coleman, U.S. Patent #2,577,106.

195. V. C. Wilson, U.S. Patent #2,728,867.

196. P. C. Ohmart, U.S. Patent #2,696,564.

197. B. R. Lindon, U.S. Patent #3,067,329.

198. S. L. Ruby, K. H. Sun, and T. Fahrner, U.S. Patent #3,101,410.

199. S. Kronenberg, U.S. Patent #3,052,797.

200. J. Handschuh, R. A. Walter, R. T. Schneider, and E. E. Carroll, Jr., Trans. IEEE NS-20, No. 1, 633 (1973).

201. L. E. Fay, III, Semiconductor Products, May 1960, p. 39.

202. E. P. Sisson, Anal. Chem. 43, No. 7, 67a (June 1971).

203. G. E. Pearson, Rev. Sci. Inst. 19, 263 (1948).

204. D. Silverman, Electro-Technology, p. 113 (June 1963).

205. R. J. Higgins, Rev. Sci. Inst. 36, 1536 (1965).

206. G. R. Henning, Electrical Manufacturing 61, 132 (April 1958).

207. A. Roth, "Vacuum Sealing Techniques," Pergamon Press, New York, 1966.

208. E. M. Bernstein, Phys. Rev. Lett. 8, 100 (1962).

BIBLIOGRAPHY (Concluded)

209. N. F. Peak, J. A. Jungerman, and C. G. Patten, Phys. Rev. 136B, 330 (1964).

210. G. T. Ewan, R. L. Graham, and J. S. Geiger, Nucl. Phys. 29, 153 (1962).

211. C. P. Bhalia, Phys. Rev. 157, 1136 (1967).

212. C. T. Hibdon and C. O. Muehlhause, Phys. Rev. 88, 943 (1952).

213. R. K. Smither, Phys. Rev. 124, 183 (1963).

214. A. Bäcklin, N. E. Holmerg, and G. Bäckström, Nucl. Phys. 80, 154 (1966).

215. F. T. Porter, M. S. Freedman, F. Wagner, Jr., and I. S. Sherman, Nucl. Inst. Meth. 39, 35 (1966).

216. C. F. Barnett and J. A. Ray, Rev. Sci. Inst. 41, 1665 (1970).

217. J. H. Neiler and P. R. Bell, chapter 5 in "Alpha, Beta and Gamma Spectroscopy," K. Siegbahn, Editor; North-Holland Publishing Company, Amsterdam, 1965.

218. H. Paul and I. Hofmann, Nucl. Inst. Meth. 22, 141 (1963).

# VITA

Samir Abdul-Majid Alzaidi was born in Baghdad, Iraq in May 1943. In 1964 he graduated from the Institute of Civil Aviation Facilities in Baghdad. For the next five years he was involved in different kinds of activities in the field of Air-Traffic Control, made a complete design of the Instrument Landing System for Baghdad's new airport, and began his university study. In 1968 he received his B.Sc. in Physics and continued working in the field of air traffic. In 1970 he worked as a teacher of physics and mathematics in Mecca, Saudi-Arabia for one academic year. In 1971 he started his graduate study at the Georgia Institute of Technology, receiving the Master's degree in the field of nuclear engineering in 1972. After six months leave in Iraq, Mr. Abdul-Majid Alzaidi returned to Georgia Tech where he continued his graduate study toward the Ph.D. degree. During the period of his doctoral study, Mr. Abdul-Majid Alzaidi received graduate research and teaching assistance from the School of Nuclear Engineering.